AD

SHOCK INDUCED DETONATION ON PROJECTILES IN HYPERSONIC FLOWS OF DETONABLE GAS MIXTURES

Final Technical Report

by

JOSEF ROM

(June 1995)

United States Army

EUROPEAN RESEARCH OFFICE OF THE U.S. ARMY

London England

CONTRACT NUMBER N6817194C9065

R&D 7115-AN-01

TECHNION RESEARCH AND DEVELOPMENT FOUNDATION
TECHNION CITY
HAIFA 32000, ISRAEL

REPORT DOCUMENTATION PAGE

Form Approved
OMB No. 0704-0188

1. AGENCY USE ONLY (Leave blank)	2. REPORT DATE	3. REPORT TYPE AND DATES COVERED
	30 June 1995	Final Report, 1 May 94 - 31 April 95

4. TITLE AND SUBTITLE

SHOCK INDUCED DETONATION ON PROJECTILES IN HYPERSONIC FLOWS OF DETONABLE GAS MIXTURES

5. FUNDING NUMBERS

N6817194C9065

6. AUTHOR(S)

JOSEF ROM

7. PERFORMING ORGANIZATION NAME(S) AND ADDRESS(ES)

Technion R&D Foundation
Technion City,
Haifa 32000 Israel

8. PERFORMING ORGANIZATION REPORT NUMBER

160-783 Final Report

9. SPONSORING/MONITORING AGENCY NAME(S) AND ADDRESS(ES)

Naval Regional Contracting Center
Detachment London, Block 2, Wing 11
DoE Complex. Eastcote Road
Ruislip. Middx, HA4 SB5

10. SPONSORING/MONITORING AGENCY REPORT NUMBER

11. SUPPLEMENTARY NOTES

12a. DISTRIBUTION/AVAILABILITY STATEMENT

12b. DISTRIBUTION CODE

13. ABSTRACT (Maximum 200 words)

This Final Report presents the developments in the research program during the period of contract N6817194C9065, May 1, 1994 to April 31, 1995. During this period the following subjects were investigated: A. CFD results on the External Propulsion Accelerator (EPA) projectile configurations. B. An analytical study on the stability of hypersonic reacting flow at the stagnation region of a blunt body using Dynamical System Analysis. C. The Use of the EPA for Scramjet Combustion Research. D. The Use of the EPA for Hypersonic Aerodynamic Test Facility. E. . Analysis of the Initiation of Detonation on a Hypervelocity Projectile and It's Maximum Velocity in the EPA. F. Preparations for testing at the Army Research Laboratories Ram Accelerator facility at Aberdeen, MD. The CFD calculations on the projectile configurations indicated a well established external combustion zone and reasonably large thrust. Analysis using energy balance considerations indicated that the maximum projectile velocity in the EPA is about 6 times the detonation speed while that for the Ram Accelerator is about 1.3 times the detonation speed of the mixture. Therefore, the EPA is capable to accelerate missile-projectile to beyond the escape velocity and can be considered also for single stage to orbit missions.

14. SUBJECT TERMS

Hypersonic Flow, Detonation, Projectile, Dynamical Systems, External Propulsion

15. NUMBER OF PAGES

74

16. PRICE CODE

17. SECURITY CLASSIFICATION OF REPORT	18. SECURITY CLASSIFICATION OF THIS PAGE	19. SECURITY CLASSIFICATION OF ABSTRACT	20. LIMITATION OF ABSTRACT
UNCLASSIFIED	UNCLASSIFIED	UNCLASSIFIED	

TABLE OF CONTENTS

SHOCK INDUCED DETONATION ON PROJECTILES IN HYPERSONIC FLOWS OF DETONABLE GAS MIXTURES

This Final Report on Contract N6817194C9065 presents the developments in the research program in the period 1 May 1994 to April 30, 1995. The research effort and results which were obtained in the period May 1994 to January 1995 were presented in the Interim Reports 1, 2 and 3. During the period of this research contract the investigations included the following programs: A. CFD results on the External Propulsion Accelerator (EPA) projectile configurations. B. An analytical study on the stability of hypersonic reacting flow at the stagnation region of a blunt body using Dynamical System Analysis. C. The Use of the EPA for Scramjet Combustion Research. D. The Use of the EPA for Hypersonic Aerodynamic Test Facility. E. . Analysis of the Initiation of Detonation on a Hypervelocity Projectile and It's Maximum Velocity in the EPA. F. Preparations for testing at the Army Research Laboratories Ram Accelerator facility at Aberdeen, MD. The results of these investigations are summarized in this report and presented in its Annexes. A summary of the research results will be presented at the 31st AIAA Joint Propulsion Conference, July 1995 (Ref. 1) and is included in Annex 1

The research performed under this contract provides a numerical proof of concept for the principles of the External Propulsion Accelerator. The numerical results indicate that considerable thrust can be obtained on a properly designed projectile enabling accelerations of tens of thousands of g's. Such accelerator can be utilized to increase the muzzle velocity of conventional gun projectiles as well as for new artillery systems. The EPA can be used for launching hypervelocity missiles for theater missile defense, either for terminal intercept or for boost phase intercept. A very intriguing application can be for single stage to orbit as the maximum velocity achievable in the EPA is estimated to be 6 times the detonation velocity, well beyond escape velocity from the earth gravitational force. It is now necessary to carry out experimental tests to verify the concept. A single firing is planed to be performed at ARL in the fall of 1995, as a result of the present program. However, a much more extensive test program is required in order to have a reasonable proof of concept experimental verification. This remains to be done in the next phase of the research program.

1. SCIENTIFIC WORK

a. Introduction

The question of the establishment and stabilization of a combustion or detonation front on a projectile flying at hypersonic speeds in a detonable mixture is of interest both as a fundamental combustion problem and for its practical applications in the External Propulsion Accelerator and it is also relevant to the Oblique Detonation Wave engine, the Ram Accelerator and various scramjet engines. The External Propulsion Accelerator was proposed by J. Rom (Ref. 2) and certain aspect of its characteristics were presented in Refs. 3 and 4. Some analytical investigations, based on many simplifying assumptions, for the establishment of combustion front ahead of the forward facing step and on spherical nosed blunt bodies in hypersonic flows of detonable mixtures, including the studies of the oscillations that may occur were investigated by Tivanov and Rom (Ref. 5, 6 and 7).

The External Propulsion Accelerator has been developed following the development of the Ram Accelerator by A. Hertzberg (Ref. 8) at the University of Washington. The Ram Accelerator method utilizes the idea of using a premixed fuel/oxidizer mixture in the launcher barrel and injecting a projectile at supersonic speeds into this mixture. Thrust is generated by the ramjet combustion obtained between the tube wall and the projectile, where the projectile acts as a ramjet centerbody and the barrel is basically a long cowling, and combustion is initiated and stabilized by the interaction of the shock waves from the projectile nose with the barrel walls. However, in deference from the Ram Accelerator, in the External Propulsion Accelerator the thrust is generated purely by the interactions between the shock waves from the projectile nose with combustion generated by normal shock waves generated on the projectile body by a ramp or a forward facing step or by a ring wing, completely independent of the barrel walls. Since the projectile flies in a premixed fuel/oxidizer atmosphere, the difficult problem of mixing the fuel and oxidizer, which plagues all airbreathing propulsion methods proposed for hypersonic flight, is eliminated. However, there are the remaining difficult issues of the ability to initiate and stabilize the combustion front on the projectile in such a way that positive thrust can be generated. The previous studies (Refs. 3 and 4) indicated that, if a relatively

small forward facing step on the projectile shoulder will be able to induce a detonation wave, then reasonable thrust levels, about the same as those obtained in the Ram Accelerator, can be achieved.
In order to further investigate the flow over the configuration with a forward facing step a cooperative program was established with the Ram Accelerator project group at the Army Research Laboratory in Aberdeen, MD. During the period from March 1994 to September 1994 the Principal Investigator, J. Rom, was at the University of Maryland and established this cooperation with the Ram Accelerator Project group at the Aberdeen Proving Ground and with the Hypersonic Research Center of the department of Aerospace Engineering at the University of Maryland, College Park, MD. During this period a very significant progress was achieved in this research program. The main results are presented under the following subjects:

A. CFD results on the External Propulsion Accelerator (EPA) projectile configurations.

The application of the solution of the Navier-Stokes equations for flows with chemical processes to the flow around the EPA projectile was achieved by the adaptation of the Ram Accelerator calculations done at ARL by Nusca (Refs. 9, 10) to the External Propulsion projectile geometry. This calculation uses the Rockwell Science Center USA-RG (Unified Solution Algorithm Real Gas) code written by Chakravarthy et al (Refs. 11, 12). This CFD code includes the full 3D unsteady Reynolds-Averaged Navier-Stokes (RANS) equations including equations for chemical kinetics (finite-rate and equilibrium). These equations are cast in conservation form and converted to algebraic equations using upwind finite-difference and finite-volume formulations. The equations are solved using a second-order TVD (total variation diminishing) scheme which is used to insure non-oscillatory numerical behavior. The results of these calculations indicated that combustion-detonation is established on forward facing steps of height greater than 0.5 mm. Based on these calculation a projectile configuration giving reasonably high thrust levels was selected for an experimental shot in the Ram Accelerator facility at ARL. The experiment will be performed using a conical nosed model with a forward facing step which will be shot into methane-oxygen-nitrogen mixture in the ARL Ram Accelerator facility (Refs. 13, 14) using subcaliber diameter model. Part of the results of these calculations are presented in AIAA Paper 95-0259 (Ref. 15) and is included in Annex 2.
The first projectile design is composed of a shallow sharp nosed cone (10° half angle) followed by a forward facing step, a short length of a cylindrical body and a conical afterbody with a blunt base. In the present calculations effects of varying step height on generating the combustion front are investigated. It is shown that for steps of height above 0.5 mm at flow Mach number of 6 there is a sizable combustion front followed by combustion over the afterbody and in the wake behind the blunt base. The combustion results in a region of high pressure, high temperature gas engulfing the back parts of the projectile resulting in significant net positive thrust. This region of combustion is confined by the hypersonic flow structure generated by the interactions of the shock wave from the conical nose with the detached shock wave ahead of the step which is followed by the combustion - detonation front. This is an excellent demonstration of external propulsion in which supersonic combustion is confined by the external flow without any structural confinement.
The calculations program includes the parametric study of the effects of step height, flow pressure and Mach number and projectile geometry on the combustion process and their effects on the thrust generated on the projectile. Particular emphasis is placed on the investigation of the flow ahead of the forward facing step, including the formation of the combustion-detonation front. Some of these results are presented in Ref. 15 and Annex 2.

B. Studies of the Stability of Detonations in the Hypersonic Flow using Dynamical System Analysis.

The analytical studies of the combustion-detonation in the stagnation region of blunt nosed bodies at hypersonic speeds indicated a very interesting analogy between the combustion-detonation phenomena in the hypersonic stagnation flow and the mechanical - electrical vibrating systems. Therefore, the methods of Dynamical systems analysis can be applied to the combustion-detonation process resulting in very good results. Some of this work is presented in a paper entitled: "Stability of Hypersonic Reacting Stagnation Flow of a Detonable Gas Mixture by Dynamical Systems Analysis" by Tivanov and Rom. This paper is accepted for publication in Combustion and Flame (Ref. 16) and the paper is presented in Annex 3.

C. The Use of the EPA for Scramjet Combustion Research.

The possibility of using a ring wing model for scramjet combustion research is being studied first by CFD solutions on the ring wing configuration. The projectile in this case will consist of a nose cone, cylindrical mid-section (no step!) and aft-cone shaped to conform to the scramjet engine design. A ring, which will simulate the scramjet engine cowling will be attached so that the projectile will act as the scramjet engine centerbody. Firing such projectiles in the EPA will enable studies of combustion characteristics in scramjet engine configurations using various premixed fuels. In particular this facility can be used for studies of initiation of supersonic combustion and dynamics of combustion of premixed hydrocarbon fuels. This concept is presented in a paper at the 35th Israel Annual Conference on Aerospace Sciences, held in Tel-Aviv and Haifa in February 15-16, 1995 (Ref. 16) and is included in Annex 4.

D. The Use of the EPA for Hypersonic Aerodynamic Test Facility

It is proposed to use the EPA as the launcher of aerodynamic models to hypersonic speeds in a ground test facility. The models, encased in a properly designed sabot, are accelerated in the EPA to the desired hypersonic speed and then fired into an instrumented ballistic range. Since the EPA is capable theoretically to launch projectiles to velocity of up to about 6 times the detonation velocity of the fuel-oxidizer mixture which can be in the order of 12,000 m/sec to 18,000 m/sec, it is well suited to be a launcher for hypersonic ballistic ranges. Using enclosed ballistic ranges will enable simulation of various altitudes in air or in any other gas mixture, which can be used to simulate atmospheres of other planets. The concept is presented at the AIAA Hypersonic Technology Conference held in Chattanoga, Tenn. on April 3-7, 1995 (Ref. 18) and is attached as Annex 5.

E. Analysis of the Initiation of Detonation on a Hypervelocity Projectile and It's Maximum Velocity in the EPA.

The initiation and the subsequent acceleration of the projectile in the in-tube chemical launchers for accelerating projectiles to hypervelocity are investigated using an energy balance analysis. It is shown that the energy balance analysis can be used to evaluate the velocity required to initiate the detonation process on the rear part of the projectile. This analysis indicated that the initiation of detonation by a step on the projectile in the EPA as well as in the Ram Accelerator can be achieved at velocities lower then the detonation velocity.
The energy balance analysis can be used to evaluate the maximum velocity that can be achieved in the in-tube chemical accelerators by balancing the drag work of the projectile with the utilization of the total available chemical reaction energy. It is shown that the EPA is capable to reach maximum velocities of about 6 times the detonation velocity while the Ram Accelerator is limited to about 1.3 times the detonation velocity of the mixture. This analysis is presented in Technion Aerospace Engineering (TAE) Report 729, December 1994 (Ref. 19) which is enclosed as Annex 6. The paper is accepted for presentation at the 20th International Symposium on Shock Waves, July 23-28 1995 in Pasadena, CA.

F. Preparations for Test Firing at the ARL Facility at the Aberdeen Proving Grounds, MD. USA.

In order to prove the concept of the external propulsion on the step model a test program was initiated at the ARL Ram Accelerator facility. The first experiment was performed using the 120mm gun launcher using a conical nosed model with a forward facing step. The first test of a subcaliber model of 32 mm diameter was tested in the 120 mm Ram Accelerator facility at ARL on July 26, 1994. The projectile was not accelerated correctly and disintegrated in the launching gun probably due to the sabot failure.
For the experimental validation, a new test is planned, probably in the fall of 1995, which will be done utilizing the lessons learned from the failure of the sabot system in the previous test of July 1994. The experiment will be performed using a conical nosed model with a forward facing step which will be shot into methane-oxygen-carbon dioxide mixture in the modified ARL Ram Accelerator facility (Refs. 13, 14). Since it was decided to examine a more suitable mixture for the EPA operation using the mixture composed of methane-oxygen diluted with carbon dioxide.

The projectile is designed to be aerodynamically stable at the flight Mach numbers. Preliminary aerodynamic characteristics are measured in the supersonic wind tunnel at the Technion and the results will be used to finalize the fins size required for stable flight trajectory.

REFERENCES

1. Rom, J., Nusca, M., Kruczynski, D., Lewis, M., Gupta, A.K. and Sabean, J., "Recent Results with the External Propulsion Accelerator", AIAA Paper 95-2491, to be presented at the 31st AIAA Joint Propulsion Conference to be held in San Diego, July 1995.
2. Rom, J., "Method and Apparatus for Launching a Projectile at Hypersonic Velocity" U.S. Patent 4,932,306, June 12 1990.
3. Rom, J. and Kvity, Y., "Accelerating Projectiles up to 12 km/sec. Utilizing the Continuous Detonation Propulsion Method", AIAA Paper 88-2969, 1988.
4. Rom, J. and Avital, G., "The External Propulsion Accelerator: Scramjet Thrust Without Interaction with the Accelerator Barrel", AIAA Paper 92-3717, 1992.
5. Tivanov, G. and Rom, J., "Investigation of Hypersonic Flow of a Detonable Gas Mixture Ahead of a Forward Facing Step" AIAA Paper 93-0611, 1993.
6. Tivanov, G. and Rom, J., "Stability of Hypersonic Flow of a Detonable Gas Mixture in the Stagnation Region of a Blunt Body and a Forward Facing Step ", Proceedings of the 33rd Israel Annual Conference of Aeronautics and Astronautics, Feb. 1993.
7. Tivanov, G. and Rom, J., "Analysis of the Stability Characteristics of Hypersonic Flow of a Detonable Gas Mixture in the Stagnation Region of a Blunt Body", AIAA Paper 93-1918, 1993.
8. Hertzberg, A., Bruckner, A.P. and Bogdanoff, D.W., "Ram Accelerator: A New Chemical Method for Accelerating Projectiles to Ultrahigh Velocities" AIAA Journal, Vol. 26, No. 2, 1988, pp 195-203.
9. Nusca, M.J., "Numerical Simulation of Fluid Dynamics with Finite-Rate and Equilibrium Combustion Kinetics for the 120 mm Ram Accelerator" AIAA Paper 93-2182, 1993.
10. Nusca, M.J., "Numerical Simulation of Gas Dynamics and Combustion Kinetics for a 120 mm Ram Accelerator" First International Workshop on Ram Accelerator, ISL, France, 1993.
11. Chakravarthy, S.R., Szema, K.Y., Goldberg, U.C., Gorski, J.J. and Osher, S., "Application of a New Class of High Accuracy TVD Schemes to the Navier-Stokes Equations" AIAA Paper 85-0165, 1985.
12. Palaniswamy, S., Ota, D.K. and Chakravarthy, S.R., "Some Reacting Flow Validation Results for USA-Series Codes" AIAA Paper 91-0583, 1991.
13. Kruczynski, D.L. and Nusca, M.J., "Experimental and computational Investigation of Scaling Phenomena in a Large Caliber Ram Accelerator" AIAA Paper 92-3425, 1992.
14. Kruczynski, D.L., "New Experiments in a 120 mm Ram Accelerator at High Pressures" AIAA Paper 93-2589, 1993.
15. Rom, J., Nusca, M., Kruczynski, D., Lewis, M., Gupta, A.K. and Sabean, J., "Investigation of the Combustion Induced by a Step on a Projectile Flying at Hypersonic Speed in an External Propulsion Accelerator", AIAA Paper 95-0259, Jan. 1995.
16. Tivanov, G. and Rom, J., "Stability of Hypersonic Reacting Stagnation Flow of a Detonable Gas Mixture by Dynamical Systems Analysis", Accepted for publication in Combustion and Flame.
17. Rom, J., Nusca, M.J., Lewis, M., Gupta, A.K. and Sabean, J., "Calculations of Combustion in a Scramjet Engine Model using the External Propulsion Accelerator as a test Facility", Proceedings of the 35th Israel Annual Conference on Aerospace Sciences, February 1995, pp 133-135.
18. Rom, J., Lewis, M.J., Gupta, A.K. and Sabean, J., "Hypersonic Aerodynamics Test Facility Using the External Propulsion Accelerator", AIAA Paper 95-6138, April 1995.
19. Rom, J. "Analysis of the Initiation of Detonation on a Hypervelocity Projectile and it's Maximum Velocity in the External Propulsion Accelerator" TAE Report No. 729, Dec. 1994.

2. PRESENTATION OF PAPERS AND PARTICIPATION IN CONFERENCES.

During the period of this contract the Principal Investigator, J. Rom presented papers and participated in the following conferences:

1. The Seventh Multinational Conference on Theater Missile Defense, on June 21-24, 1994 in Annapolis, Maryland.

2. The 30th AIAA Joint Propulsion Conference, on June 27-29, 1994 in Indianapolis, Indiana.

3. The 45th International Astronautical Congress, on October 10-14, 1994 in Jerusalem, Israel.

4. The 33rd AIAA Annual Meeting, on January 8-12, 1995 in Reno, Nevada.
paper presentation:
Rom, J., Nusca, M., Kruczynski, D., Lewis, M., Gupta, A.K. and Sabean, J., "Investigation of the Combustion Induced by a Step on a Projectile Flying at Hypersonic Speed in an External Propulsion Accelerator", AIAA Paper 95-0259, Jan. 1995.

5. The 35th Israel Annual Conference on Aerospace Sciences, on February 15-16, 1995, Tel Aviv, Israel.
paper presentation:
Rom, J., Nusca, M.J., Lewis, M., Gupta, A.K. and Sabean, J., "Calculations of Combustion in a Scramjet Engine Model using the External Propulsion Accelerator as a test Facility", Proceedings of the 35th Israel Annual Conference on Aerospace Sciences, February 1995, pp 133-135.

6. AIAA 6th International Aerospace Plane and Hypersonic Technologies Conference, on April 3-7, 1995, Chattanooga, TN.
paper presentation:
Rom, J., Lewis, M.J., Gupta, A.K. and Sabean, J., "Hypersonic Aerodynamics Test Facility Using the External Propulsion Accelerator", AIAA Paper 95-6138, April 1995.

7. The 31st AIAA Joint Propulsion Conference to be held in San Diego, CA. July 10-13, 1995.
paper presentation:
Rom, J., Nusca, M., Kruczynski, D., Lewis, M., Gupta, A.K. and Sabean, J., "Recent Results with the External Propulsion Accelerator", AIAA Paper 95-2491, to be presented at the 31st AIAA Joint Propulsion Conference to be held in San Diego, July 1995.

8. The 20th International Symposium on Shock Waves to be held in Pasadena, CA July 23-28, 1995.
paper presentation:
Rom, J., "Analysis of the Initiation of Detonation on a Hypervelocity Projectile and it's Maximum Velocity in the External Propulsion Accelerator"

3. PUBLICATIONS (during the period of the contract)

1. Rom, J. "Analysis of the Initiation of Detonation on a Hypervelocity Projectile and it's Maximum Velocity in the External Propulsion Accelerator" TAE Report No. 729, Dec. 1994.

2. Rom, J., Nusca, M., Kruczynski, D., Lewis, M., Gupta, A.K. and Sabean, J., "Investigation of the Combustion Induced by a Step on a Projectile Flying at Hypersonic Speed in an External Propulsion Accelerator", AIAA Paper 95-0259, Jan. 1995.

3. Rom, J., Lewis, M.J., Gupta, A.K. and Sabean, J., "Hypersonic Aerodynamics Test Facility Using the External Propulsion Accelerator", AIAA Paper 95-6138, April 1995.

4. Rom, J., Nusca, M.J., Lewis, M., Gupta, A.K. and Sabean, J., "Calculations of Combustion in a Scramjet Engine Model using the External Propulsion Accelerator as a test Facility", Proceedings of the 35th Israel Annual Conference on Aerospace Sciences, February 1995, pp 133-135.

5. Tivanov, G. and Rom, J., "Stability of Hypersonic Reacting Stagnation Flow of a Detonable Gas Mixture by Dynamical Systems Analysis", Accepted for publication in Combustion and Flame.

ANNEX 1

RECENT RESULTS WITH THE EXTERNAL PROPULSION ACCELERATOR

J. Rom[1], M.J. Nusca[2], D. Kruczynski[3] M.J. Lewis[4], A.K. Gupta[5] and J. Sabean[6]

ABSTRACT

The present paper presents the results of recent developments in the research on the External Propulsion Accelerator (EPA). This research is motivated by the fact that the chemical propellants are about three order of magnitude more compact in weight and size than electromagnetic energy production and storage systems. Therefore, there is great interest in developing accelerators of hypervelocity projectiles using chemical propellants. There are two methods for in-tube chemical accelerators utilizing premixed gaseous detonative mixtures; the Ram Accelerator (RA) and the External Propulsion Accelerator (EPA). These in-tube chemical launchers for accelerating projectiles to hypervelocity utilize, in the superdetonative mode of operation, the possibilities of generating continuous thrust by initiating detonation in the premixed fuel/oxidizer mixture by shock wave interactions. The first method proposed for an in-tube chemical launcher was the Ram Accelerator, originated and developed by A. Hertzberg and his colleagues at the University of Washington. The second method for operating the chemical in-tube accelerator is based on the utilization of the external propulsion cycle, proposed by J. Rom at the Technion-Israel Institute of Technology. In the External Propulsion Accelerator the projectile is fired into the launcher tube which is filled with premixed fuel/oxidizer mixture, however, here the projectile diameter is much smaller than the tube diameter (about 25%) so that there is no interaction between the flow over the projectile and the tube wall over the complete length of the projectile. In this case the detonation is established by aerodynamic means on the projectile, such as a forward facing step on the projectile shoulder or by the blunt leading edge of a ring wing positioned on the center/rear part of the projectile. By the interactions of the detonation wave with the nose shock wave an "external combustion chamber" is produced. This aerodynamically confined region which is filled with the hot chemical reaction products is then expanded on the rear part and into the base region of the projectile, producing thrust on the projectile. In this paper we present some investigations of the operational performance limits of the Ram and the External Propulsion Accelerators using an energy balance analysis. The energy balance analysis is applied to evaluate the maximum velocity which can be achieved in the in-tube accelerators when the available chemical reaction energy is utilized. It is shown that the maximum velocity of the projectile in the RA is limited, due to the high drag caused by the choking, to about 1.3 the detonation velocity while the maximum velocity of the projectile in the EPA can reach up to 6 times the detonation velocity. Then the results of numerical simulation of the flow over projectile configurations and some performance parameters of the External Propulsion Accelerator are presented. The applications of the EPA to ground test facilities such as a launcher for a hypersonic range and as a facility for combustion research in scramjet engines are discussed.

INTRODUCTION

The present paper presents the results of recent developments in the research on the External Propulsion Accelerator (EPA). This research is motivated by the fact that the chemical propellants are about three order of magnitude more compact in weight and size than electromagnetic energy production and storage systems.

[1] Professor, Lady Davis Chair, Faculty of Aerospace Engineering, Technion - Israel Institute of Technology, Visiting Professor, Department of Mechanical Engineering, University of Maryland, Fellow AIAA.
[2] Aerospace Engineer, Weapons Technology Directorate, Aberdeen Proving Ground, Army Research Laboratory.
[3] Aerospace Engineer, Weapons Technology Directorate, Aberdeen Proving Ground, Army Research Laboratory.
[4] Associate Professor, Department of Aerospace Engineering, University of Maryland.
[5] Professor, Department of Mechanical Engineering, University of Maryland, Fellow AIAA.
[6] Graduate student, Department of Aerospace Engineering, University of Maryland.

Therefore, there is great interest in developing accelerators of hypervelocity projectiles using chemical propellants. There are two methods for in-tube chemical accelerators utilizing premixed gaseous detonative mixtures; the Ram Accelerator and the External Propulsion Accelerator. These in-tube chemical launchers for accelerating projectiles to hypervelocity utilize, in the superdetonative mode of operation, the possibilities of generating continuous thrust by initiating detonation in the premixed fuel/oxidizer mixture by shock wave interactions. The first method proposed for an in-tube chemical launcher was the Ram Accelerator, originated and developed by A. Hertzberg and his colleagues at the University of Washington (Ref. 1). The concept of the Ram Accelerator, operating in the superdetonative mode, is based on utilization of the scramjet cycle, where the projectile acts as a free centerbody and the tube as an extended cowling (Fig. 1). The sharp nosed projectile diameter is slightly less (typically 70% to 80%) than the tube diameter, therefore, the nose shock wave is reflected from the tube wall into the projectile centerbody. Under proper conditions this reflected shock wave initiates a detonation process so that when the products of the chemical reactions are expanded on the rear part of the projectile, thrust is generated.

Another method for operating the chemical in-tube accelerator is based on the utilization of the external propulsion cycle, proposed by Rom (Ref. 2). In the External Propulsion Accelerator the projectile is fired into the launcher tube which is filled with premixed fuel/oxidizer mixture, however, here the projectile diameter is much smaller than the tube diameter (about 25%) so that there is no interaction between the flow over the projectile and the tube wall over the complete length of the projectile (Fig. 2). In this case the detonation is established by aerodynamic means on the projectile, such as a forward facing step on the projectile shoulder or by the blunt leading edge of a ring wing positioned on the center/rear part of the projectile. By the interactions of the detonation wave with the nose shock wave an "external combustion chamber" is produced. This aerodynamically confined region which is filled with the hot chemical reaction products is then expanded on the rear part and into the base region of the projectile, producing thrust on the projectile.

Some characteristics of the EPA and various applications are discussed in Refs. 3, 4, and 5. The CFD calculations indicate that it is possible to establish and stabilize a combustion-detonation front on projectiles of various geometry flying at hypersonic speeds in detonable gas mixtures. The characteristics of the hypersonic combustion-detonation on the projectiles in the External Propulsion Accelerator are also relevant to the Oblique Detonation Wave engine, the Ram Accelerator and various scramjet engines. Certain characteristics of the EPA were presented in Refs. 6, and 7. Some analytical investigations, based on many simplifying assumptions, for the establishment of combustion front ahead of the forward facing step and on spherical nosed blunt bodies in hypersonic flows of detonable mixtures, including the studies of the oscillations that may occur were investigated by Tivanov and Rom (Ref. 8, 9 and 10).

In this paper we present some investigations of the operational performance limits of the Ram and the External Propulsion Accelerators using an energy balance analysis. The energy balance analysis is applied to evaluate the maximum velocity which can be achieved in the in-tube accelerators when the available chemical reaction energy is utilized. It is shown that the maximum velocity of the projectile in the RA is limited due to the high drag caused by the choking, to about 1.3 the detonation velocity while the maximum velocity of the projectile in the EPA can reach up to 6 times the detonation velocity. Then the results of numerical simulation of the flow over projectile configurations and some performance parameters of the External Propulsion Accelerator are presented. The applications of the EPA to ground test facilities such as a launcher for a hypersonic range and as a facility for combustion research in scramjet engines are discussed.

AN ENERGY BALANCE ANALYSIS FOR THE DETONATION DRIVEN PROJECTILE IN THE IN-TUBE CHEMICAL ACCELERATORS

The performance limits of the in-tube chemical accelerators, the RA and EPA, can be evaluated using an energy balance analysis. In this analysis we equate the energy of the chemical reaction with the drag work of the flying projectile. Using the energy required to initiate detonation is used to determine the minimum projectile velocity which is needed to initiate the detonation. While utilizing the total energy available in the mixture will determine the maximum velocity of the projectile.

A. The Minimum Projectile Velocity Required to Initiate Detonation

The minimum velocity of the projectile flying in the Ram Accelerator (RA) or in the External Propulsion Accelerator (EPA) needed to initiate detonation can be evaluated by equating the energy required to initiate detonation in the fuel/oxidizer mixture with the drag work of the flying projectile, as presented in Ref. 12. The energy for the initiation of detonation by the hypervelocity projectile is evaluated by the use of the blast wave analogy (Ref. 12). It

is shown in Ref. 12 that for the flow of the fuel/oxidizer mixture at hypersonic velocity over the projectile in the EPA, as illustrated in Fig. 2, the minimum Mach number for the initiation of detonation on a projectile with a forward facing step can be evaluated by

$$\frac{V_\infty^2}{D^2} = 2.504 \frac{H}{d}\left(\frac{D\tau_r}{H}\right)^2 \frac{1}{C_{D_{step}}} . \qquad (1)$$

Where d is the projectile diameter, the step height is H (where H/d << 1), D is the Chapman-Jouguet detonation speed and τ_r is the reaction time. Since typical H/d values can be 1/30 and smaller , $D\tau_r$ /H should be less than 1 (probably in the range of 1/3 to 1/5) for detonation to occur and C_{Dstep} , the drag coefficient for a forward facing step is about 1. Therefore, introducing these values into Eq. 1, the minimum projectile velocity that produces energy to balance the critical initiation energy for detonation is evaluated to be much below the detonation velocity. Since the projectile in the EPA is expected to fly well above the detonation speed then there is no problem of securing the energy required to initiate the detonation both in the step and also the ring wing configurations.

This energy balance, presented in Eq. 1, is also applicable to the projectile in the RA. In this case, the drag coefficient is equated with that of the drag of the projectile including the effects of the interaction between the projectile and the tube wall and the reference area is the cross section of the projectile body. As the projectile speed increases the drag force on the projectile increases so as to provide the energy for initiation of the detonation. At the lower initial speeds the required drag is provided by the perforated piston orbutrator which is used in the RA for initiation of the process.

B. The Maximum Projectile Velocity in the In-Tube Chemical Accelerators.

It is obvious that the flow as well as the combustion process are very different in the cases of the RA and in the EPA, however, in both cases the work done by the drag force acting on the hypervelocity projectile is balanced by the energy released by the detonating gas mixture.

1. Maximum velocity of the projectile in the EPA.

Following the discussion in Ref. 12, the maximum velocity is

$$\frac{V_{\infty_{max}}^2}{D^2} = \frac{\beta^2 \eta_c}{C_D(\gamma^2 - 1)} , \qquad (2)$$

and following Lee (Ref. 13), we can assume a value of 2/3 for η_c (assuming high combustion temperature of 3000° K and low temperature of 1000° K). In Eq. 2, β is defined as the ratio of the outside diameter of the external combustion zone to the projectile diameter. In the EPA the thickness of the external combustion layer varies as a function of the flow Mach number. It was found from the numerical calculations, which are reported in part in Refs. 3, 11 that for the 32 mm diameter projectile with a 1 mm step the combustion layer thickness varies from 3 step heights at Mach number 5 to 5.5 step heights at Mach number 6 and to 17 step heights at Mach number 10. The value of C_D for the cone with the 1 mm step is about 0.26-0.28 for Mach numbers above 5 (for cone-cylinder without the step the drag coefficient is about 0.07-0.08). Then, using Eq. 2, the maximum projectile velocity can be about 1.9 times the detonation velocity at Mach number 5, about 2.1 times the detonation velocity at Mach number 6 and about 3.3 times the detonation velocity at Mach number 10. At higher flight Mach numbers the combustion may extend to the tube wall, then for the 120 mm tube with the 32 mm projectile the maximum velocity is about 6 times the detonation velocity, which is well above the escape velocity to orbit into space. Therefore, when the projectile is injected at initial velocity between Mach 5 to 6, only about 21% to 28% of the energy of combustion is used to overcome the drag, so that about 72% to 79% of the combustion energy is available for accelerating the projectile. Actually the available combustion energy increases as the Mach number increases, reaching to about 90% at Mach number 10 and will be even higher as the Mach number is increased further. In this case of accelerating the projectile in the EPA we can conclude that only a small fraction of the available combustion energy which can be released in the detonation process is needed to overcome the drag of the hypervelocity projectile and this available energy can be used for accelerating the projectile to higher hypervelocity. Of course as the projectile velocity increases the problems of heating and ablation of the projectile surfaces and the aerodynamic and acceleration loads on the projectile structure become more critical.

2. Maximum Velocity of the Projectile in the RA

The maximum velocity of the projectile in the RA is evaluated using a similar analysis (Ref. 12). Such evaluation was first done by Lee in Ref. 13. Lee assumes a value of the drag coefficient for the projectile flying in the RA tube to be of order 1, $C_D = O(1)$, which is equal to the drag coefficient of a blunt body at hypersonic speeds. So, using Eq. 2 with $\gamma = 1.4$ and $\beta = 1.5$, he estimates the

value of the maximum projectile velocity to be about 1.3 times the detonation velocity. He then concludes that when the projectile velocity is equal to the detonation velocity about 75% of the available energy is used to overcome the drag so that only a small fraction of the energy is available for additional acceleration of the projectile. This result is in agreement with the experimental data on projectiles obtained in the RA of the University of Washington. The projectiles tested at the University of Washington and ARL, as presented in Refs. 1 and 11, have a drag coefficient of about 0.2 -0.25 at Mach numbers above 5 in free flight without the tube wall interference. However, the multiple shock wave reflections from the tube wall to the projectile center-section and the blunt leading edges of the fins which may initiate detonation increase the drag coefficient of the projectile considerably in its flight in the accelerator tube. At these conditions the assumption of a drag coefficient of about 1, which is the value for a blunt body, seems reasonable. As the projectile velocity increases the strength of the reflected oblique shock waves increase and the total pressure loss in the shock interference region on one hand provides energy for the initiation of the detonation but on the other hand due to the extremely high drag consumes an increasing portion of the available reaction energy until the energy required to overcome the drag force will be larger than the available energy from the chemical reaction and we will face the conditions of "unstart" if the projectile will deform and disintegrate or it will exit the tube at this maximum velocity. The fact that the "unstart" is obtained at about 1.15 to 1.2 the detonation velocity is shown in Figs. 3a and 3b, based on the data of Ref. 14, for aluminum projectiles. Using a titanium projectile, which did not deform, the maximum velocity is obtained and the projectile flies at this maximum velocity for the last 3 meters of the tube, as shown in Fig. 4. This maximum velocity is 1.2 the detonation velocity and is in very good agreement with the energy analysis value.

THE PERFORMANCE OF PROJECTILES FLYING AT HYPERSONIC SPEED IN THE EXTERNAL PROPULSION ACCELERATOR

A. Description of the External Propulsion Accelerator (EPA)

An outline of an EPA facility is presented in Fig. 5.

The first stage of the EPA facility can be a large caliber smooth bore conventional powder gun for the initial acceleration of the sabot-projectile/missile payload. Since the projectile/missile must be accelerated to velocities higher than the detonation velocity of the fuel/oxidizer mixture in the accelerator tube (detonation speeds of 1000 m/sec to 1500 m/sec), we require muzzle exit velocities of 1300 m/sec to 1800 m/sec in order to accommodate various mixture compositions. These muzzle velocities can be achieved in large caliber powder guns with barrel lengths of 6 m to 10 m.

The second stage must be a sabot separation section. There are various methods used for sabot separation, mechanical and/or aerodynamic methods, which can be utilized in this design. In Fig. 5 a sabot stripper plate is used. The "clean" projectile/missile flies through the sabot stripper and enters at a velocity which is higher than the detonation velocity into the fuel/oxidizer mixture in the accelerator tube.

The third stage is the accelerator section. This section is a large tube, its diameter should be in the order of 4 times the projectile/missile maximum diameter, which is filled with various premixed gaseous fuel and oxidizer mixtures. Both ends of the accelerator tube must be sealed, either by diaphragms which are pierced by the flying missile or by quick acting valves which are opened in synchronization with the flying missile. This tube can be divided into sections closed by separating diaphragms, so that different mixtures can be filled into each of these subsections. In this way mixtures of increasing detonation speeds can be matched to the projectile/missile velocity as this velocity increases due to the acceleration of the projectile/missile as it flies down the tube through these sub-sections.

The tube, in this case, acts only as a containing vessel for the premixed fuel/oxidizer atmosphere through which the projectile/missile flies. The tube structure must be designed to withstand the initial mixture pressure which can be of the order of 20 atm. to 200 atm., if we wish to use the tube for a single shot operation, or it can be made to withstand the peak pressures experienced after the passage of the gun blast and the explosion of the remaining mixture after the passage of the projectile/missile.

At the exit of the accelerator section the projectile/missile emerges, after piercing the exit diaphragm, at its highest velocity. The exit velocity is determined by the thrust which is generated on the projectile/missile and the length of the accelerator section. The calculations reported in Ref. 3 indicate that thrust levels of F/pA (where F is the thrust force, p is the initial pressure in the tube and A is the maximum cross section of the projectile/missile) of about 3 can be achieved. This thrust level can be increased by using more energetic fuels and by optimizing the projectile/missile design. This thrust level is sufficient to accelerate reasonable size projectile/missile to above 50,000 g's. We use this acceleration level since there are guidance and control systems as well as telemetering units hardened to operate at this 50 Kg's level. The added velocity at the exit of the accelerator tube as a function of the tube length is shown in Fig. 6. Thus, assuming initial velocity of 1500 m/sec., the exit velocity for a 8 m long accelerator tube will be 3500 m/sec. and for 32 m long tube the exit velocity will be 5500 m/sec. It was shown in

Ref. 12, using an energy balance analysis, that it is possible to reach in the EPA a maximum velocity of about 6 times the detonation velocity of the mixture used in the tube. Therefore, using mixtures with detonation speeds of 2,500 m/sec. and up to 3,000 m/sec. enable the utilization of the EPA to reach about 18,000 m/sec., well beyond escape velocity from earth. This may be a very promising method to obtain a "single stage to orbit" mission.
The diameter of the acceleration section is about 1 m for a 25 cm diameter projectile/missile and 40 cm. for a 10 cm. diameter projectile/missile, or smaller or larger for smaller or larger projectile/missiles.

B. Aerodynamic design of the EPA projectile.
After being stripped from its sabot and upon entering the acceleration tube section the projectile flies freely in the gas mixture which is in the tube. The projectile is aimed to pierce the entrance diaphragm near its center and should fly near the tube center. Therefore, the projectile is designed to be aerodynamically stable, both statically and dynamically. In order to insure stability over the range of flight Mach numbers the basic configuration needed for external propulsion, i.e. the cone, forward facing step - cylindrical with boattail aft section, is fitted with small elongated fins at the end of the boattail section. At first, a design with fins with a span equal to the maximum body diameter is investigated. This configuration with 6 fins is shown in Fig. 7. In order to stabilize the flight trajectory in the center of the tube the possibility of imparting a slow spin by canting the fins is also tested. In Fig. 7 the fins are canted to 3° to the model axis while the tail with parallel fins is also shown. The aerodynamic coefficients are measured in the supersonic wind tunnel of the Aerodynamic Laboratory in the Technion. The aerodynamic coefficient are measured at M = 3.4 and these values are extrapolated to the hypersonic flight Mach number using slender body analysis methods. Preliminary wind tunnel results indicate that the aerodynamic center of the 6 fins configuration is positioned so as to obtain reasonable stability margin for the positions of the center of gravity of the projectile. The aerodynamic coefficient evaluated from the wind tunnel results are used to evaluate the flight trajectory by a six degrees of freedom program. This work is currently underway and will be included in future report. In parallel, a firing test is being planed using the Ram Accelerator facility at the Army Research Laboratories of the US Army at Aberdeen Proving Grounds in Maryland, USA.
Following this investigation on the aerodynamic stabilization and flight trajectory it is planned to study the heat transfer rates to the projectile surfaces and determine a practical method for thermal protection at the hypersonic speeds that can be achieved by projectiles in the EPA.

C. Evaluation of the combustion characteristics on the projectile.
The performance characteristics of the projectile flight in the accelerator tube is evaluated by the use of the computer code which is based on the solution of the Navier-Stokes equations for flows with chemical processes. This computer code was developed for the Ram Accelerator calculations at ARL by Nusca (Refs. 16, 17). This program uses the Rockwell Science Center USA-RG (Unified Solution Algorithm Real Gas) code written by Chakravarthy et al (Refs. 18, 19). This CFD code includes the full 3D unsteady Reynolds-Averaged Navier-Stokes (RANS) equations including equations for chemical kinetics (finite-rate and equilibrium). These equations are cast in conservation form and converted to algebraic equations using upwind finite-difference and finite-volume formulations. The equations are solved using a second-order TVD (total variation diminishing) scheme which is used to insure non-oscillatory numerical behavior. The flow field with the combustion generated by the forward facing step is presented in Fig. 8 and for the model with the ring wing in Fig. 9. Following these calculations, test runs of the forward facing step configurations and the ring wing projectiles are being planned in the ARL Ram Accelerator facility (Refs. 20, 21) using subcaliber models.

USE OF THE EXTERNAL PROPULSION ACCELERATOR AS TEST FACILITIES

A. HYPERSONIC FLIGHT RANGE

The External Propulsion Accelerator (EPA) can be used as the launcher of aerodynamic models to hypersonic speeds in a ground test facility. The models, encased in a properly designed sabot, are accelerated in the EPA to the desired hypersonic speed and fired into an instrumented ballistic range. The EPA is theoretically capable to launch projectiles to velocities of up to 6 times the detonation velocity of the fuel-oxidizer mixture, in the order of 12,000 m/sec to 18,000m/sec, so that it is well suited to be a launcher for the hypersonic ballistic range. The free flight range technology seems to enable the best simulation of atmospheric free flight conditions in a ground based facility. The range concept is most suitable since it uses quiescent arbitrary gas in its test sections in which the model flies at the design hypersonic speed. While in other test facilities, such as the various types of shock tunnels and gun tunnels, it is required to compress and heat the test gas to high stagnation temperatures and pressures followed by a rapid expansion in high Mach number nozzles. So that in such facilities the simulation is distorted by the effects of dissociation and ionization of the gas in the shock tunnel stagnation chamber as well as disturbances due to nozzle flow non-uniformities, effects of boundary layer disturbances, etc. The test range can be

divided into sections separated by diaphragms, enabling simulation of flight at various pressure altitudes in a single shot. Therefore, such a hypersonic range with the EPA launcher can be an excellent tool for hypersonic aircraft research and development.

The requirements for a hypersonic ground based flight test range and the feasibility of the use of light-gas gun launcher was discussed by Witcofski et al (Ref. 22). In this study the use of an Electromagnetic launcher (EML) and of the Ram Accelerator (RA) where also considered. It was concluded that with the present state of technology the most suitable candidate is the two-stage light-gas gun which can be made to launch models of about 20 cm. span and length of up to 90 cm. to speeds of up to 6 km/sec. It was contemplated, that at a later stage, using more advanced launcher technology, the models can be increased to 30 cm to 45 cm in span and the velocity range will be increased to 10 km/sec to 15 km/sec.

THE TEST FACILITY

In this application, the hypersonic testing facility is basically similar to the AHAF concept presented in Ref. 22. The facility will be comprised from: 1. The Accelerator section. 2. Sabot separation section. 3. Ballistic Range for aerodynamic models free flight testing. 4. Decelerator section for model retrieval. An artist view of such facility, reproduced from Ref. 22, is shown in Fig. 10.

1. The Accelerator Section

The accelerator is comprised of two parts, an initial accelerator for accelerating the model with its sabot to the required insertion speed of 1,400 to 1,800 m/sec. (Mach number between 5 to 6.6) and the External Propulsion launcher tube which will accelerate the projectile, in which the model is inserted, into the test range. The flight Mach Number in the ballistic range can be then set to the required hypersonic speed with the possibility of reaching M = 30. The type of initial accelerator and the length of the External Propulsion Launcher depend on the allowable acceleration for the model. Simple aerodynamic shapes used for hypersonic flight, such as blunt reentry bodies, slender shuttle type configurations and wave riders with hardened on board instrumentation can be built to operate up to 50,000 g's acceleration level. In this case, a gun powder launcher can be used for the initial acceleration and the acceleration level of the External Propulsion launcher can be adjusted to the desired level. The gun launcher will require lengths of 5 to 20 meters. This section will be followed by the External Propulsion launcher. The lengths of the EPA section will depend on the achievable and allowable acceleration levels. Using the level of 50,000 g's, the required lengths of the EPA (Fig. 6) will be about 2 meters for M = 7 testing, 8 meters for M = 11 testing, about 18 meters for M = 15 testing and for Mach number 30 testing a launcher length of about 120 meters will be required. Using the conservative evaluation for the thrust coefficient, F/pA = 3, the thrust generated on a 25 cm diameter projectile is nearly 300,000 Kg. for initial pressure of 50 atm. The projectile weight, including the model and sabot, is then about 58 Kg. for the 50,000 g's acceleration. This weight can be doubled if the initial pressure is increased to 100 atm. enabling robust structure for the model and sabot as well as for the onboard instrumentation. The initial accelerator as well as the EPA can be "cushioned" for lower acceleration levels. The length of this launcher varies inversely as the acceleration levels, i.e. lower acceleration will require the correspondingly longer launcher lengths.

The External Propulsion launcher diameter should be about 4 times the model maximum diameter or span. Therefore, a launcher of 1m diameter will enable launching of models of 25 cm. span encased in a projectile of comparable diameter. The launcher tube diameter can be reduced to 40 cm for 10 cm projectile diameter. Of course larger models can be considered with increase in the diameter of the accelerator.

2. Blast Chamber and Sabot Separation Section.

The blast of the combusting gas mixture as well as the blast of the gun for the initial acceleration follow the projectile and should be retained in a blast chamber at the exit of the launching tube. This chamber is followed by the sabot-model separating section, as shown in Fig. 10.

Since the projectile shape required for the initial accelerator and for the External Propulsion Accelerator should be of a specified axi-symmetric shape the aerodynamic model must be encased in a sabot. The outside shape of this sabot should be in accordance with the External Propulsion projectile design while supporting the model to withstand the acceleration levels. Upon exit from the accelerator launcher the sabot should be separated either mechanically or by special mechanism which will be initiated at the exit of the launcher and the sabot parts should be retained in this separation section while the free model flies into the test range.

3. Ballistic Range Section.

The free model can now fly in the instrumented ballistic range where its instantaneous trajectory positions and attitudes can be photographed and measured. Further offboard instrumentation may include optical instrumentation for measurements of the vibrational, translational and electron temperatures and interferometric photographs for measurements of density profiles. In addition various onboard instrumentation can be installed in the model, such as wall temperatures and pressures, accelerometers for model acceleration, strain gages for loads and stresses, and these can be monitored by telemetering system. If we consider models of 10 cm to 25 cm in diameter or span, such models are sufficiently large to include most details of the aerodynamic design,

including deflected control surfaces and/or small control jets actuated by small rockets or gas supply.

The ballistic range can either be an atmospheric range or be enclosed in a large tube enabling controlled atmosphere for simulation of pressure-altitude effects and also atmospheric composition of other planets. The enclosed test range in a large tube can be divided into sections separated by diaphragms, enabling simulation of flight at various pressure altitudes and/or various gases in a single shot.

4. Deceleration Section.

The energy imparted to the model traveling at Mach 6 to 30 is very large and must be absorbed in order to stop the model. For simple models, the models can be expandable and a conventional "catcher" can be used. For more sophisticated and expansive models there may be some possibilities of some energy absorbing methods for arresting the models, at least in the lower hypersonic speed range.

B. THE HYPERSONIC SCRAMJET TEST FACILITY

The combustion-detonation phenomena in a scramjet engine as well as in an Oblique Detonation Wave Engine can be studied in the External Propulsion Accelerator. This facility provides the means to investigate the combustion-detonation process independently from the fuel mixing process. In this case, a projectile simulates the engine geometry and the combustion of the premixed fuel/oxidizer mixture is initiated in the model flying in the External Propulsion Accelerator. The scramjet combustion also provides net thrust for the model flight in the Accelerator. Thus, this facility enables testing of the combustion characteristics as function of inlet, combustor and nozzle geometry, fuel/oxygen chemical parameters and flight velocity. The effects of various fuel/oxidizer mixtures can be studied by including sections separated by diaphragms in the accelerator tube. These sections can be filled with various mixtures to different initial pressures, so that effects of various pressure levels can also be simulated in this facility.

The scramjet model will be composed of a shallow sharp nosed cone acting as the scramjet inlet, a ring wing simulating the cowling of the scramjet around a cylindrical center body and a conical afterbody simulating the scramjet exhaust. Combustion is generated behind the shock wave established in front of the wedge shape lip of the ring wing. The flow field is illustrated in Fig. 9. The scramjet combustion in this configuration will produce high temperature high pressure combustion products resulting in significant net positive thrust.

THE SCRAMJET TEST FACILITY

In this application, the hypersonic scramjet testing facility will be comprised from: 1. The External Propulsion Accelerator section. 2. Transparent test section. 3. Deccelerator section for model retrieval.

1. The External Propulsion Accelerator Section

The tests are conducted in a regular External Propulsion Accelerator using a specially designed model for the scramjet simulation. The model with its sabot are accelerated by a gun powder charge to the required insertion speed of 1,000 up to 1,900 m/sec. (Mach number between 3 to 5). In a simple configuration the projectile body will simulate the engine centerbody and a properly shaped ring wing around this centerbody will represent the engine cowling. The shapes of the engine intake and the shape of the combustion region inside the engine can be also simulated by this model. Combustion-detonation will be initiated by the shock waves generated at the intake to the ring wing and it will cause combustion in the space between the centerbody and the ring-cowling. The flow will be then expanded on the aft-body of the model, simulating the engine exhaust and nozzle flow characteristics. The operation of the scramjet will produce net thrust for the acceleration of the model. Therefore, measurements of the model acceleration-deceleration will enable the evaluation of the thrust obtained by this scramjet engine as a function of model velocity. More sophisticated measurements can be obtained using on-board instrumentation with telemetering. Models with hardened on-board instrumentation can be built to operate up to 50,000 g's acceleration level. The acceleration level in the projectile will depend on the thrust generated by the scramjet. Since the gas mixtures can be varied in the accelerator, this will be a method to study the effects of various chemical fuel compounds on the combustion and the thrust generation. Such studies can be made when the accelerator tube is divided into a number of sections separated by diaphragms. Each section of the accelerator tube can be filled with a certain fuel/oxidizer mixture at various initial pressures. So that in a single experiment the combustion characteristics of flight in various mixtures at specified initial pressures can be studied These test sections can be positioned at the end of the basic accelerator tube in which the projectile is accelerated to the desired velocity.

The length of the facility will be determined by the acceleration of the model and the speed range for the tests. For the External Propulsion launcher at 50,000 g's, the required lengths of the EPA (Fig. 6) will be about 2 meters for M = 7 testing, 8 meters for M = 11 testing, about 18 meters for M = 15 testing and for Mach number 30 testing a launcher length of about 120 meters will be required. More sophisticated models requiring lower values of acceleration can be used by proper modifications to the launcher. Lower initial accelerations can be achieved by initial acceleration of either a Ram Accelerator stage initiated by a small light gas gun or a small rocket or the

initial acceleration be achieved directly by a rocket motor which will separate at the entrance to the External Propulsion launcher. The length of this launcher varies inversely as the acceleration levels, i.e. lower acceleration will require the correspondingly longer lengths.

The External Propulsion launcher diameter should be about 4 times the model maximum diameter. Therefore, a launcher of 1m diameter will enable launching of models of 25 cm. diameter and the launcher tube diameter can be reduced to 40 cm for 10 cm models. Of course larger models can be considered with increase in size of the facility.

2. Transparent Test Section.

The possibility of including a transparent section into the Ram Accelerator facility was studied at ARL by Kruczynski et al. (Ref. 15). Such a transparent section at the end of the launcher tube will enable flow visualization photographs on the model, particularly, at the intake and exhaust regions.

3. Deceleration Section.

The energy imparted to the model traveling at Mach 6 to 15 is very large and must be absorbed in order to stop the model. For simple models, the models can be expandable and a conventional "catcher" can be used. For more sophisticated and expansive models there may be some possibilities of some energy absorbing methods for arresting the models, at least in the lower hypersonic speed range.

SUMMARY AND CONCLUSIONS

The two methods for in-tube chemical accelerators utilizing premixed gaseous detonative mixtures; the Ram Accelerator (RA) and the External Propulsion Accelerator (EPA) are examined using an energy balance analysis. It is shown that the maximum velocity of the projectile in the RA is limited, due to the high drag caused by the choking, to about 1.3 the detonation velocity while the maximum velocity of the projectile in the EPA can reach up to 6 times the detonation velocity.

The results of numerical simulation of the flow over projectile configurations using a Navier-Stokes code with chemical reactions show that combustion can be generated by a small step on the shoulder of the projectile. These calculations indicate that positive thrust is obtained.

It is shown that the projectile can be stabilized aerodynamically by 6 small fins which can be canted to impart roll to the flying projectile.

The applications of the EPA to ground test facilities such as a launcher for a hypersonic flight range and as a facility for combustion research in scramjet engines are discussed.

REFERENCES

1. Hertzberg, A., Bruckner, A.P. and Bogdanoff, D.W., " Ram Accelerator: A New Chemical Method for Accelerating Projectiles to Ultrahigh Velocities", AIAA Journal, Vol. 26, No. 2, 1988, pp. 195-203.

2. Rom, J., "Method and Apparatus for Launching a Projectile at Hypersonic Velocity", U.S. Patent 4,932,306, June 12, 1990.

3. Rom, J., Nusca, M.J., Kruzcynski, D., Lewis, M., Gupta, A.K. and Sabean, J., "Investigations of the Combustion Induced by a Step on a Projectile Flying at Hypersonic Speeds in the External Propulsion Accelerator", AIAA Paper 95-0259, 1995.

4. Rom, J., Nusca, M., Lewis, M., Gupta, A.K. and Sebian, J. " Calculations of combustion in a Scramjet engine model in the External Propulsion Accelerator as a test facility" Proceedings of the 35th Israel Annual Conference on Aerospace Sciences, February 1995.

5. Rom, J., Lewis, M., Gupta, A.K. and Sebian, J., "Hypersonic aerodynamic test facility using the External Propulsion Accelerator", to be presented at the 6th International AIAA Aerospace plane and hypersonic technologies, April 1995.

6. Rom, J. and Kivity, Y., "Accelerating Projectiles up to 12 km/sec. Utilizing the Continuous Detonation Propulsion Method", AIAA Paper 88-2969, 1988.

7. Rom, J. and Avital, G., "The External Propulsion Accelerator: Scramjet Thrust Without Interaction with the Accelerator Barrel", AIAA Paper 92-3717, 1992.

8. Tivanov, G. and Rom, J., "Investigation of Hypersonic Flow of a Detonable Gas Mixture Ahead of a Forward Facing Step", AIAA Paper 93-0611, 1993.

9. Tivanov, G. and Rom, J., "Stability of Hypersonic Flow of a Detonable Gas Mixture in the Stagnation Region of a Blunt Body and a Forward Facing Step ", Proceedings of the 33rd Israel Annual Conference of Aeronautics and Astronautics, Feb. 1993.

10. Tivanov, G. and Rom, J., "Analysis of the Stability Characteristics of Hypersonic Flow of a Detonable Gas Mixture in the Stagnation Region of a Blunt Body", AIAA Paper 93-1918, 1993.

11. Nusca, M.J., "Reacting Flow Simulations for Large Scale Ram Accelerator", AIAA Paper 94-2963, 1994.

12. Rom, J., "Analysis of the Initiation of Detonation on a Hypervelocity Projectile and it's Maximum Velocity in the External Propulsion Accelerator", TAE Report 729, December 1994.

13. Lee, J.H.S., "On the Initiation of Detonation by a Hypervelocity Projectile", Paper presented at the Zeldovich Memorial Conference on Combustion, Sept. 12-17, 1994, Voronovo, Russia.

14. Knowlen, C., Higgins, A. and Bruckner, A., "investigation of Operational Limits to the Ram Accelerator", AIAA Paper 94-2967, 1994.

15. Hinkey, J.B., Burnham, E.A. and Bruckner, A.P., "Investigation of Ram Accelerator Flow Fields Induced by Canted Projectiles", AIAA Paper 93-2186, 1993.

16. Nusca, M.J., "Numerical Simulation of Fluid Dynamics with Finite-Rate and Equilibrium Combustion Kinetics for the 120 mm Ram Accelerator" AIAA Paper 93-2182, 1993.

17. Nusca, M.J., "Numerical Simulation of Gas Dynamics and Combustion Kinetics for a 120 mm Ram Accelerator" First International Workshop on Ram Accelerator, ISL, France, 1993.

18. Chakravarthy, S.R., Szema, K.Y., Goldberg, U.C., Gorski, J.J. and Osher, S., "Application of a New Class of High Accuracy TVD Schemes to the Navier-Stokes Equations" AIAA Paper 85-0165, 1985.

19. Palaniswamy, S., Ota, D.K. and Chakravarthy, S.R., "Some Reacting Flow Validation Results for USA-Series Codes" AIAA Paper 91-0583, 1991.

20. Kruczynski, D.L. and Nusca, M.J., "Experimental and computational Investigation of Scaling Phenomena in a Large Caliber Ram Accelerator" AIAA Paper 92-3425, 1992.

21. Kruczynski, D.L., "New Experiments in a 120 mm Ram Accelerator at High Pressures" AIAA Paper 93-2589, 1993.

22. Witcofski, R., Scallion, W., Carter, D. Jr. and Courter, R., "An Advanced Hypervelocity Aerophysics Facility: A Ground-Based Flight-Test Range", AIAA Paper 91-0296, 1991

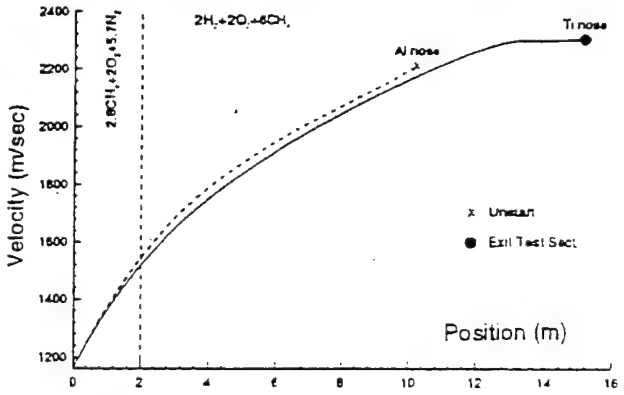

Figure 4. Velocity-distance data comparing aluminum and titanium nose projectiles (from Ref. 14)

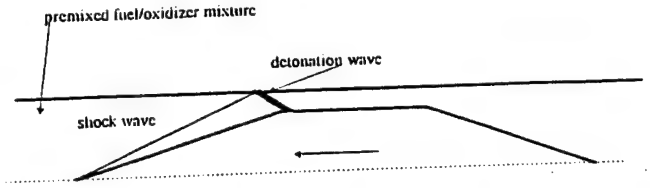

Figure 1. The Ram Accelerator projectile in the detonative mode (Ref. 1)

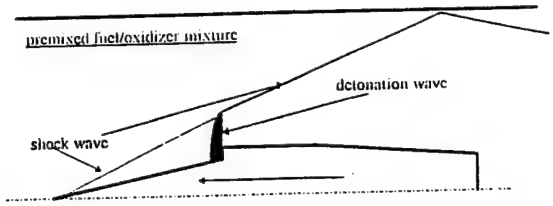

Figure 2. The External Propulsion Accelerator projectile with a forward facing step (Ref. 2)

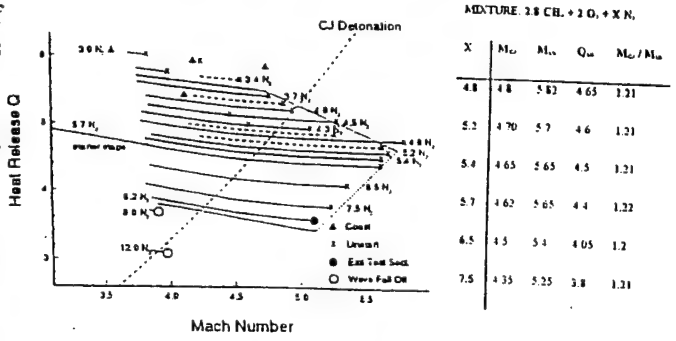

Figure 3a. Results of variable nitrogen experiments plotted as thermally choked heat release vs. flight Mach number (from Ref. 14)

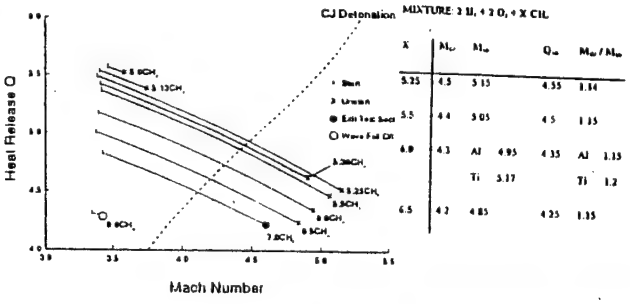

Figure 3b. Results of variable methane experiments plotted as thermally choked heat release vs. flight Mach number (from Ref. 14)

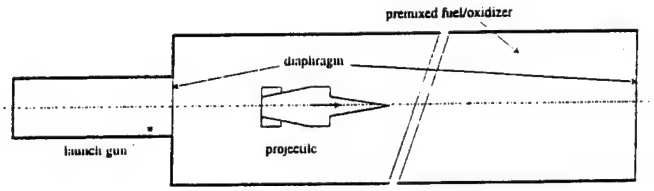

Figure 5. Schematic of the External Propulsion Accelerator facility

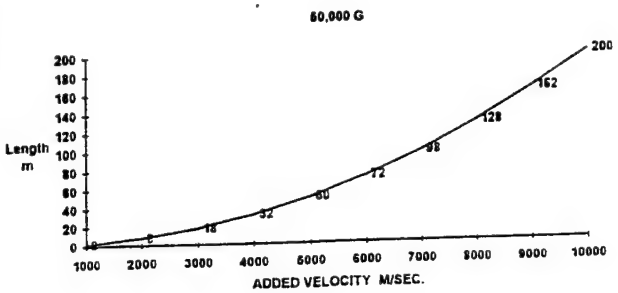

Figure 6. The added velocity as a function of accelerator tube length for 50,000 g's acceleration

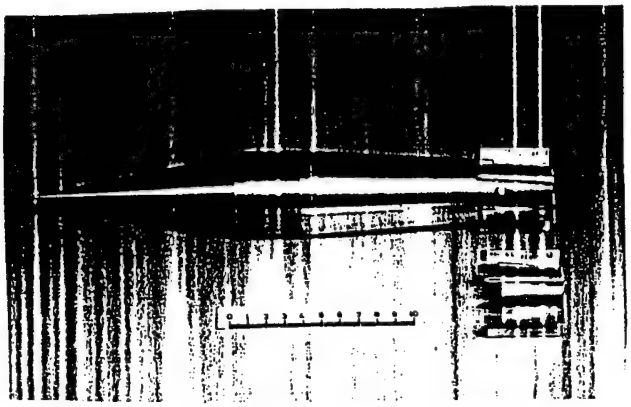

Figure 7. An External Propulsion Accelerator projectile with a 1 mm step and 6 fins tail

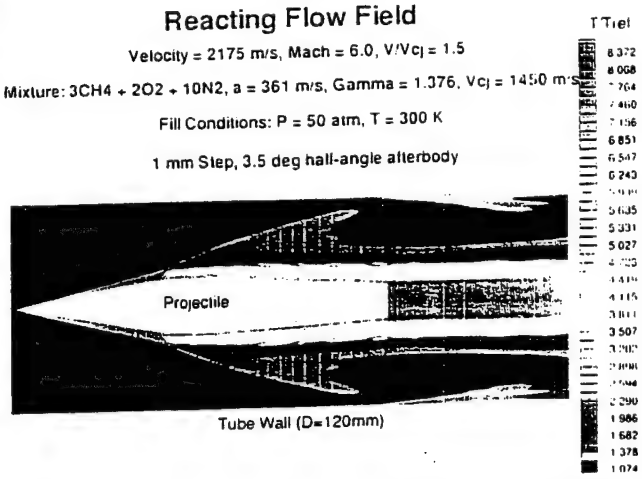

Figure 8. The temperature ratio distribution around the 1 mm step model for Mach number 6 flow with chemical reactions in the EPA.

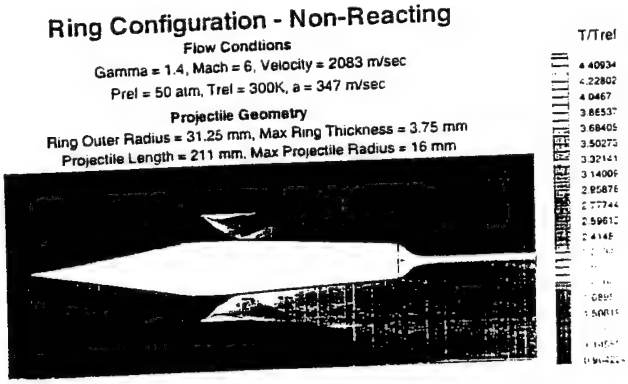

Figure 9. The temperature ratio distribution around the ring wing model for Mach number 6 flow without chemical reactions in the EPA.

Figure 10. Schematic view of the hypersonic flight range facility using EPA launcher

AIAA 95-0259

Investigation of the Combustion Induced by a Step on a Projectile Flying at Hypersonic Speed in an External Propulsion Accelerator

J. Rom, Technion, Israel Institute of Technology
Haifa, Israel

M. Nusca, D. Kruczynski, Army Research Laboratory, Aberdeen Proving Ground, MD

M. Lewis, A. Gupta, J. Sabean, University of Maryland, College Park, MD

33rd Aerospace Sciences Meeting
January 9-12, 1995 / Reno, Nevada

INVESTIGATION OF THE COMBUSTION INDUCED BY A STEP ON A PROJECTILE FLYING AT HYPERSONIC SPEED IN AN EXTERNAL PROPULSION ACCELERATOR

J. Rom[1], M.J. Nusca[2], D.L. Kruczynski[3], M.J. Lewis[4], A.K. Gupta[5], and J. Sabean[6]

Abstract

The establishment of combustion by a small forward facing step on a hypervelocity projectile, in the External Propulsion Accelerator, is demonstrated via a computational fluid dynamics simulation. Computations of the flow over the projectile flying at hypersonic speeds in a combustible mixture are presented. The computations indicate that a small forward-facing step, of the order of 1 mm, can initiate detonation at the step and sustain combustion over the afterbody and blunt base of the projectile, flying at Mach numbers above 5. The interaction between the shock wave from the shallow cone forebody and the detached shock-detonation wave from the forward-facing step, positioned on the shoulder of the projectile (i.e., the forebody-afterbody junction) results in confinement of a combustion layer on the external surface of the projectile afterbody and on the blunt base. The high pressure, high temperature products of the combustion, which are confined to the external combustion layer, are then expanded over the afterbody and into the wake of the projectile and can be used to generate thrust. Thus this layer, confined by the aerodynamic interactions, acts as an external combustion chamber. This is an excellent demonstration of the external propulsion method. Some preliminary computed results are presented for a 32mm projectile flying in a 120mm accelerator tube, at Mach numbers of 6 and 10. The tube is filled with a fuel-rich methane/oxygen/nitrogen mixture at an initial pressure of 50 atm. The results show that for projectiles with step heights of 0.5, 1, and 1.5 mm, combustion is established and maintained.

[1]Professor, Lady Davis Chair, Faculty of Aerospace Engineering, Technion, Israel Institute of Technology. Visiting Professor, Dept. of Mechanical Engineering, University of Maryland. Fellow AIAA.

[2]Aerospace Engineer, US Army Research Lab., Aberdeen Proving Ground, MD, Senior Member, AIAA.

[3]Mechanical Engineer, US Army Research Lab., Aberdeen Proving Ground, MD, Member, AIAA.

[4]Associate Professor, Dept. of Aerospace Engineering, University of Maryland.

[5]Professor, Dept. of Mechanical Engineering, University of Maryland. Fellow AIAA.

[6]Graduate Student, Dept. of Aerospace Engineering, University of Maryland.

Introduction

The question of establishment and stabilization of a combustion or detonation front on a projectile flying at hypersonic speeds in a detonable mixture is of interest both as a fundamental combustion problem and for practical application in the External Propulsion Accelerator. It is also relevant to the Oblique Detonation Wave (ODW) engine, the Ram Accelerator, and various scramjet engines. The External Propulsion Accelerator was proposed by J. Rom[1] and certain aspects of its characteristics were presented in References 2 and 3. Some aspects of the establishment of a combustion front ahead of the forward-facing step on a hypervelociy projectile, and on a spherically blunted body in hypersonic flow of a detonable mixture (including oscillations) were investigated by Tivanov and Rom.[4,5,6]

The External Propulsion Accelerator has been developed following that of the Ram Accelerator by Hertzberg and colleagues at the University of Washington.[7] The Ram Accelerator is based on the idea of using a premixed fuel/oxidizer/diluent mixture in a sealed launch barrel, and injecting a projectile at supersonic speeds into the mixture. Thrust is generated by the ramjet combustion obtained between the tube wall and the projectile, where the projectile acts as a ramjet centerbody and the barrel is basically a long cowl. In the supersonic mode combustion is initiated by the interaction of shock waves, generated at the projectile nose, and reflected between the tube walls and the projectile body.

Unlike the Ram Accelerator, for the External Propulsion Accelerator, thrust is generated by combustion initiated by a normal shock wave generated on the projectile body by a ramp or forward-facing step (or by a ring wing[1]) independent of the barrel walls. Since the projectile flies in a premixed fuel/oxidizer atmosphere, the problem of mixing fuel and oxidizer, which plagues air-breathing proplusion methods proposed for hypersonic flight, is eliminated. However, there are remaining difficult issues such as the ability to initiate and stabilize the combustion front on the projectile in such a way that positive thrust can be generated. Previous studies[2,3] indicated that, if a relatively small forward-facing step on the projectile shoulder (i.e. the forebody-afterbody junction) is able to induce a detonation wave and a sustained combustion front, then reasonable thrust levels may be achieved.

Therefore, the present investigation will study the ability of a small forward-facing step to ignite the premixed fuel/oxidizer mixture flowing at hypersonic speeds over the projectile, and study the flow field and combuston front generated by the interaction of the shock wave from the projectile nose, and the detonation wave generated by the step. This interaction results in the confinement of a high pressure, high temperature region below a contact surface. This region, between the projectile body and the contact surface, acts like the combustion chamber of an engine. However, in this case, the contact surface acts as the "engine cowling" without a structural boundary. This is an example of a true external propulsion "combustion chamber". The high temperature and pressure combustion products are then expanded over the afterbody and the base of the projectile to produce thrust. The flow field, with chemical reactions, are studied in detail using the numerical solution of the Reynolds Averaged Navier-Stokes (RANS) equations, including the equations for chemical species.

The present investigation utilizes the solution of the RANS equations for flows with chemical processes adapted for the Ram Accelerator configuration at the US Army Research Laboratory (ARL) by Nusca[8-11] and are summarized in this paper. In the present calculations we use the same mixture of CH_4, O_2, and N_2 selected at the ARL for the Ram Accelerator firings. The chemical reaction rate constants for a mixture, used in the calculations for the ARL Ram Accelerator, yielded good results when compared with experimental data.[8-11] Although the combustion conditions in the case of the External Propulsion Accelerator are different from those in the Ram Accelerator (i.e. scale of the projectile and method of ignition) it has been assumed in this paper that by using the same mixture with the same kinetics model, good results can be achieved for the External Propulsion Accelerator as well. Actually, more sutiable mixtures for the External Propulsion mode of operation are available and should be used, but in the present investigation we chose to use this mixture for which the chemical reaction model was validated for the Ram Accelerator. This paper presents calculations of the effects of step height and Mach number for several projectile geometries, on the combustion process and thrust generated on the projectile. These calculations are also used to study the flow ahead of the forward-facing step, including the formation of a combustion-detonation front.

Reacting Flow Model

Computational fluid dynamics (CFD) flow simulations for the ram accelerator projectile were performed at U.S. Army Research Laboratory (ARL) using the Rockwell Science Center USA-RG (Unified Solution Algorithm Real Gas) code.[12-14] This code has been used successfully at the ARL for simulation of a full-bore 120mm ram accelerator projectile by Nusca[8-11] This CFD code solves the full, 3D, unsteady Reynolds-Averaged Navier-Stokes (RANS) equations including equations for chemical kinetics (finite-rate and equilibrium). These partial differential equations are cast in conservation form and converted to algebraic equations using an upwind finite-volume formulation. Solution takes place on a mesh of nodes distributed in a zonal fashion around the projectile and throughout the flow field such that sharp geometric corners and other details are accurately represented. The conservation law form of the equations assures that the end states of regions of discontinuity (shocks, detonations, deflagrations) are physically correct even when smeared over a few computational cells. The Total Variation Diminishing (TVD) technique is employed to discretize inertia terms of the conservation equations, while the viscous terms are evaluated using an unbiased stencil. Flux computations across cell boundaries are based on Roe's scheme for hyperbolic equations.[15] Spatial accuracy of third-order can be maintained in regions of the flow field with continuous variation while slope limiting, used near large flow gradients, reduces the accuracy locally to avoid spurious oscillations.

The RANS equations for 2D/axisymmetric reacting flow (N species mixture) are written in the following conservation form[13] for dependent variables of energy (e), density (ρ), axial and radial momentum flux ($\rho u, \rho v$), and species flux ($\rho\sigma$).

$$\frac{\partial W}{\partial t} + \frac{\partial (F_1 - G_1)}{\partial x} + \frac{\partial (F_2 - G_2)}{\partial y} = \Omega \qquad (1)$$

$$W = \begin{pmatrix} e \\ \rho \\ \rho u \\ \rho v \\ \rho\sigma_1 \\ . \\ . \\ . \\ \rho\sigma_{N-1} \end{pmatrix}, F_1 = \begin{pmatrix} (e+p)u \\ \rho u \\ \rho u^2 + p \\ \rho uv \\ \rho u\sigma_1 \\ . \\ . \\ . \\ \rho u\sigma_{N-1} \end{pmatrix}$$

$$F_2 = \begin{pmatrix} (e+p)v \\ \rho v \\ \rho vu \\ \rho v^2 + p \\ \rho v\sigma_1 \\ . \\ . \\ . \\ \rho v\sigma_{N-1} \end{pmatrix}, \Omega = \begin{pmatrix} 0 \\ 0 \\ 0 \\ 0 \\ \sum_k \omega_{1k} \\ . \\ . \\ . \\ \sum_k \omega_{(N-1)k} \end{pmatrix}$$

$$G_1 = \begin{pmatrix} \kappa_m \frac{\partial T}{\partial x} + \sum_i \rho D(h_i - h_N)\frac{\partial \sigma_i}{\partial x} + u\tau_{xx} + v\tau_{xy} \\ 0 \\ \tau_{xx} \\ \tau_{xy} \\ \rho D \frac{\partial \sigma_1}{\partial x} \\ . \\ . \\ . \\ \rho D \frac{\partial \sigma_{N-1}}{\partial x} \end{pmatrix}$$

$$G_2 = \begin{pmatrix} \kappa_m \frac{\partial T}{\partial y} + \sum_i \rho D(h_i - h_N)\frac{\partial \sigma_i}{\partial y} + u\tau_{yx} + v\tau_{yy} \\ 0 \\ \tau_{yx} \\ \tau_{yy} \\ \rho D \frac{\partial \sigma_1}{\partial y} \\ . \\ . \\ . \\ \rho D \frac{\partial \sigma_{N-1}}{\partial y} \end{pmatrix}$$

The shear stress terms are given by,

$$\tau_{xx} = 2\mu_m \frac{\partial u}{\partial x} - \frac{2}{3}\mu_m \left(\frac{\partial u}{\partial x} + \frac{\partial v}{\partial y}\right) \quad (2)$$

$$\tau_{yy} = 2\mu_m \frac{\partial v}{\partial y} - \frac{2}{3}\mu_m \left(\frac{\partial u}{\partial x} + \frac{\partial v}{\partial y}\right) \quad (3)$$

$$\tau_{xy} = \tau_{yx} = \mu_m \left(\frac{\partial u}{\partial y} + \frac{\partial v}{\partial x}\right) \quad (4)$$

In these equations σ_i and ω_i are the mass fraction and chemical production term for the i-th species. The species viscosity (μ) and thermal conducivity (κ) are referenced to μ_o, κ_o and T_o using Sutherland's law,

$$\frac{\mu_i}{\mu_{o_i}} = \left(\frac{T}{T_{o\mu}}\right)^{3/2} \frac{T_{o\mu} + S_\mu}{T + S_\mu} \quad (5)$$

$$\frac{\kappa_i}{\kappa_{o_i}} = \left(\frac{T}{T_{o\kappa}}\right)^{3/2} \frac{T_{o\kappa} + S_\kappa}{T + S_\kappa} \quad (6)$$

where T_o and S vary with species.[16] The mixture viscosity and thermal conductivity are determined using Wilke's law[17] denoting f as μ or κ,

$$f_m = \sum_{i=1}^{N} \left[X_i f_i \left(\sum_{j=1}^{N} X_j \phi_{ij} \right)^{-1} \right] \quad (7)$$

$$\phi_{ij} = (8)^{-1/2} \left(1 + \frac{\mathcal{M}_i}{\mathcal{M}_j}\right)^{-1/2} \left[1 + \left(\frac{f_i}{f_j}\right)^{1/2} \left(\frac{\mathcal{M}_j}{\mathcal{M}_i}\right)^{1/4}\right]^2 \quad (8)$$

where X_i and $\mathcal{M}_i$ are the mole fraction and molecular weight of the i-th species, respectively. Fick's law is used to relate the mixture diffusivity to the mixture viscosity through the Schmidt number $\mathrm{Sc} = \mu_m/(\rho D)$. The specific heat, enthalpy and Gibbs free energy of each species (per mass) are given by the following fourth order temperature (T) polynomial curve fits,[18] (ΔH_{f_i} is the heat of formation, and $\Re_i$ is the specific gas constant for the i-th species).

$$\frac{c_{p_i}}{\Re_i} = A_i + B_i T + C_i T^2 + D_i T^3 + E_i T^4 \quad (9)$$

$$h_i = \Re_i \left(A_i + \frac{B_i}{2}T + \frac{C_i}{3}T^2 + \frac{D_i}{4}T^3 + \frac{E_i}{5}T^4\right) T + \Delta H_{f_i} \quad (10)$$

$$\frac{g_i}{\Re_i} = A_i(T - T\ln T) - \frac{B_i}{2}T^2 - \frac{C_i}{6}T^3 - \frac{D_i}{12}T^4 - \frac{E_i}{20}T^5 + \frac{\Delta H_{f_i}}{\Re_i} - F_i T \quad (11)$$

The mixture enthalpy, total energy per unit volume, and ratio of specific heats are given by,

$$h = \sum_{i=1}^{N} \sigma_i \int^T c_{p_i} \mathrm{d}T + \sum_{i=1}^{N} \sigma_i \Delta H_{f_i} \quad (12)$$

$$e = \frac{p}{\gamma - 1} + \rho\frac{(u^2 + v^2)}{2} + \sum_{i=1}^{N} \rho\sigma_i \Delta H_{f_i} \quad (13)$$

$$\gamma = 1 + \left[\frac{c_{pm}}{\overline{\Re}\sum_i(\sigma_i/\mathcal{M}_i)} - 1\right]^{-1} \quad (14)$$

$$c_{pm} = \frac{1}{T}\sum_{i=1}^{N} \sigma_i \int^T c_{p_i} \mathrm{d}T \quad (15)$$

A co-volume equation of state is used to relate pressure (p) to temperature (T).

$$p(V - b) = n\overline{\Re}T; \quad b = \sum_{i=1}^{N} n_i b_i \quad (16)$$

where, V is the volume, b is the covolume (see Ref. 19), n is the number of moles of gas, and $\overline{\Re}$ is the universal gas constant.

The system of Navier-Stokes equations (Eq. 1) is valid for the laminar flow of a viscous, Newtonian fluid. In reality, the flow will remain laminar up to a certain critical value of the Reynolds number, $\rho UL/\mu$, where U and L are representative values of the velocity and length. Above this critical value the flow becomes turbulent and is characterized by the appearance of fluctuations in all variables (U, p, ρ, T, etc.) around mean values. These fluctuations are statistical in nature and cannot be described in a deterministic way. The current model uses the Reynolds-averaging approximation along with algebraic turbulence models that relate fluid viscosity (μ) to other variables. See Reference 10 for further details.

Hydrocarbon mixtures such as $3CH_4 + 2O_2 + 10N_2$, pressurized to 50-100 atm, are commonly used for ram accelerator testing at ARL. A single test can incorporate several different gas mixtures in different sections of the accelerator tube, separated by diaphragms. Fuel rich mixtures are used with fuel equivalence ratios as high as 3. For these conditions a good understanding of CH_4/O_2 chemical kinetics, especially for $P \geq 10$ atm, is not available.[20] Accurate numerical simulation of hydrocarbon-based reacting flow is very demanding in terms of computational resources since the number of intermediate species and the number of kinetic steps are prohibitively large (i.e., ≥ 15). For high pressure systems the computational investment may not be justified due to uncertainty in measured reaction kinetics. Thus, global reaction mechanisms (neglecting intermediate steps) have been used,

$$\begin{aligned} CH_4 + 2O_2 &\Leftrightarrow CO + 2H_2 + 1.5O_2 \\ CO + .5O_2 &\Leftrightarrow CO_2 \\ 2H_2 + O_2 &\Leftrightarrow 2H_2O \end{aligned} \tag{17}$$

The reaction rate is defined using the Law of Mass Action and an Arrhenius expression for C, the specific reaction rate constant.

$$\begin{aligned} \omega &= C \prod_{i=1}^{N} \sigma_i^{\nu_i} \\ &= AT^{\alpha} \exp\left(\frac{-E_a}{\overline{\Re} T}\right) \sigma_{CH_4}^{a} \sigma_{O_2}^{b} \sigma_{CO}^{c} \sigma_{H_2}^{d} \sigma_{CO_2}^{e} \sigma_{H_2O}^{f} \end{aligned} \tag{18}$$

where AT^{α} is the collision frequency, the exponential term is the Boltzmann factor, E_a is the activation energy, and ν_i represents the stoichiometric coefficient. Exponents a thru f are chosen to fit results from flame experiments using large kinetic mechanisms.[21]

An Arrhenius reaction rate may not be correct for the high pressure flows, and much of the necessary reaction rate data for hydrocarbon fuels has not been measured above 10 atm.[20] In addition, the 3-step kinetics mechanism described above is based on the low pressure work of Westbrook[21] where the exponents are determined by matching experimentally measured flame speed. For the ARL full-bore ram accelerator, where mixture ignition is largely determined by shock-induced (i.e. reflected shocks from the accelerator tube wall) and viscous heating, the exponents a thru f were altered to the degree necessary in order to match accelerator tube wall pressures measured at the ARL (See References 8-11). It was found that ram accelerator performance was determined to a large degree by the reaction induction length (i.e. ignition delay time) which is a function of scale and mixture (as well as pressure). For the preliminary CFD computations described in the present paper, no attempt has been made to alter the kinetic steps or the reaction rate expression for the current sub-bore projectile with ignition via a step on the projectile. Experimental confirmation of mixture ignition (i.e. location, extent, and resulting tube wall pressure history) is required in order to validate the kinetics model used in the CFD code. However, the code has been extensively validated for high speed compressible gas dynamics.[14]

An additional issue that must be resolved is turbulence modeling. No attempt has been made in the present work (or that described by Nusca for the ARL projectile) to test the dependence of results on various models of turbulence. Nusca[10] has documented the effects of viscosity for the full-bore projectile and has achieved good results for that shape using algebraic turbulence models. No attempt has been made in the present applications to alter those models.

Results

Figure 1 shows the computational mesh for the projectile with a step located at the forebody-midbody junction, 1mm in height. The forebody is conical, 85.1 mm in length with cone half-angle 10 degs. The midbody is cylindrical, 30 mm in length and 32 mm in diameter. The afterbody is conical, 98.6 mm in length and with a half-angle of 3.5 degs. The grid was generated in zones so that sharp body junctions are accurately represented. Approximately 11000 grid cells cover the projectile and 600 grid cells reside in the wake (for the half-plane).

A gas mixture of $3CH_4+2O_2+10N_2$ was used for the CFD simulations described in this section. The mixture has a frozen speed of sound $a = 361$ m/s, ratio of specific heats $\gamma = 1.376$, and a Chapman-Jouget detonation velocity $V_{CJ} = 1450$ m/s. The initial pressure and tem-

perature of the mixture (before projectile injection) was 50 atm and 300 K, respectively.

Figure 2 shows the computed, frozen flow Mach number contours in grey-scale (bright white represents zero value, i.e. the projectile, while dark black represents a value of 6) for the projectile geometry displayed in Figure 1 (step height of 1 mm) and a freestream Mach number of 6 (V = 2175 m/s, V/V_{CJ} = 1.5). Important gas dynamic features are labeled. A bow shock extends from the projectile nose, while the step produces a normal shock and a small stagnation region. The merging of these shocks produces a curved "transmitted shock" that reflects from the accelerator tube wall, downstream of the projectile. Behind the transmitted shock, a contact surface is formed (not fully visible in Mach number contours) that separates flows of different density, temperature and velocity (i.e. flow having passed thru different shock waves). The recirculation zone behind the projectile (wake) is clearly subsonic. The results for a freestream Mach number of 10 (V= 3610 m/s, V/V_{CJ} = 2.5), displayed in Figure 3, show a dowstream bending of the bow and transmitted shocks as well as a strengthening (i.e. producing lower values of the downstream Mach number flow, greyer color) of the transmitted shock and step-generated normal shock.

Figures 4 and 5 show water (H_2O is a major product of the combustion) mass fraction contours in grey-scale (bright white representing the absence of water and dark black representing a mass fraction of 0.07 and above) for a freestream Mach number of 6. Figure 5 is closer view of the step region. Major combustion activity is predicted, using the current kinetics mechanism (Eq. 17 and 18), in the step-generated stagnation region (behind the normal shock) and continuing around the step and then over the projectile surface. This region of strong combustion and combustion products effectively resides between the contact surface and the wall. The projectile wake entrains combustion products. Note in Figure 5 that the production of H_2O is reduced somewhat (i.e. lighter grey colors) after expansion around the step, but is not extinguished. Figure 5 also shows a close view of the same step height but at a freestream Mach number of 10. The H_2O mass fraction distribution if more uniform and extends farther into the flowfield radially away from the projectile.

A close examination of the flow structures is instructive. The bow shock wave from the nose does not initiate chemical reaction. The detached normal shock wave ahead of the step initiates a very strong detonation wave which intersects the bow wave. At the intersection point a transmitted shock wave is directed towards the tube wall. The strength of this transmited wave depends on the flow Mach number and step height. The transmited shock weakens as its distance from the projectile increases, until reaching the tube wall and reflecting. The pressure behind this reflected shock wave is much lower in comparison to the pressure behind the reflected shock waves obtained in the Ram Accelerator. At the intersection point between the bow shock wave and the detonation wave, ahead of the step, a contact-combustion surface is also generated. This contact surface begins at the intersection point, which is a few step heights above the surface, and is propagated from there nearly parallel to the projectile surface towards the projectile base and further downstream, above the wake. The temperature of the flow with combustion products, behind the step, is about 5 to 8 times the freestream temperature, and the pressure is about 10 to 15 times the freestream pressure. This contact surface separates the hot flow of the combustion products, processed by the detonation ahead of the step, and the outer flow that passed through the transmited shock wave. Therefore, the contact surface acts as an aerodynamic cowling while the region between the contact surface and the projectile body surface acts in a similar way as the combustion chamber in a conventional ramjet engine. However, the "combustion chamber" is confined by the aerodynamic contact surface without the structural cowling of a conventional engine. The high pressure, high temperature combustion products in this aerodynamic "combustion chamber" can then be expanded over the projectile afterbody to produce thrust. This is the first demonstration, by a numerical simulation, of an aerodynamically confined combustion region external to the projectile, which can be utilized for thrust generation.

Figure 6 shows water mass fraction contours in the vicinity of the 0.5 and 1.5 mm steps for a freestream Mach number of 6. The H_2O mass fraction distributions are similar to those for the 1 mm step height but with the combustion region remaining close to the projectile body for the 0.5 mm step and extending farther into the flowfield for the 1.5 mm step. The larger step causes a more extensive stagnation region in front of the step (behind the normal shock).

As the step height is increased, the conditions and the position of the contact surface are effected, resulting in increased mass of combustion products at higher pressures and temperatures, but with an increase in drag due the increased step height. It is interesting to note that, at a certain Mach number, the height of the combustion layer above the projectile, normalized by step height, is nearly constant for the three step heights (0.5, 1, 1.5 mm) considered. This ratio is found to be about 5.5±0.2 at Mach 6. The observation that combustion can be initiated and sustained for the 0.5mm step is in

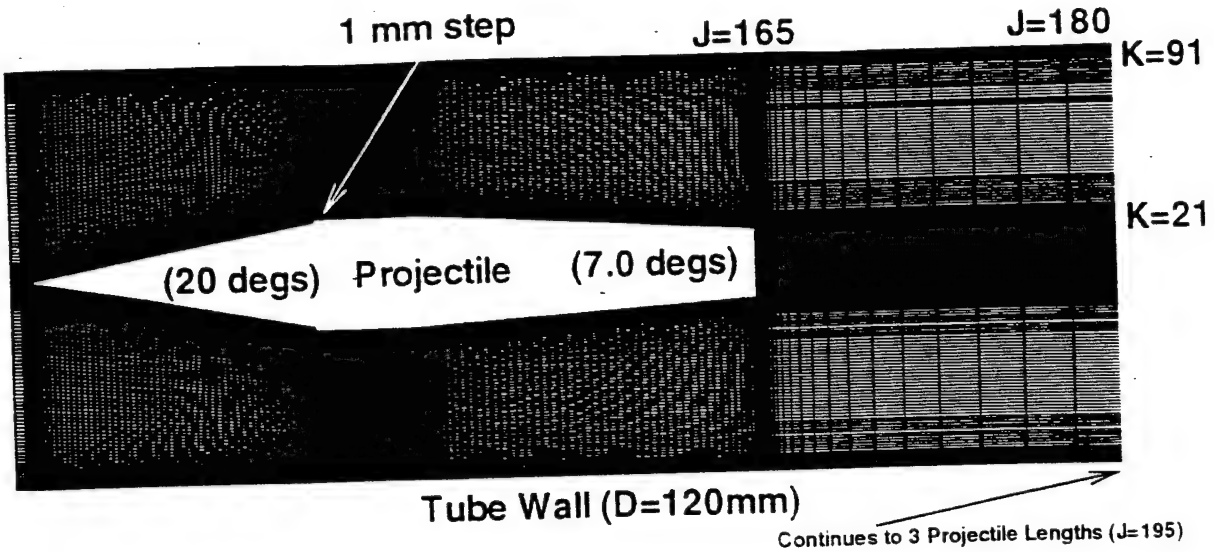

Figure 1: Computational Mesh. Projectile with 1 mm step.

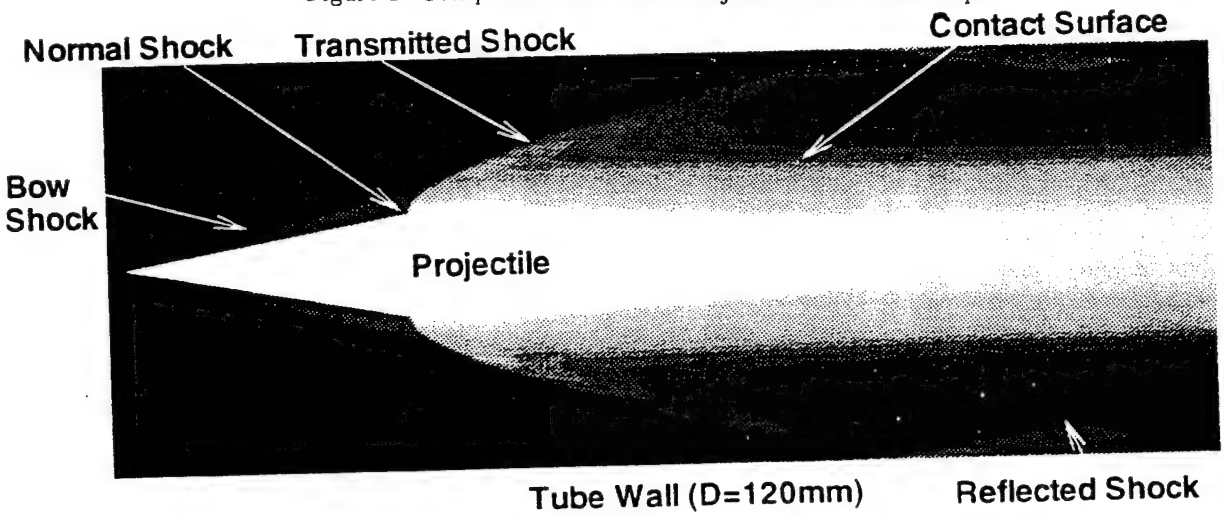

Figure 2: Non-Reacting Mach Number Contours (bright white = 0, dark black = 6). $M_\infty = 6$, 1 mm Step.

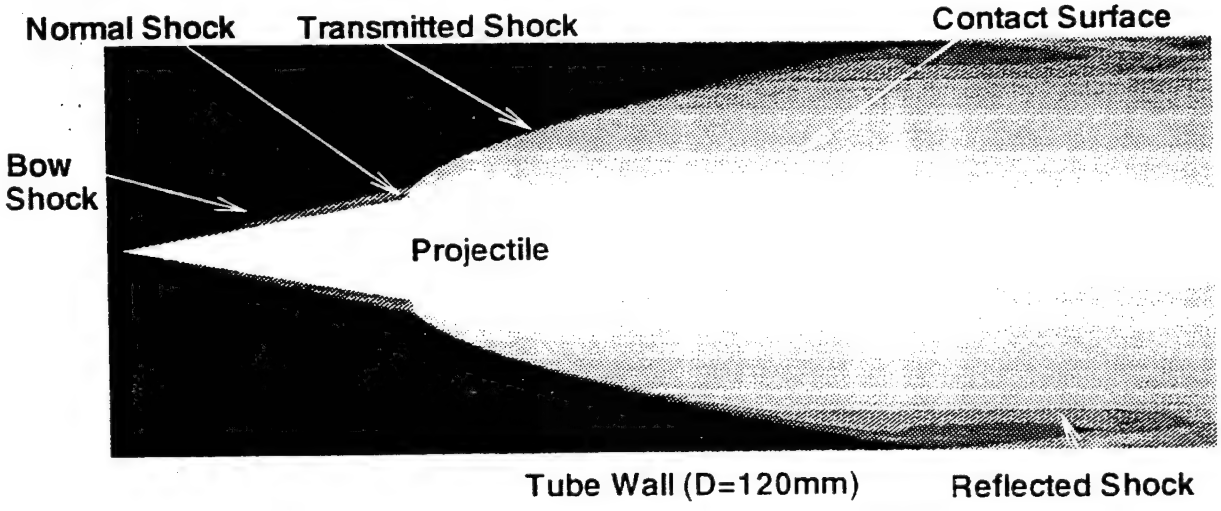

Figure 3: Non-Reacting Mach Number Contours (bright white = 0, dark black = 10). $M_\infty = 10$, 1 mm Step.

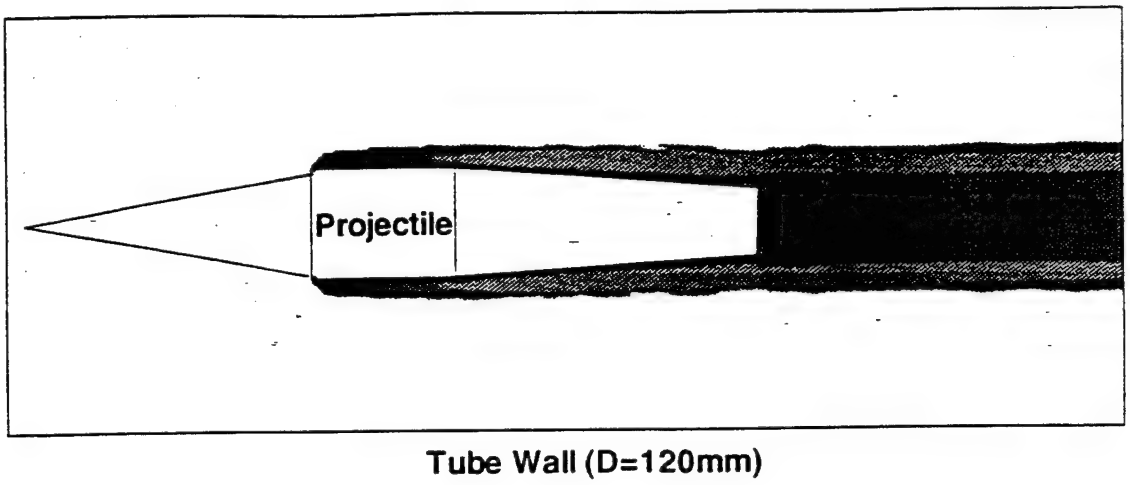

Figure 4: Reacting H_2O Contours (bright white = 0, dark black $\geq$ 0.07), $M_\infty = 6$, 1 mm Step.

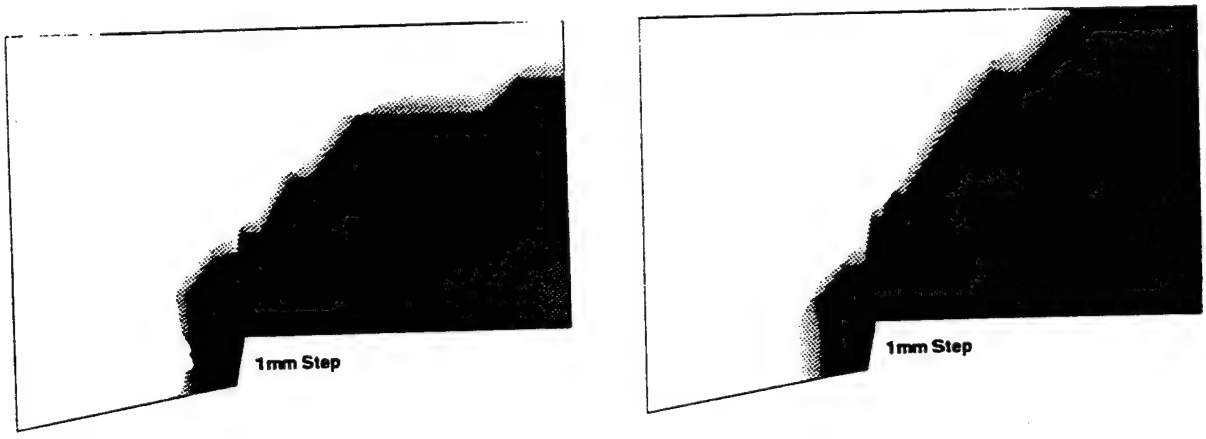

Figure 5: Reacting H_2O Contours (bright white = 0, dark black $\geq$ 0.07), $M_\infty = 6$ and 10, 1 mm Step.

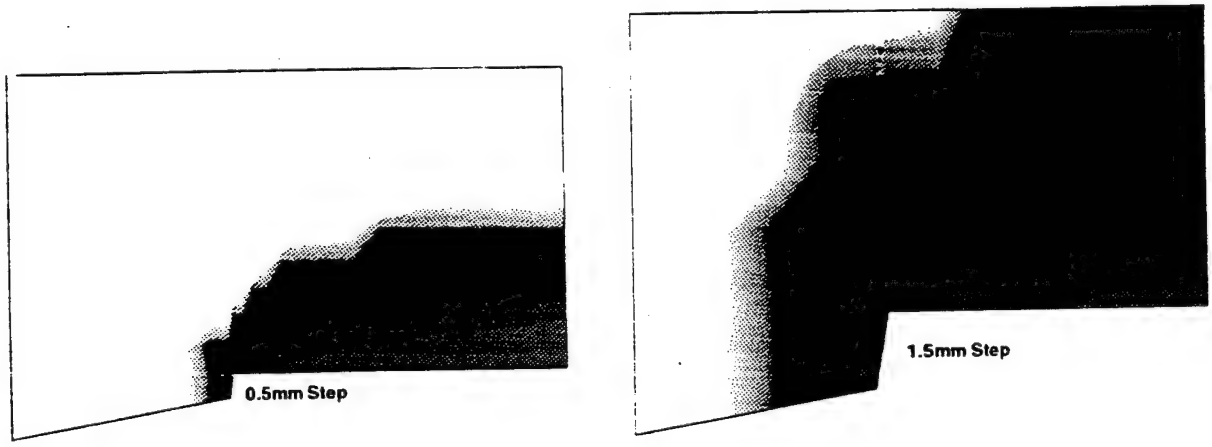

Figure 6: Reacting H_2O Contours (bright white = 0, dark black $\geq$ 0.07), $M_\infty = 6$, 0.5 and 1.5 mm Steps.

general agreement with the approximate analysis of Reference 4, where the minimum step height for establishing a combustion-detonation front ahead of a step for stoichiometric CH_4, O_2 mixture is evaluated. This step height is about 0.7 mm at Mach number 6 and pressure of one atmosphere. The agreement between the prediction of the approximate analysis[4] and the present numerical simulation is good.

The computed pressure distributions on the projectile surface were integrated to form a thrust coefficient, F/PA, where P is the initial mixture pressure (50 atm) and A is the cross sectional area of the accelerator tube (diameter of 120mm). For a freestream Mach number of 6 and the 1 mm step, the non-reacting flow yielded F/PA = -0.4 (i.e. drag), while the reacting flow yielded F/PA = 3.1. Projectiles with step heights of 0.5 mm and 1.5 mm, and non-reacting flow yielded F/PA = -0.3 and -0.9, respectively. With chemical reactions, these cases yielded F/PA = 3.4 and 3.06, respectively. The 0.5 mm step yields a smaller drag that must be cancelled by the thrust produced by combustion and thus yields a larger thrust coefficient. The 1.5 mm step yields a larger drag that must be cancelled by the thrust produced by combustion. Nevertheless the more extensive combustion for this step height yields a slightly smaller thrust coefficient.

The authors feel confident about the fidelity of the CFD code with regards to gas dynamic phenomena displayed in this section. Grid resolution studies should be conducted to ensure accurate representation of the wake region. The accuracy of the assumed chemical kinetics mechanism can be argued, especially at high pressure and fuel rich conditions. Further research and validation is warranted. The presented results should therefore be considered preliminary.

Conclusions

The present numerical simulation of the effects of a forward-facing step positioned on the body of a hypervelocity projectile, clearly indicates that the step will produce chemical reactions. The present calculations also show that these reactions do not extinguish after flow expansion around the step, and are sustained over the afterbody and the wake of the projectile, and can be used to produce thrust. However, since the projectile shape and combustion scales are different in the present External Propulsion case from those in the Ram Accelerator case, these results must be validated by an experimental firing of a projectile with a step. Such an experimental program is planned by the third author at the ARL, and should be reported in future publications.

It is shown that the interaction between the shockwave from the shallow nose cone and the detached shock-detonation wave from the forward-facing step, which is positioned on the shoulder of the projectile, results in confinement of a combustion layer on the external surface of the projectile afterbody and behind the blunt base. The high pressure, high temperature products of the combustion, which are confined to the external combustion layer, are then expanded into the rear and the base flow of the projectile and can be used to generate thrust. Thus, this layer, confined by the aerodynamic interactions, acts as an external combustion chamber. This is an excellant demonstration of the external propulsion method.

Acknowledgements

The participation of the first author in this research program was supported in part by the U.S. Government through the European Office of the U.S. Army Research Office, contract No. N6817194C9065. The second and third coauthors were supported by the U.S. Army Research Laboratory's Hybrid In-Bore Ram (HIRAM) program. The first, fourth, fifth, and sixth coauthors were supported by the NASA Hypersonics Center program, under grant NAGW3715, with Mr. Stephen Wander as techical monitor.

References

1. Rom, J., "Method and Apparatus for Launching a Projectile at Hypersonic Velocity," U.S. Patent 4,932,306, June 12, 1990.

2. Rom, J., and Kivity, Y., "Accelerating Projectiles up to 12 km/sec Utilizing the Continuous Detonation Propulsion Method," AIAA Paper No. 88-2969, 1988.

3. Rom, J., and Avital, G., "The Exernal Propulsion Accelerator: Scramjet Thrust Without Interaction with the Accelerator Barrel," AIAA Paper No. 92-3717, 1992.

4. Tivanov, G., and Rom, J., "Investigation of Hypersonic Flow of a Detonable Gas Mixture Ahead of a Forward Facing Step," AIAA Paper No. 93-0611, 1993.

5. Tivanov, G., and Rom, J., "Stability of Hypersonic Flow of a Detonable Gas Mixture in the Stagnation Region of a Blunt Body and a Forward Facing Step," Proceedings of the 33rd Israel Annual Conference of Aeronautics and Astronautics, Feb. 1993.

6. Tivanov, G., and Rom, J., "Analysis of the Stability Characteristics of Hypersonic Flow of a Detonable Gas Mixture in the Stagnation Region of a Blunt Body," AIAA Paper No. 93-1918, 1993.

7. Hertzberg, A., Bruckner, A.P., and Bogdanoff, D.W., "Ram Accelerator: A New Chemical Method for Accelerating Projectiles to Ultrahigh Velocities," AIAA Journal, Vol. 26, No. 2, 1988, pp. 195-203.

8. Nusca, M.J., "Numerical Simulation of Reacting Flow in a Thermally Choked Ram Accelerator Projectile Launch System," AIAA-91-2490, Proceedings of the 27th AIAA/SAE/ASME/ASEE Joint Propulsion Conference, Sacramento, CA, 24-26 June 1991.

9. Kruczynski, D.L., and Nusca, M.J., "Experimental and Computational Investigation of Scaling Phenomena in a Large Scale Ram Accelerator," AIAA-92-3245, Proceedings of the 28th AIAA/SAE/ASME/ASEE Joint Propulsion Conference, Nashville, TN, 6-8 July 1992.

10. Nusca, M.J., "Numerical Simulation of Fluid Dynamics with Finite-Rate and Equilibrium Combustion Kinetics for the 120-MM Ram Accelerator," AIAA-93-2182, Proceedings of the 29th AIAA/SAE/ASME/ASEE Joint Propulsion Conference, Monterey, CA, 29-30 June 1993.

11. Nusca, M.J., "Reacting Flow Simulation for a Large Scale Ram Accelerator," AIAA-94-2963, Proceedings of the 30th AIAA Joint Propulsion Conference, Indianapolis, IN, 27-29 June 1994.

12. Chakravarthy, S.R., Szema, K.Y., Goldberg, U.C., Gorski, J.J., and Osher, S., "Application of a New Class of High Accuracy TVD Schemes to the Navier-Stokes Equations," AIAA-85-0165, Proceedings of the AIAA 23rd Aerospace Sciences Meeting, Jan. 14-17, 1985, Reno, NV.

13. Palaniswamy, S., and Chakravarthy, S.R., "Finite Rate Chemistry for USA Series Codes: Formulation and Applications," AIAA-89-0200, Proceedings of the 27th AIAA Aerospace Sciences Meeting, Jan. 9-12, 1989, Reno, NV.

14. Palaniswamy, S., Ota, D.K., and Chakravarthy, S.R., "Some Reacting-Flow Validation Results for USA-Series Codes," AIAA-91-0583, Proceedings of the 29th AIAA Aerospace Sciences Meeting, Jan. 7-10, 1991, Reno, NV.

15. Roe, P.L., "Approximate Riemann Solvers, Parameter Vectors, and Difference Schemes," Journal of Computational Physics, Volume 43, 1981, pp. 357-372.

16. Stull, D.R., and Prophet, H., "JANNAF Thermochemical Tables," 2nd ed., National Bureau of Standards, NSRDS-Rept. 37, June 1971.

17. Wilke, C.R., "A Viscosity Equation for Gas Mixtures," Journal of Chemistry and Physics, Vol. 18, No. 4, pp. 517-519, 1950.

18. Drummond, J.P., Rogers, C., and Hussaini, M.Y., "A Numerical Model for Supersonic Reacting Mixing Layer," Computer Methods in Applied Mechanics and Engineering, Vol. 64, 1987.

19. Hirschfelder, J.O., Curtiss, C.F., and Bird, R., Molecular Theory of Gases and Liquids, John Wiley & Sons, 1954.

20. Anderson, W.R., and Kotlar, A.J., "Detailed Modeling of CH_4/O_2 Combustion for Hybrid In-Bore Ram Propulsion (HIRAM) Application," 28th JANNAF Combustion Meeting, Brooks Air Force Base, San Antonio, Texas, Oct. 28 - Nov. 1, 1991.

21. Westbrook, C.K., and Dryer, F.L., "Simplified Reaction Mechanisms for the Oxidation of Hydrocarbon Fuels in Flames," Combustion and Science Technology, Vol. 27, 1981, pp 31-43.

ANNEX 3

CNF 372

Stability of Hypersonic Reacting Stagnation Flow of a Detonable Gas Mixture by Dynamical Systems Analysis

at? O.K

GENADI TIVANOV* and JOSEF ROM†
Technion—Israel Institute of Technology, Haifa 32000, Israel

The stability characteristics of the reacting hypersonic flow of the fuel/oxidizer mixture in the stagnation region of a blunt body are studied. The conditions for oscillations of the combustion front are assumed to be determined mainly by the flow conditions at the stagnation region. The density at the stagnation region is assumed to be constant at hypersonic flow conditions. By assuming a simplified flow model, the time dependent flow equations, including the heat addition due to the chemical reactions, are reduced to a second-order nonlinear differential equation for the instantaneous temperature. The solutions are analyzed assuming a one-step chemical reaction with zero-order and first-order processes using dynamical systems methods. These methods are used to determine the stability boundaries in terms of the flow and chemical reaction parameters. It is shown that the zero-order reaction has nonperiodic solutions that may lead to explosion whereas the first-order and higher-order reactions may have periodic solutions indicating oscillations. The zero-order analysis also reaffirms the requirements for a minimum size blunt body for the establishment of a detonation (in agreement with classical detonation theory) and the first-order analysis indicates a minimum body size for establishment of oscillations. The oscillation frequencies are calculated using the small perturbation approximation for the temperature oscillations. These frequencies are compared with results from published data on spheres and hemisphere cylindrical bodies fired into hydrogen–oxygen and acetylene oxygen mixtures. Very good agreement is found between the measured and calculated results.

NOMENCLATURE

a	speed of sound
A_n	preexponential factor for chemical reaction of order n
b	$\frac{\varepsilon}{2}\left[\ln\frac{4}{3\varepsilon}+\frac{\varepsilon}{2}\left(\ln\frac{4}{3\varepsilon}+1\right)\right]$
B	$\left(\frac{RT^{*2}}{E}\right)\left(\frac{c_v}{Q}\right)$
c_p	specific heat at constant pressure
c_v	specific heat at constant volume
D	detonation velocity
Dam	Damkohler number $= \frac{t^* F u_\infty}{H}$
e	natural log base
E	activation energy
f	frequency
F	defined in Eq. 10
H	step height; body radius
M	Mach number
n	order of chemical reaction
p	pressure
Q	heat of reaction
R	gas constant
R_{ch}	chemical reaction rate
R_s	distance between detached shock wave and body or step face
S	defined by Eq. 23
t	time
t^*	$\frac{c_v \mu T^* \exp\frac{1}{\mu}}{Q A_n \bar{\rho}^{n-1}}$
T	temperature; period
T^*	reference temperature
u	velocity component in the x-direction
u_∞	free stream velocity
v	velocity component in the y-direction
x, y	Cartesian coordinates

Greek Symbols

α	$\frac{(2-\gamma)F u_\infty t^*}{H} = (2-\gamma)\mathrm{Dam}$
β	mass fraction of main reaction component
γ	specific heat ratio
ε	ρ_∞/ρ_s; infinitesimal value
κ_0, κ_1	constants, $0 < \kappa_i < 1$
μ	$RT^*/E = p^*/\bar{\rho}E$
η	$1-\beta$
ρ	density

* Research Fellow, Faculty of Aerospace Engineering
† Professor, Lady Davis Chair, Faculty of Aerospace Engineering, Visiting Professor, Department of Mechanical Engineering, University of Maryland. Fellow AIAA

COMBUSTION AND FLAME 00: 000–000 (1995)

Published by Elsevier Science Inc.

0010-2180/95/$9.50
SSDI 0010-2180(95)00097-P

$\bar{\rho}$ average density

θ $\dfrac{E(T - T^*)}{RT^{*2}}$

τ $\dfrac{t}{t^*}$

INTRODUCTION

Under certain flow conditions, oscillations of the combustion front occur on blunt bodies fired into detonable mixtures at hypersonic speeds [1, 2]. The conditions for the stability of the chemically reacting hypersonic flow, the establishment of a steady detonation or oscillatory reaction, are very important because blunt bodies are used for the generation and stabilization of reaction fronts in supersonic and hypersonic propulsion systems such as the Oblique Detonation Wave Engine (ODWE) [3, 4] and the External Propulsion Accelerator [5, 6]. Studies of the development of combustion and detonation fronts on blunt bodies in supersonic and hypersonic flows were presented in Refs. 7–11. Although the oscillation of the combustion front is discussed in these studies, the problem is not analyzed in detail. A wave interaction model that explains the mechanism for the establishment of oscillations near the stagnation region of a blunt body was presented by McVey and Toong [12]. In the last few years investigations utilizing numerical methods to calculate the details of the time dependent flow structure near the stagnation region of a blunt body at hypersonic speeds including the effects of chemical reactions were presented [13–15]. These studies used numerical computations to map the instantaneous wave structure near the stagnation region of a blunt body and to infer the oscillation frequencies for these conditions. A numerical parametric study of the effects of varying body diameter is presented in Ref. 16, showing that the oscillations are not only a function of the projectile velocity in relation to the Chapman–Jouguet detonation velocity, but also depend on the projectile diameter as well as on the induction time, reaction rate constant, activation energy and heat release.

It can be seen both in the experimental flow photographs [1, 2] as well as in the results of the numerical calculations [13–16] that the detached shock wave remains steady and is only slightly affected by the oscillating combustion front in the stagnation region. Therefore, the oscillating combustion is bounded on one side by the solid body surface and on the other side by the steady structure of the detached shock wave. In effect, the combustion front is oscillating like a membrane in a region bounded by the solid body surface on one side and the stationary detached shock wave surface on the other side. This results in a "whistle" effect of the vibrating combustion front. This oscillation model suggests the application of the dynamical system analysis for the study of combustion oscillations in hypersonic stagnation flow and provides the motivation and is the justification for the present analysis.

The oscillations are observed to occur at projectile velocities close to the detonation velocity. When the projectile velocity is increased considerably above the detonation speed the combustion front merges into the shock to form a detonation wave and no oscillations are expected.

In order to investigate the stability of the hypersonic flow of the fuel/oxidizer mixture in the stagnation region of a blunt-nosed body, the time dependent flow equations including the effects of chemical reactions are studied. The approximations of inviscid flow and constant density in the stagnation region are used. These approximations are suitable for hypersonic flows at high Reynolds numbers. For example, in the External Propulsion Accelerator the initial pressures are in the range of 20 to 200 atm. resulting in very high Reynolds numbers and very thin boundary layers. The fact that the density in the stagnation region of a blunt body in hypersonic flow is roughly constant is discussed by Hayes and Probstein [17] and more recently in Ref. 18.

Studies of the critical conditions in chemically reacting systems by the examination of the equations for the instantaneous temperature (from the energy equation) and the species consumption rate (from the chemical reaction equation) are presented in Refs. 19–22. It is shown that a nonlinear second order differential equation describes the instantaneous temperature field. This nonlinear differential equation can be studied using the theory of

nonlinear oscillators presented by Andronov, et al. [23] and the developments of the mathematical theory for these equations is presented in Refs. 24–26. This dynamical systems analysis can be used to determine the conditions for stability of the solutions and their periodic behavior.

THE EQUATIONS FOR THE STAGNATION REGION FLOW WITH CHEMICAL REACTIONS

The time-dependent energy equation for the flow of the fuel/oxidizer mixture including the heat addition due to the chemical reactions (neglecting effects of heat conduction and mass diffusion) is

$$c_v \rho \left(\frac{\partial T}{\partial t} + u\frac{\partial T}{\partial x} + v\frac{\partial T}{\partial y} \right) = u\frac{\partial p}{\partial x} + v\frac{\partial p}{\partial y} + Q\beta^n A_n \exp\left(-\frac{E}{RT} \right), \tag{1}$$

where the chemical reaction rate is expressed by the Arrhenius rate equation

$$-\frac{d\beta}{dt} = -\frac{\partial \beta}{\partial t} - u\frac{\partial \beta}{\partial x} - v\frac{\partial \beta}{\partial y} = \beta^n A_n \exp\left(-\frac{E}{RT} \right). \tag{2}$$

The initial and boundary conditions on the temperatures are: at $t = 0$, $T(0) = T_0$ and on the downstream side of the shock wave T (shock wave) $= T_s$ while the projectile body temperature is T_w. Assuming a one-step reaction, the main component of reaction varies during the reaction from the initial value $\beta = \beta_0$ ($t = 0$) to the final value $\beta = \beta_{end}$. Usually $\beta_0 = 1$ and for complete reaction $\beta_{end} \to 0$.

For hypersonic flow it is justified to assume, as a first approximation, that the density in the stagnation region behind the detached shock wave is constant [17, 18], represented by an average density $\bar{\rho}$. In this case, using the ideal gas equation $p = \bar{\rho}RT$, in Eq. 1, gives

$$\frac{\partial T}{\partial t} = -(2-\gamma)\left(u\frac{\partial T}{\partial x} + v\frac{\partial T}{\partial y} \right) + \frac{QA_n \beta^n}{c_v \bar{\rho}} \exp\left(-\frac{E}{RT} \right). \tag{3}$$

In order to accentuate the dynamics of the reactive flow system, we assume a simplified model for the flow in the stagnation region. It is assumed that near the stagnation point of the blunt body the temperature and species density vary linearly, so the temperature gradients and the species density gradients in the x and the y directions can be expressed by the approximate linear relations. For these relations we shall assume an effective temperature, T^*, and an effective mass fraction of the main reaction component, β^*. In this case these gradients are:

$$\frac{\partial T}{\partial x} \cong \frac{T - T^*}{R_s}, \qquad \frac{\partial T}{\partial y} \cong -\frac{T - T^*}{H}, \tag{4a}$$

$$\frac{\partial \beta}{\partial x} \cong \frac{\beta - \beta^*}{R_s}, \qquad \frac{\partial \beta}{\partial y} \cong -\frac{\beta - \beta^*}{H}. \tag{4b}$$

Introducing these values into the equations for the temperature and the species concentrations, Eqs. 2 and 3, gives

$$\frac{dT}{dt} \cong \frac{QA_n \beta^n}{c_v \bar{\rho}} \exp\left(-\frac{E}{RT} \right) - (2-\gamma)\left(\frac{u}{R_s} - \frac{v}{H} \right)(T - T^*) \tag{5a}$$

and

$$\frac{d\beta}{dt} \cong -A_n \beta^n \exp\left(-\frac{E}{RT} \right) - \left(\frac{u}{R_s} - \frac{v}{H} \right)(\beta - \beta^*). \tag{5b}$$

The standoff distance of the detached shock wave, R_s, can be estimated from the solution

for the hypersonic flow over a blunt flat-nosed body [17],

$$R_s = \frac{H}{1-b}, \tag{6}$$

where $b = \frac{\varepsilon}{2}\left[\ln\frac{4}{3\varepsilon} + \frac{\varepsilon}{2}\left(\ln\frac{4}{3\varepsilon} + 1\right)\right]$

and $\varepsilon = \frac{\rho_\infty}{\rho_s}$.

From Ref. 17 the velocity components u and v near the stagnation point are

$$u = u_\infty\sqrt{\frac{8\varepsilon}{3}}\left[1 + \frac{y\left(1-\frac{8\varepsilon}{3}\right)}{\varepsilon R_s\sqrt{\frac{8\varepsilon}{3}}}\right]\frac{x_1}{R_s}, \tag{7}$$

$$v = -u_\infty\varepsilon\left(\frac{x}{x_1}\right)^2, \tag{8}$$

and

$$\frac{x}{x_1} = \sqrt{\frac{3\varepsilon}{1-3\varepsilon}}\sinh\left[\frac{y\sqrt{1-3\varepsilon}}{\varepsilon R_s}\right]. \tag{9}$$

The quantity x_i is the x coordinate of the point being investigated, and the quantity x is the coordinate at entry into the shock layer of the streamline passing through the point being investigated [17]. Near the stagnation point, let $y = \kappa_0 H$ and $x_1 = \kappa_1 R_s$ where the parameters κ_0 and κ_1 range between 0 and 1. Using these expressions for u, v, x, and y (Eqs. 6–9), it is now possible to evaluate

$$\frac{u}{R_s} - \frac{v}{H} = \frac{u_\infty F}{H},$$

where

$$F = (1-b)\sqrt{\frac{8}{3\varepsilon}}\left[\kappa_1 + \frac{\kappa_0\kappa_1\left(1-\frac{8\varepsilon}{3}\right)}{\varepsilon(1-b)\sqrt{\frac{8\varepsilon}{3}}}\right] + \varepsilon\sqrt{\frac{3\varepsilon}{1-3\varepsilon}}\sinh\left[\frac{\kappa_0\sqrt{1-3\varepsilon}}{\varepsilon(1-b)}\right]. \tag{10}$$

Introducing the following dimensionless variables:

$$\theta = \frac{E}{RT^{*2}}(T - T^*), \qquad \mu = \frac{RT^*}{E},$$

$$\beta = \frac{\rho_i}{\rho}, \qquad \tau = \frac{t}{t^*},$$

$$B = \frac{\mu c_v T^*}{Q}, \qquad \alpha = \frac{(2-\gamma)Fu_\infty t^*}{H},$$

$$t^* = \frac{\mu c_v T^* \exp\frac{1}{\mu}}{QA_n\bar{\rho}^{n-1}},$$

and the Damkohler number,

$$\mathrm{Dam} = \frac{t^* u_\infty F}{H} = \frac{\alpha}{2-\gamma},$$

and using these variables in Eqs. 5a and 5b gives

$$\frac{d\theta}{d\tau} = \beta^n \exp\left(\frac{\theta}{1+\mu\theta}\right) - (2-\gamma)\mathrm{Dam}\,\theta, \tag{11a}$$

$$\frac{d\beta}{d\tau} = -B\beta^n \exp\frac{\theta}{1+\mu\theta} - \mathrm{Dam}(\beta - \beta^*) \tag{11b}$$

The phase plane equation is

$$\frac{d\theta}{d\beta} = \frac{\beta^n \exp\left(\frac{\theta}{1+\mu\theta}\right) - (2-\gamma)\mathrm{Dam}\,\theta}{-B\beta^n \exp\left(\frac{\theta}{1+\mu\theta}\right) - \mathrm{Dam}(\beta - \beta^*)}. \tag{12}$$

Equations 11a and 11b can be combined to eliminate β and provide a single equation for θ. At the stagnation region with uniform reactive mixture, we can assume that $\partial\beta/\partial x$ and $\partial\beta/\partial y \ll 1$, therefore, the value of $(\beta - \beta^*) \to 0$, and then the combined dynamic reaction equation is

$$\ddot{\theta} + \alpha\dot{\theta} - \frac{\dot{\theta}(\dot{\theta} + \alpha\theta)}{(1+\mu\theta)^2} + nB(\dot{\theta} + \alpha\theta)^{(2n-1)/n}\exp\left(\frac{\theta}{1+\mu\theta}\right)^{1/n} = 0, \tag{13}$$

where the dot represents differentiation with respect to τ and the n represents the order of the chemical reaction.

The dynamic reaction equation, Eq. 13, is a second-order nonlinear differential equation of the form

$$\ddot{\theta} + f(\theta, \dot{\theta})\dot{\theta} + g(\theta) = 0. \quad (14)$$

The terms $f(\theta, \dot{\theta})$ and $g(\theta)$ can be viewed as representing "damping" and a "restoring force" effects, respectively. It should be noted that these terms are largely determined by the body size parameter $\alpha = (2 - \gamma)Fu_\infty t^*/H$ (which is proportional to the Damkohler number) and by the mixture chemical and physical properties represented by B and μ. This analogy is demonstrated by the "energy" formulation presented in Appendix A.

This formulation of the dynamic reaction equation developed here for the hypersonic stagnation flow is analogous to the mechanical and electrical vibration equations. Therefore, the large mathematical literature and the methods developed for the analysis of Dynamical systems can be applied to this reacting system. The solution of this equation and the singularities which appear in these solutions can be used to define the stability boundaries of the reactions, the possibility of divergence leading to explosion or existence of periodic solutions indicating oscillations. In this analysis we shall use the solutions of similar differential equations presented by Andronov et al. [23], and in Refs. 24–26 and 30–34.

Some indications of the properties of these equations can be obtained from numerical solutions. The calculation of the temperature parameter, θ, variation as a function of time parameter, τ, for the case of $\alpha = 0.1$ and for chemical reactions of the order $n = 0, 1, 2$ and autocatalytic are presented in Fig. 1. The case of zero-order reaction shows fast increasing temperature leading to explosion. The effect of increasing values of α on the temperature rise is shown in Fig. 2. For small α the temperature rises fast leading to explosion. As α increases the temperature rise decreases. Since this parameter α is inversely proportional to the body size H, it is seen that above a certain body size the temperature of reaction diverges

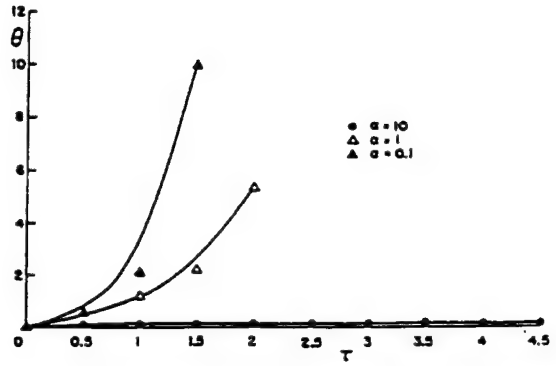

Fig. 1. The variation of θ as a function of τ for various chemical reactions, with $n = 0, 1, 2$ and autocatalytic.

and for small body size the temperature size is limited. This indicates that there is a minimum body size required to generate explosive reaction, which is in agreement with both experimental observations [27] and analysis [18].

Solutions for the Zero-Order Chemical Reaction, $n = 0$

In the case of zero-order reaction Eqs. 11a and 11b are

$$\frac{d\theta}{d\tau} = \exp\left(\frac{\theta}{1 + \mu\theta}\right) - (2 - \gamma)\text{Dam}\ \theta \quad (15a)$$

$$\frac{d\beta}{d\tau} = -B \exp\left(\frac{\theta}{1 + \mu\theta}\right) - \text{Dam}(\beta - \beta^*) \quad (15b)$$

For this case there is decoupling between the equations, so that the temperature variation can be obtained from Eq. 15a as shown in Figs.

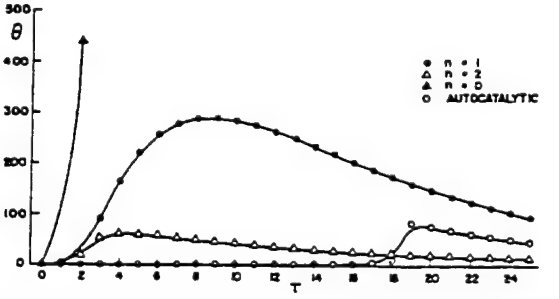

Fig. 2. The variation of θ as a function of τ for zero-order reaction for various values of α.

1 and 2. It is of interest to examine the stationary states in the θ–α plane, using the relation $\alpha = \dfrac{\exp\dfrac{\theta}{1+\mu\theta}}{\theta}$, obtained from Eq. 15a. The diagram of the stationary states is shown in Fig. 3 for cases where $\mu < 1/4$. There are two extreme points, A and B, corresponding to values of (θ_1^*, α_1^*) for A and (θ_2^*, α_2^*) for B, as noted on the graph, where

$$\theta_{1,2}^* = \frac{(1-2\mu) \pm \sqrt{1-4\mu}}{2\mu^2} \quad \text{and}$$

$$\alpha_{1,2}^* = \frac{\exp\left(\dfrac{\theta_{1,2}^*}{1+\mu\theta_{1,2}^*}\right)}{\theta_{1,2}^*}.$$

The low-temperature reaction following the curve up to point A, where $\theta < \theta_1^*$, represents the slow low temperature combustion process. The region of operation between A and B, where $\theta_1^* < \theta < \theta_2^*$, represents a metastable state and the high temperature region of the curve above point B, where $\theta > \theta_2^*$, may be interpreted as an explosive process. In fact, this is a bifurcation $\theta(\alpha)$ where α_1^*, α_2^* are the bifurcation values when the "jump" conditions are realized. This is a duck trajectory with unstable state within θ_1^*, θ_2^*, and stable states when $\alpha < \alpha_2^*$; $\theta < \theta_1^*$, and when $\alpha > \alpha_1^*$; $\theta > \theta_2^*$, where slow combustion or explosive regimes, respectively, exist.

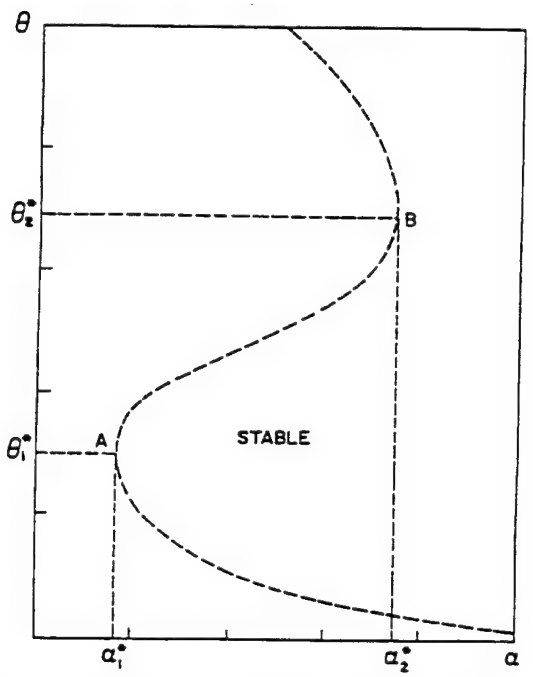

Fig. 3. Diagram of the stationary state in the θ–α plane for the zero-order reaction.

These extreme points can be used to define the minimum body size. Since α is inversely proportional to the body radius the maximum value of α_2^* defines a minimum value of $H_{\min}$. Therefore, to obtain stable detonation we must have

$$H \geq H_{\min} = \frac{(2-\gamma)Fu_\infty t^*}{\alpha_2^*}. \tag{16}$$

This result is in good agreement with the minimum body size estimated in Ref. 18.

Solutions of the First-Order Reaction Equations, $n = 1$

Using the formulation of the two first-order equations for the time-dependent temperature and species concentration parameters, Eqs. 11a and 11b, these become for the $n = 1$ case:

$$\frac{d\theta}{d\tau} = \beta \exp\left(\frac{\theta}{1+\mu\theta}\right) - (2-\gamma)\mathrm{Dam}\,\theta, \tag{17a}$$

$$\frac{d\beta}{d\tau} = -B\beta \exp\left(\frac{\theta}{1+\mu\theta}\right) - \mathrm{Dam}(\beta - \beta^*). \tag{17b}$$

In the stagnation region, for the case of uniform combustion, we can assume $\mathrm{Dam}(\beta - \beta^*) = 0$. Then, the diagram of the null-cline curves in the phase plane $\theta - \beta$ is shown in Fig. 4 for various values of α. These curves have the duck shape with two extreme points, and an example of these points on one curve at $(\theta_1^{**}, \beta_2^{**})$ and at $(\theta_2^{**}, \beta_1^{**})$ is indicated on Fig. 4. These curves indicate three regions of stability; θ lower than θ_1^{**} region of stable low temperature; θ between θ_1^{**} and θ_2^{**} a metastable state and for θ above θ_2^{**} explosive regime.

The shape of the null-cline curve is used as a guide for the construction of the phase dia-

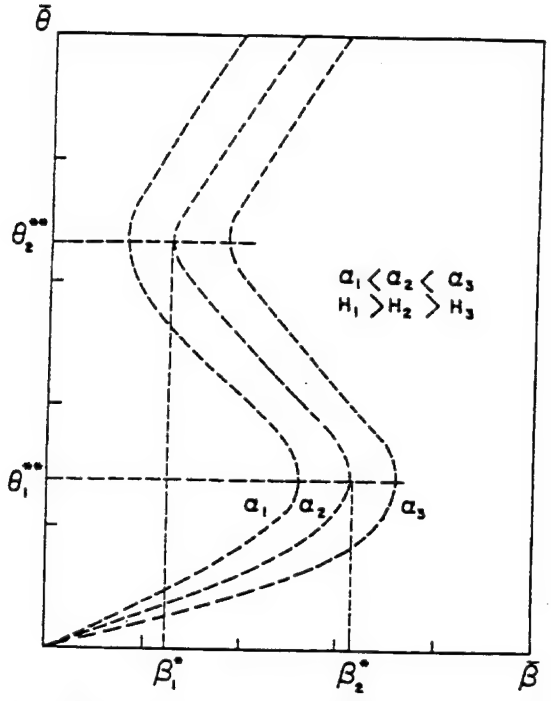

Fig. 4. Diagram of the null-cline in the phase plane θ–β for the first-order reaction.

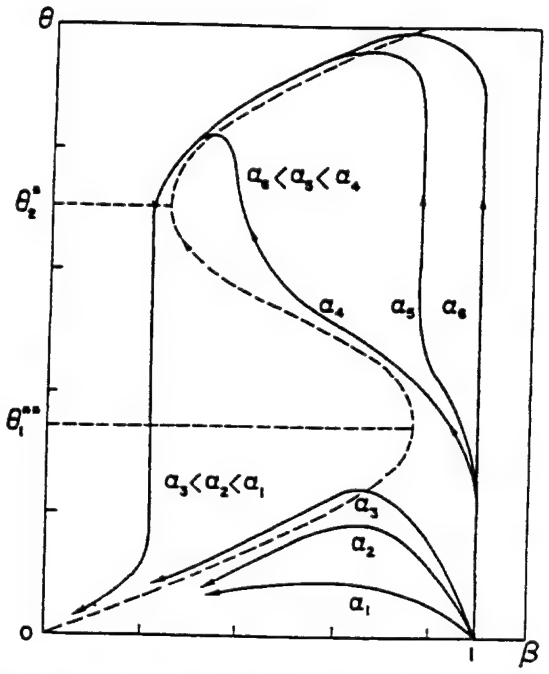

Fig. 5. Phase diagram of the solutions in the θ–β plane for various α for first-order reaction.

gram for a range of values for α, as shown in Fig. 5. Starting from the point $\theta = 0$; $\beta = 1$, in the cases of large α (small H) the solutions follow the stable low temperature reaction region. For moderate values of α, the solutions follow the metastable region (α_4 in Fig. 5). For small α (α_6 in Fig. 5), the temperature jumps to the explosive reaction region.

The second-order equation, Eq. 14, is used for the investigation of the possibility of periodic solutions. In the case of zero-order reaction, $n = 0$ and $g(\theta) = 0$, there can be no periodic solutions. For the first-order reaction case, $n = 1$ in Eq. 14, the expressions for $f(\theta, \dot{\theta})$ and $g(\theta)$ are, respectively,

$$f(\theta, \dot{\theta}) = \alpha - \frac{\alpha\theta - \dot{\theta}}{(1 + \mu\theta)^2} + B \exp\left(\frac{\theta}{1 + \mu\theta}\right), \tag{18a}$$

$$g(\theta) = B\alpha\theta \exp\left(\frac{\theta}{1 + \mu\theta}\right). \tag{18b}$$

Since $\theta g(\theta) > 0$ for $\theta > 0$, the point $[\theta(t = 0), \dot{\theta}(t = 0)]$ is a singular point. This singular point is inside the closed trajectories of the energy curves, as shown in Ref. 25, where the energy curves are

$$w(\theta, \dot{\theta}) = G(\theta) + \frac{1}{2}\dot{\theta}^2 = \text{const},$$

where

$$\int_0^{\infty} g(\theta)\, d\theta = G(\theta). \tag{19}$$

Since $g(-\theta) \neq -g(\theta)$, these paths are not symmetrical trajectories near the initial point $[\theta(t = 0), \dot{\theta}(t = 0)]$. The conditions defined by Eq. 19 are sufficient to obtain oscillations of θ and $\dot{\theta}$ or to obtain monotonic decay of the function $\theta(t)$, so that $\lim \theta(t)_{t \to 0} = \lim \dot{\theta}(t)_{t \to 0} = 0$. It is expected that the periodic solutions of Eq. 14, for $n = 1$, will be cycles located around the origin of coordinates. The existence of a unique solution of this equation and its periodic behavior are discussed in Refs. 25, 26, and 30–34. Since these analyses present general theorems, their application to the present case requires specific considerations which are presented in Ap-

pendix B. When $\alpha = 0$, the trajectories are open, indicating nonperiodic solution and possible divergence to explosion as in the zero-order case. As α increases the trajectories become closed indicating a limit cycle with decreasing amplitude, as shown in Fig. 6 for various initial conditions. As discussed in Ref. 24, the existence of a limit cycle indicates that periodic solutions are possible. These periodic solutions can be studied from the characteristics of the singular points of the system. The oscillatory solutions and their frequencies can be also studied using perturbation analysis.

EVALUATION OF OSCILLATION FREQUENCIES USING PERTURBATION ANALYSIS FOR THE FIRST-ORDER REACTION, $n = 1$

We apply small perturbation analysis to the instantaneous temperature and reacting species equations for the first-order reactions, Eqs. 17a and 17b, respectively, by assuming small disturbances imposed on the average flow parameters, $\theta = \bar{\theta} + \alpha'$, $\beta = \bar{\beta} + \beta'$.

In the stagnation flow, for first-order reaction, $n = 1$, and $\mathrm{Dam}(\beta - \beta^*) = 0$, $\bar{\theta}$ and $\bar{\beta}$ are evaluated using Eqs. 17a and 17b to obtain

$$\bar{\beta} \exp\left(\frac{\bar{\theta}}{1 + \mu\bar{\theta}}\right) - (2 - \gamma)\mathrm{Dam}\,\bar{\theta} = 0, \quad (20a)$$

$$B\bar{\beta} \exp\left(\frac{\bar{\theta}}{1 + \mu\bar{\theta}}\right) = 0. \quad (20b)$$

By introducing the perturbation values into Eqs. 17a and 17b, the following linearized equations are obtained:

$$\frac{d\theta'}{d\tau} = \left[\frac{\bar{\beta} \exp\left(\dfrac{\bar{\theta}}{1 + \mu\bar{\theta}}\right)}{1 + \mu\bar{\theta}} - \alpha\right]\theta' + \exp\left(\frac{\bar{\theta}}{1 + \mu\bar{\theta}}\right)\beta', \quad (21a)$$

$$\frac{d\beta'}{d\tau} = -\frac{B\bar{\beta} \exp\dfrac{\bar{\theta}}{1 + \mu\bar{\theta}}}{1 + \mu\bar{\theta}}\theta' - \left[B \exp\left(\frac{\bar{\theta}}{1 + \mu\bar{\theta}}\right)\right]\beta'. \quad (21b)$$

This linearization requires $\beta\theta' \ll 1$, $\mu\theta' \ll 1$, and

$$\exp\left(\frac{\theta'}{1 + \mu\bar{\theta}}\right) \equiv 1 + \frac{\theta'}{1 + \mu\bar{\theta}}.$$

The stability of the solutions of these equations and their oscillation frequencies can be studied by the solution of the characteristic equation for the eigenvalues,

$$\lambda^2 + \left[\left(B - \frac{\bar{\beta}}{1 + \mu\bar{\theta}}\right)\exp\left(\frac{\bar{\theta}}{1 + \mu\bar{\theta}}\right)\right]\lambda + B\alpha \exp\left(\frac{\bar{\theta}}{1 + \mu\bar{\theta}}\right) = 0. \quad (22)$$

It is well known that the stability and frequencies of oscillations are determined by the complex roots of this characteristics equation. For the hydrogen–oxygen mixture, flowing at 5000 m/s, where $\mu = 0.2$, $B = 0.5$, $\gamma = 1.4$, $t^* = 3.5 \times 10^{-7}$, and using κ_0, $\kappa_1 = 0.5$, the eigenvalues for this case, for $\alpha = (0.01, 0.2, 1, 2)$, are plotted in Fig. 7. It is seen that small $\alpha < 1$, there are positive real parts indicating regimes of diverging temperatures. Here we have the possibility of explosion. The range of values of the imaginary parts of the eigenvalues for this mixture indicate that the frequencies of the oscillations, $f = \mathrm{Im}(\lambda)/2\pi t^*$, are between 0.05 and 5.00 MHz,

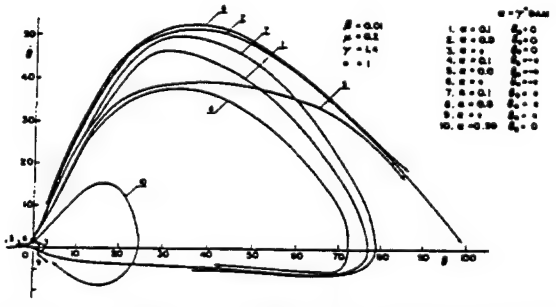

Fig. 6. Phase portrait for first-order reaction for various initial conditions and various α.

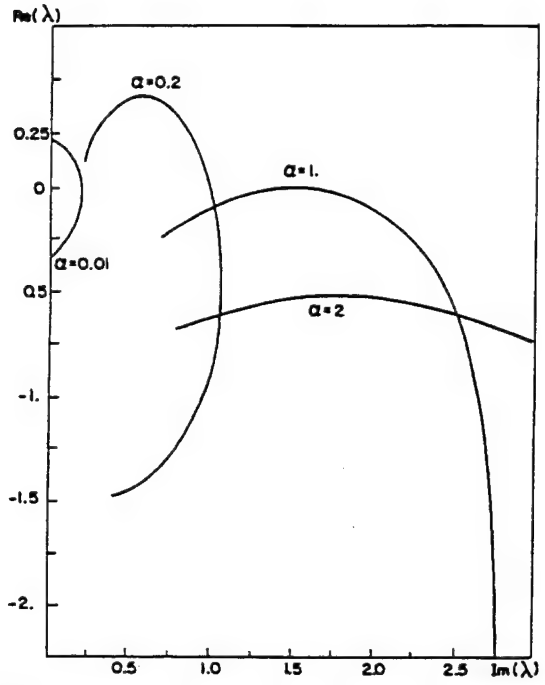

Fig. 7. Variation of the real and imaginary parts of the eigenvalues for a hydrogen–oxygen mixture.

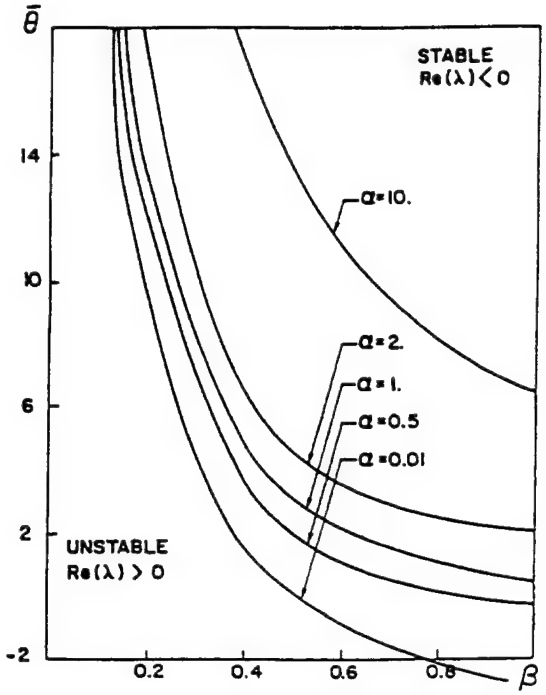

Fig. 8. Neutral stability curves, $\mathrm{Re}(\lambda) = 0$, for hydrogen–oxygen mixture.

which agrees well with frequencies measured in experiments.

The complex eigenvalues vary as a function of the temperature parameter for a known mixture. The oscillations occur when the imaginary part is nonzero. The range where the imaginary part is not zero, i.e., the range of oscillations, is obtained from the solution of

$$S = \left[\left(B - \frac{\bar{\beta}}{1+\mu\bar{\theta}}\right)\exp\left(\frac{\bar{\theta}}{1+\mu\bar{\theta}}\right) + \alpha\right]^2 - 4B\alpha\exp\left(\frac{\bar{\theta}}{1+\mu\bar{\theta}}\right) \le 0. \qquad (23)$$

The boundary within which oscillation occurs is obtained when $S = 0$. The neutral stability boundaries between stable and unstable regimes, defined by the curves of $\mathrm{Re}(\lambda) = 0$, are calculated for this hydrogen-oxygen mixture, as shown in Fig. 8, for various values of α. The variation of the frequency of oscillations, as determined by the values of the imaginary part of the eigenvalues, as a function of $\bar{\theta}$ is presented in Fig. 9. For small values of α the frequencies are low, although as α increases the values of $\mathrm{Im}(\lambda)$ increase. There seems to be a peak of frequency for certain values of $\bar{\theta}$, indicating an effect like "resonance." For increasing α the peak in the values of $\mathrm{Im}(\lambda)$ increases and as $\bar{\theta}$ is increased the value of $\bar{\theta}$ at the peak of the $\mathrm{Im}(\lambda)$ also shifts to higher values of $\bar{\theta}$. The variation of this peak value of $\mathrm{Im}(\lambda)$ at increasing α and $\bar{\theta}$ is also indicated on Fig. 9.

DISCUSSION OF THE DYNAMICAL SYSTEMS ANALYSIS FOR THE PERTURBATION EQUATIONS

The perturbation equations presented in Eqs. 21a and 21b, can be expressed in the "classic" form

$$\dot{\theta}' = a\theta' + b\beta',$$

$$\dot{\beta}' = -c\theta' - d\beta',$$

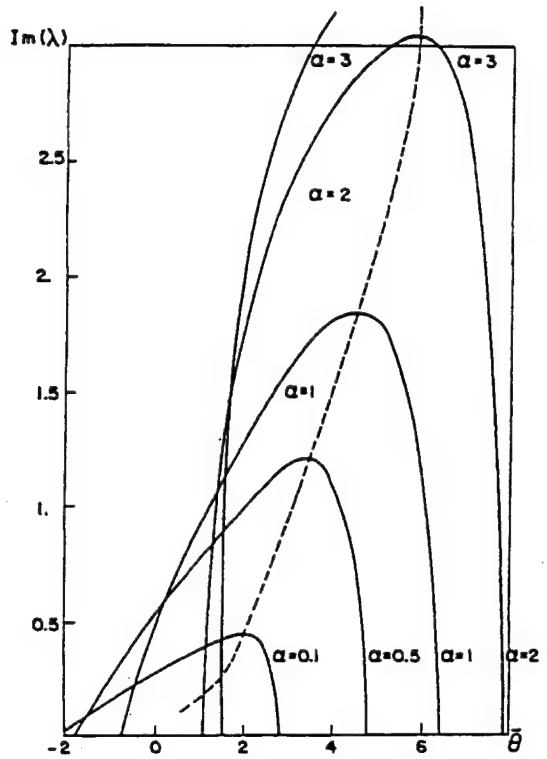

Fig. 9. Variation of $\mathrm{Im}(\lambda)$ as a function of θ for various values of α.

where a, b, c, and d are

$$a = \left[\frac{\bar{\beta} \exp\left(\frac{\bar{\theta}}{1 + \mu\bar{\theta}} \right)}{1 + \mu\bar{\theta}} - \alpha \right],$$

$$b = \exp\left(\frac{\bar{\theta}}{1 + \mu\bar{\theta}} \right),$$

$$c = \frac{B\bar{\beta} \exp \frac{\bar{\theta}}{1 + \mu\bar{\theta}}}{1 + \mu\bar{\theta}},$$

$$d = \left[B \exp\left(\frac{\bar{\theta}}{1 + \mu\bar{\theta}} \right) \right].$$

Following the analysis of Ref. 23 we define

$$\sigma = a - d, \qquad \Delta = -ad + bc$$

as the trace and the determinant of the matrix of coefficients.

Then

$$\sigma = \left(\frac{\bar{\beta}}{1 + \mu\bar{\theta}} - B \right) \exp\left(\frac{\bar{\alpha}}{1 + \mu\bar{\theta}} \right) - \alpha \qquad (24)$$

$$\Delta = \alpha B \exp\left(\frac{\bar{\theta}}{1 + \mu\bar{\theta}} \right) \qquad (25)$$

In Fig. 10, the well known diagram of σ vs. Δ is presented, showing the regions of stability and instability as well as the type of singularities in each region. The stationary states are evaluated by Eqs. 20a and 20b and the nature of singularities near these stationary states can be evaluated by analyzing the perturbation equations using the parameters σ and Δ as defined in Eqs. 24 and 25, respectively. It was already shown that for the first-order reaction case, $n = 1$, there is only one singular point at the origin, where $\bar{\theta} = \bar{\beta} = 0$ and the eigenvalues are $\lambda_1 = -\alpha$ and $\lambda_2 = -B$ indicating a stable node type singularity. This result can be shown to apply also to higher order reaction cases where $n \geq 1$.

We examine the condition $\sigma = 0$. The real part of the eigenvalue, $\lambda_r = 0$, but the imaginary part $\lambda_i \neq 0$, indicates neutral oscillations corresponding to a singularity of a center type. The corresponding body size which is evaluated from the corresponding value of α can be

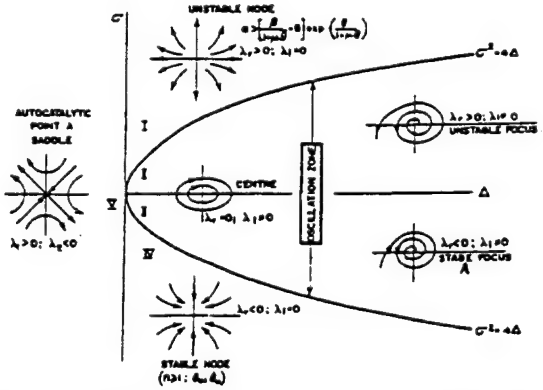

Fig. 10. Relation between states of equilibrium and types of singularities of the characteristics equation.

calculated from Eq. 24, when $\sigma = 0$, so that this critical value of H_{crit} is

$$H_{crit} = \frac{(2-\gamma)Fu_{\infty}(1-\mu\theta)\exp\left(\dfrac{-\theta}{1+\mu\theta}\right)}{\beta - B(1+\mu\theta)}. \tag{26}$$

This is the body radius required for obtaining neutral oscillations of the reactions in the stagnation point value for first-order reactions. This critical body size is different from the minimum body radius required for establishment of detonation evaluated from the appropriate criterion for the zero-order reaction, presented in Eq. 16.

COMPARISON WITH EXPERIMENTAL DATA

Minimum Body Size

The analysis for the zero-order reaction case resulted in the evaluation of a minimum body radius for establishment of detonation in the stagnation point, presented in Eq. 16. The minimum radius can be calculated using the proper parameters for various mixtures, such as hydrogen–oxygen, methane–oxygen and acetylene–oxygen. For these mixtures the calculated body radius is about 1–3 mm at flow Mach number of 5 down to 0.1–0.3 mm at Mach number of 10. These results are in good agreement with the previous estimates of Ref. 18. Experimental evidence showing the requirement for a minimum size cylindrical rod for establishment of detonation is presented in Ref. 27. The experiments are carried out in an expansion tube filled with methane–oxygen–nitrogen mixture accelerated to velocity of about 2300 m/s at initial pressure of 0.5 atm. For these conditions detonation was not achieved for rod diameters lower than 3 mm. This value is within the range of estimated values by the present analysis, Eq. 16. The minimum body size, obtained here by the dynamical systems analysis, is in agreement with previous results obtained using classical homogeneous ignition theory [35–37].

An indication that there is a minimum body diameter for oscillations to occur, as indicated by the critical body size in Eq. 26, can be seen from the numerical study on the effect of body size variation presented in Ref. 16. It was shown there that whereas oscillations were observed on a 15 mm sphere, such oscillations were not obtained for the same flow conditions on a 2.5 mm sphere.

Frequencies of Oscillations

There are few experimental measurements of the oscillations obtained on spheres and spherical nosed cylindrical projectiles flying at high supersonic speeds in hydrogen/oxygen diluted with nitrogen or with argon and acetylene/oxygen mixtures [1, 2, 12, 28, 29]. The test conditions and the measured frequencies reported in these cited references are presented in Table 1.

It was shown here that for reactions of order one and higher, oscillations can be obtained when the phase trajectories are closed indicating a limit cycle. The period of oscillations is estimated from the relation for the limit cycle,

$$T = t^*\tau \cong \frac{t_{ind}c_v T^*\mu\tau\exp\left(\dfrac{1}{\mu}\right)}{Q}.$$

Introducing the values for the hydrogen–oxygen system, the estimated frequencies by this relation are in the range of 0.1 to 1.5 MHz. This range of estimated frequencies covers very well the experimental values presented in Table 1.

The oscillation frequencies are evaluated from the perturbation analysis by calculating the values of the imaginary part of the eigenvalues for the first-order reaction, $n = 1$, using Eq. 22. The oscillation frequency is then,

$$f = \frac{\mathrm{Im}(\lambda)}{2\pi t^*} = \frac{QA_n}{2c_v\mu T^*\exp\left(\dfrac{1}{\mu}\right)}\sqrt{\left[\exp\left(\frac{\bar{\theta}}{1+\mu\bar{\theta}}\right)\left(B - \frac{\bar{\beta}}{1+\mu\bar{\theta}}\right) + \alpha\right]^2 - 4B\alpha\exp\left(\frac{\bar{\theta}}{1+\mu\bar{\theta}}\right)}.$$

TABLE 1

Comparison of Measured and Calculated Frequencies of Oscillations on Blunt Bodies Flying at Hypersonic Speeds in Detonative Mixtures

Mixture	M_∞	a_∞ (m/s)	u_∞ (m/s)	p_∞ (atm)	D (m/s)	u_∞/D	H (mm)	f (MHz) Exp.	f (MHz) Calc.	Ref.
$2H_2 + O_2 + 3.76N_2$	4.18	403	1685	0.421	2055	0.82	7.5	0.15	0.12	2
$2H_2 + O_2 + 3.76N_2$	5.04	403	2029	0.421	2055	0.99	7.5	1.04	1.15	2
H_2 + Air	4.65	409	1900	0.55	1950	0.97	4.5	0.85 1.8	0.9	28
H_2 + Air	4.71	409	1925	0.55	1950	0.99	4.5	1.15	1.20	28
H_2 + Air	4.16	409	1700	0.55	1950	0.87	4.5	0.3	0.33	28
H_2 + Air (30%H_2)	4.8	409	1963	0.25	1950	1.01	10	≈ 0.1	0.12	29
$O_2 + C_2H_2$ (15 : 1)	5.16	328	1690	0.197	1692	1.00	6.35	≈ 0.06	0.07	12
$H_2 + O_2$ + Ar (1 : 2 :2)	4.54	370	1680	0.263	1910	0.88	6.35	≈ 0.26	0.29	1

These calculated frequencies are also included in Table 1, for comparison with the experimental data. The values of the parameters used in these calculations are presented in Table 2. In all cases we chose the values of $\kappa_0 = 0.5$ and $\kappa_1 = 0.75$, as these seem to fit somewhat better the results, particularly those of Ref. 28, instead of $\kappa_0 = 0.5$ and $\kappa_1 = 0.5$ which were chosen previously. There is a remarkable agreement between the measured and calculated frequencies for all the reported experiments, the differences range from 4.3% to 20%, as indicated in Table 2. These differences are relatively small considering the rough approximations used in the analysis.

DISCUSSION AND CONCLUSIONS

The present analysis shows that the chemical reaction process in the stagnation region of a blunt-nosed body in hypersonic flow of a reacting mixture behaves as a dynamical system analogous to the vibrating mechanical and electrical systems. In the stagnation region the combustion front oscillates between the nonoscillating detached shock wave and the

TABLE 2

The Physical Parameters Used in the Calculations of the Frequency of the Oscillations in Table 1[a]

Mixture	Q (MJ/kg)	T^* (K)	μ	B	$E/R \times 10^4$	$A_n \times 10^8 \times \bar{p}$	$\bar{\theta}$	f Exp (MHz)	f Calc. (MHz)	% error
$2H_2 + O_2 + 3.76N_2$	2.2	1967	0.205	0.55	0.96	1.25	1.51	0.15	0.12	20
$2H_2 + O_2 + 3.76N_2$	2.2	2200	0.23	0.69	0.96	1.25	0.74	1.04	1.15	10.6
H_2 + Air	1.98	2085	0.208	0.62	1.0	2.2	0.5	0.85	0.9	6
H_2 + Air	1.98	1800	0.18	0.46	1.0	2.2	1.54	1.15	1.20	4.3
H_2 + Air	1.98	1650	0.165	0.38	1.0	2.2	2.39	0.3	0.33	10
H_2 + Air (30% H_2)	1.98	1830	0.183	0.47	1.0	2.2	1.4	≈ 0.1	0.12	20
$O_2 + C_2H_2$ (15 : 1)	1.49	2060	0.165	0.16	1.25	$(262.0 \times \bar{p})^{(1)}$	0.41	≈ 0.06	0.07	17
$H_2 + O_2$ + Ar (1 : 2 : 2)	1.90	2050	0.214	0.81	0.96	1.25	1.2	≈ 0.26	0.29	11.5

[a] $\bar{p}$ is the pressure equal to the pressure behind the normal detached shock wave, p.

T^* is evaluated as follows: $T^* = 0.5\,(T_{C-J} + T_E)$, where T_{C-J} is the Chapman–Jouguet detonation temperature and T_E is the Eckeret effective temperature, $T_E = 0.5\,(T_w + T_s) + 0.22\,(T_r - T_s)$ where $T_s = p_s/R\rho_s$ and $T_r = T_\infty[1 + 0.5r(\gamma - 1)M_\infty^2]$ with $r = 0.85$.

$\bar{\theta}$ is evaluated by the relation

$$\bar{\theta} = \frac{E}{RT^{*2}}(\bar{T} - T^*), \qquad \text{where } \bar{T} = \frac{\gamma + 1}{2\gamma}T_{C-J}$$

(1) for the Acytelene-Oxygen mixture the A_n value is $(2.62 \times 10^2 \times \bar{p})$, where $\bar{p}$ is the average density equal to the density behind the normal detached shock wave, ρ.

acetylene?

Ac?

solid body surface. The instantaneous temperature variation in the hypersonic flow with chemical reactions which may lead to detonation or to oscillatory combustion is formulated as a second order differential equation with "damping" and "restoring force" terms. These "damping" and "restoring force" terms are dependent on the flow characteristics and on the chemical and physical parameters of the fuel/oxidizer mixture. This formulation is derived from the energy equation for the hypersonic flow at the stagnation region of a blunt-nosed body and the associated species concentration equation for the reacting mixture. In this formulation these equations can be presented either as two first-order nonlinear differential equations for the temperature and species concentration or as a second-order nonlinear differential equation for the instantaneous temperature.

In this development some rough approximations are required, as presented and discussed in the paper. These include: (1) the assumption of "constant density" in the stagnation region; (2) the assumption of linear variation of the flow parameters near the stagnation point which enabled the evaluation of the local $\partial/\partial x$ and $\partial/\partial y$ derivatives near the stagnation point in terms of average values (Eqs. 4a and 4b); (3) representing the velocity components in the stagnation region u, v by Eqs. 7–9, evaluated for blunt body in hypersonic flow [17]; (4) choosing average values of the parameters $\kappa_0 = 0.5$ and $\kappa_1 = 0.75$ for the representative y/H and x_1/R_s positions in the stagnation region, respectively, and (5) assuming uniform reactive mixture in the stagnation region, so that $(\beta - \beta^*) \rightarrow 0$ in this region.

The result is a formulation of the dynamical systems model for the combustion front which can oscillate behind the steady detached shock wave and ahead of the blunt nosed body in hypersonic flow. The full analogy between this combustion process and mechanical and electrical dynamic systems is a very intriguing subject for studies. It is shown in this investigation that it is possible to identify "damping" and "restoring force" in terms of the flow and chemical and physical parameters. This is made even clearer using the energy analogy formulation presented in Appendix A.

The analysis of the zero-order reaction indicates the existence of a solution leading to explosion when the body is large enough. This is used for the determination of the minimum blunt body size required to establish combustion–detonation process. This result, obtained here by the dynamical systems analysis, is in agreement with results obtained previously using classical homogeneous ignition theory [35–37] and with experimental observations [27]. It is also shown that for first-order reactions (and higher orders) the possibility of periodic solutions exists. Using small perturbation analysis, a characteristic equation for the eigenvalues is obtained from which the oscillation frequencies are evaluated. The calculated frequencies are compared with measured frequencies on spheres and hemispherical cylindrical bodies. The differences vary between 4% and 20%, which is a very good agreement in this case. The fact that such good agreement is obtained, in spite of the very rough approximations used, is an indication that the present formulation of the combustion process using the dynamical systems analysis is reasonable for the stability analysis of hypersonic flow of reacting mixtures in the stagnation region of blunt-nosed bodies.

The research was supported in part by the Wolfson Family Charitable Trust program for the absorption of immigrant scientists and by the Fund for Absorption of Scientists of the Ministry of Absorption, Government of Israel and by the Technion V.P.R. - Aeronautical Engineering Research Fund and also in part by the US Army Contract No. N68171-94-C-9065.

REFERENCES

1. Alpert, R. L., and Toong, T. Y., *Astronaut. Acta* 17:539–560 (1972).
2. Lehr, H. F., *Astronaut. Acta*, 17:589–597 (1972).
3. Pratt, D. T., Humphrey, J. W., and Glenn, D. E., *J. Propul. Power* 7:837–845 (1991).
4. Ostrander, M. J., Hyde, M. F., Young, R. D., and Kissinger, R. D., AIAA Paper 87-2202, 1987.
5. Rom, J., U.S. Patent 4,932,306, 1990.
6. Rom, J., and Avital, J., AIAA Paper 92-3717, 1992.
7. Chernyi, G. G., *Mekh. Zhid. Gaza* 1(6):10–24 (1966).
8. Gilinskii, S. M., Zapryanov, Z. D., and Chernyi, G. G., *Mekh. Zhid. Gaza* 1(5):8–13 (1966).

9. Chernyi, G. G., Korobeinikov, V. P., Levin, V. A., and Medvedev, S. A., *Astronaut. Acta* 15:259–265 (1970).
10. Chernyi, G. G., and Gilinskii, S. M., *Astronaut. Acta* 15:539–544 (1970).
11. Gilinsky, M. M., Moskovskii Gosudarstvennyi Universitet, Instituta Mekhaniki, Nauchnye Trudy, 32:72–84 (1974).
12. McVey, J. B., and Toong, T. Y., *Combust. Sci. Technol.* 3:63–76 (1971).
13. Matsuo, A., and Fujiwara, T., *AIAA J.* 31:1835–1841 (1993).
14. Matsuo, A., Fujiwara, T., and Fujii, K., AIAA Paper 93-0451, 1994.
15. Matsuo, A., Fujii, K., and Fujiwara, T., AIAA Paper 94-0764, 1994.
16. Ahuja, J. K., and Tiwari, S. N., AIAA Paper 94-0674, 1994.
17. Hayes, W. D., and Probstein, R. F., *Hypersonic Flow Theory*, Academic Press, New York, 1959.
18. Tivanov, G., and Rom, J., AIAA Paper 93-9611, 1993.
19. Adler, J., and Enig, J. W., *Combust. Flame* 8:97–103 (1964).
20. Gray, B. F., *Combust. Flame* 21:317–325 (1973).
21. Babushok, V. I., and Gol'dshtein, V. M., *Combust. Flame* 72:221–224 (1988).
22. Babushok, V. I., and Gol'dshtein, V. M., *Combust. Sci. Technol.* 70:81–89 (1990).
23. Andronov, A. A., Vitt, A. A., and Khaikin, S. E., *Theory of Oscillators*, Pergamon, 1966.
24. Davis, H. T., *Introduction to Nonlinear Differential and Integral Equations*, Dover, 1962.
25. Reissing, R., Sansone, G., and Conti, R., *Qualitative Theorie Nichtlinearer Differentialgleichungen*, Edizioni Cremonese, Roma, 1963.
26. Reissing, R., Sansone, G., and Conti, R., *Nichtilineare Differentialgleichungen Hocher Ordnung*, Edizioni Cremonese, Roma, 1969.
27. Srulijes, J., Smeets, G., and Seller, F., AIAA Paper 92-3246, 1992.
28. Behrens, H., Struth, W., and Wecken, F., *Tenth Symposium (International) on Combustion*, The Combustion Institute, Pittsburgh, 1965, pp. 245–252.
29. Ruegg, F. W., and Dorsey, W. W., *NBS J. Res.* C 66C(1):51–58 (1962).
30. Levinson, N., and Smith, O., *Duke Math. J* 9:382–403 (1942).
31. Dragilev, A., *Appl. Mech. Math.* 16:85–88 (1952).
32. Philippov, A., *Coll. Math.* 30:171–180 (1952).
33. Philippov, A., *Coll. Math.* 99–128 (1960).
34. Castro, A., *Rev. Math. Hisp-Amer.* 12:266–280, 317–329 (1952); 18:99–122, 146–156, 181–200 (1958).
35. Sichel, M., and Galloway, A. J., *Astronaut. Acta* 13:137–145 (1967).
36. Galloway, A. J., and Sichel, M., *Astronaut. Acta* 15:89–105 (1969).
37. Lee, H. S., *Annu. Rev. Fluid Mech.* 16:311–336 (1984).
38. Tivanov, G., and Rom, J., AIAA Paper 93-1918, 1993.

Received 24 June 1994; revised 7 April 1995

APPENDIX A: ENERGY ANALOGY FORMULATION

An additional view of the analogy between the dynamical systems in the hypersonic reacting stagnation flow and the dynamical systems in mechanical and electrical vibrations can be derived by examining the energy formulation of the dynamic equation. The energy formulation can be obtained by examining Eq. 13 for the zero-order reaction case, $n = 0$, by first differentiating this equation with respect to τ and obtaining the relation

$$\ddot{\theta} - \dot{\theta}\left[\frac{\exp\left(\dfrac{\theta}{1+\mu\theta}\right)}{(1+\mu\theta)^2} - \alpha\right] = 0. \qquad \text{(A1)}$$

Using the relation $\ddot{\theta} = \dot{\theta}\left(\dfrac{d\dot{\theta}}{d\theta}\right)$ and integrating Eq. A1 between the limits of θ_0 and θ, for convenience can assume $\mu = 0$ (since our interest is mainly to obtain the energy terms), then

$$\frac{\dot{\theta}^2}{2} + \alpha\theta\exp(\theta) - \frac{\exp(2\theta)}{2} - \frac{\alpha^2\theta^2}{2} = \frac{\dot{\theta}_0^{\,2}}{2} + \alpha\theta_0\exp(\theta_0) - \frac{\exp(2\theta_0)}{2} - \frac{\alpha^2\theta_0^{\,2}}{2}. \qquad \text{(A2)}$$

This relation has the form of an energy representation,

$$K(\dot{\theta}) + V(\alpha,\theta) = E(\alpha,\dot{\theta}_0,\theta_0), \qquad \text{(A3)}$$

where $K = \dot{\theta}^2/2$ represents the "kinetic energy,"

$V = \alpha\theta\exp(\theta) - [\exp(2\theta)/2] - \alpha^2\theta^2/2$, represents "potential energy," and

$E = \dot{\theta}_0^{\,2}/2 + \alpha\theta_0\exp(\theta_0) - [\exp(2\theta_0)/2] - \alpha^2\theta_0^{\,2}/2$ = const represents "total energy."

AU: PLEASE SEE QUERY ON MANUSCRIPT

Therefore, Eq. A3 has the form of the energy conservation of a dynamical system, and can be used as a phase trajectory equation obtained from "energy" conservation relations when E = const. The "total energy" constant E is determined by the values of θ_0, which can be viewed as determining the "energy reserve" for the system while the parameter α represents the "stiffness" of the system. This mechanical analogy shows that for this zero-order reaction no periodic solutions exist, in agreement with our analysis.

Examining the second-order differential equation for the instantaneous temperature parameter in the zero-order reaction case, A1, shows that the "damping," which is represented by the term multiplying in Eq. A1, is approximately equal to $[\exp(\theta) - \alpha]$ assuming $\mu = 0$ for this case. So when α is increased, i.e., body size is decreased, then, the "damping" is also decreased.

APPENDIX B: MATHEMATICAL CONDITIONS FOR SOLUTIONS OF THE DYNAMICAL REACTION EQUATION

Conditions for Periodic Solutions

The dynamical reaction equation, Eq. 14, is

$$\ddot{\theta} + f(\theta, \dot{\theta})\dot{\theta} + g(\theta) = 0. \tag{B1}$$

Using the analysis of Eq. 34, examining the solutions of this equation for the following conditions:

1. $f(\theta_0, \dot{\theta}_0) < 0$, where $\theta_0 = \theta(t = 0)$ and $\dot{\theta}_0 = \dot{\theta}(t = 0)$ (B2)

2. $|g(\theta)| + |\dot{\theta}| f(\theta, \dot{\theta}) \geq \varepsilon > 0$, for $|\theta| > \theta_0$ (B3)

3. $f(\theta, \dot{\theta}) + f(\theta, -\dot{\theta}) \geq 0$ for $|\theta| + |\dot{\theta}| \geq$ const. (B4)

In these cases, according to Ref. 34, the dynamical reaction equation, Eq. B1, has at least one periodic solution when the conditions exist, as follows:

For the conditions of Eq. B2, when

$$f(0,0) = \alpha - \frac{\alpha\theta_0 - \dot{\theta}_0}{[1 + \mu\theta_0]^2} + B \exp\left(\frac{\theta_0}{1 + \mu\theta_0}\right) < 0, \tag{B5a}$$

or

$$\alpha < \frac{\dot{\theta}_0 - B(1 + \mu\theta_0)^2 \exp\left(\frac{\theta_0}{1 + \mu\theta_0}\right)}{(1 + \mu\theta_0)^2 - \theta_0}, \tag{B5b}$$

when for example $\theta_0 = 0$ and $\dot{\theta} = 1$, then $\alpha < 1 - B$ for a periodic solution to exist.

For the conditions of Eq. B3, when

$$\alpha < \frac{|\dot{\theta}\left[B(1 + \mu\theta)^2 \exp\left(\frac{\theta}{1 + \mu\theta}\right) - \dot{\theta}\right]}{B(1 + \mu\theta)^2 \theta \exp\left(\frac{\theta}{1 + \mu\theta}\right) + \left|\dot{\theta}\left[(1 + \mu\theta)^2 - \theta\right]\right|}. \tag{B6}$$

For conditions of Eq. B4, when

$$\alpha \leq \frac{B(1 + \mu\theta)^2 \exp\left(\frac{\theta}{1 + \mu\theta}\right)}{\theta - (1 + \mu\theta)^2}. \tag{B7}$$

This condition requires that B should be very small, $B < \varepsilon$, which is not physically reasonable. Therefore, for this case we use another condition defined in Ref. 34, as follows:

$$\int_{-\theta_1}^{\theta_2} f(\theta, \dot{\theta})\, d\theta \geq \varepsilon$$

for only $\theta_2 \geq \theta_1$ for every $\dot{\theta}(\theta) \geq 0$,

and then it is possible to replace the condition of Eq. B7 by the relation

$$\alpha < \frac{\int \left[B \exp\left(\frac{\theta}{1 + \mu\theta}\right) - \frac{\dot{\theta}}{(1 + \mu\theta)^2}\right] d\theta}{\int \left[1 - \frac{\theta}{(1 + \mu\theta)^2}\right] d\theta}. \tag{B8}$$

This requirement is still very restrictive in comparison to those presented in relations B5b or B6, which lead to the conditions

$\alpha < 1 - B$ if $\theta_0 = 0$ from Eq. B5b,

$\alpha < 1$ if $B \ll \varepsilon$; $\mu \ll \varepsilon$ from Eq. B6

(where ε is an infinitesimal value) while from the condition of Eq. B8, it can be shown that

$$\alpha < 1 + \sum_{n=2} \frac{\theta^{n-1}}{n!}. \tag{B9}$$

So that in order to obtain periodic solutions, it is required that $\alpha < 1 + \varepsilon$. In such cases when α is kept constant and for various initial temperatures, θ_0, the solution is a family of closed trajectories as outlined in the phase portrait shown in Fig. 11. Solutions are shown when starting from the stationary state $\bar{\theta}$, which is a stable node evaluated from Eq. 17a, and for various other initial conditions. An example of a phase portrait for various values of α and various initial conditions is shown in Fig. 6. Some of these curves are not completely closed; this is an indication that "jump" conditions may occur due to effect of energy source. The study of these effects requires analysis using at least a two-step chemical reaction model and cannot be treated with the present one-step reaction analysis.

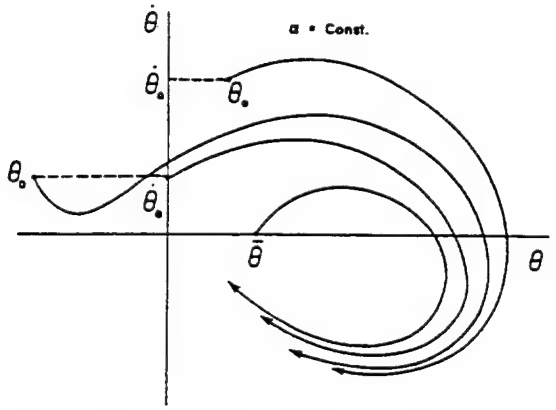

Fig. 11. Phase portrait for first-order reaction for α = const.

Conditions on the "Damping" and "Restoring Force" Parameters

Examining the dynamic reaction equation, Eq. B1, neutral free oscillations occur when

$f(\theta, \dot{\theta}) = 0$; then

$$f(\theta, \dot{\theta}) = \alpha - \frac{\alpha\theta - \dot{\theta}}{(1 + \mu\theta)^2} + B \exp\left(\frac{\theta}{1 + \mu\theta}\right) = 0. \tag{B10}$$

Therefore, in this case, when the chemical and physical parameters fulfill the relation

$$B = \frac{RT^{*2}c_v}{EQ} = \exp\left(-\frac{\theta}{1 + \mu\theta}\right)\left[\frac{\beta \exp\left(\frac{\theta}{1 + \mu\theta}\right)}{(1 + \mu\theta)^2} - \alpha\right],$$

the conditions for free oscillations exist.

The term $f(\theta, \dot{\theta})$ in Eq. B1 can be interpreted as being analogous to a "damping" term for the dynamic system. So that increasing or decreasing $f(\theta, \dot{\theta})$ will correspondingly affect the oscillations frequencies and amplitudes. The variations of $f(\theta, \dot{\theta})$ for obtaining the conditions for the limit cycle to exist are now examined. Let $f(\theta, \dot{\theta})$ vary in the range $0 \leq f(\theta, \dot{\theta}) \leq \bar{f}(\theta, \dot{\theta})$, where $\bar{f}$ has a finite value. The characteristics of nonlinear differential equations indicate that, if $f(0, 0) < 0$ and since $\bar{f}$ is larger than $f(\theta, \dot{\theta})$, then the periodical solutions that exist for $f(\theta, \dot{\theta})$ exist also at the conditions of $\bar{f}(\theta, \dot{\theta})$. Therefore, oscillations (when they occur) are not destroyed by the increase of the "damping" term in the equation but are affected when the stationary (equilibrium) state becomes unstable. The condition $\theta g(\theta) > 0$ can be interpreted as being proportional to the "restoring force," in an analogy to

a mechanical dynamic system, acting to return the system towards its equilibrium state, towards the point $\dot{\theta} = \theta = 0$. The term $g(\theta)$ in Eq. B1 represents the "restoring force" in the dynamic equation, therefore, $g(\theta) \geq 0$. since $g(-\theta) \neq -g(\theta)$ this restoring force is unharmonic.

Oscillatory solutions are obtained when $f(\theta, \dot{\theta})$ changes sign as θ increases as the process develops with time. Also, starting from the initial conditions $\theta_0 = \theta(t = 0)$ and $\dot{\theta}_0 = \dot{\theta}(t = 0)$, the function $f(\theta_0 + \varepsilon, \dot{\theta}_0 + \varepsilon)$ should decrease to $f < 0$. This is illustrated in the phase diagram presented in Fig. 12 where the variation of $f(\theta, \dot{\theta})$ and $\dot{\theta}$ as a function of θ for various values of α are shown. It is seen in this figure that the curves for $f(\theta, \dot{\theta})$ first decrease to negative values and as θ increases this function increases to positive values. Physically this process can be explained as indicating, first, as $f < 0$, the system absorbs the external energy so that the oscillation energy is increasing, then, as $f > 0$, the oscillation energy decreases. This pattern is seen for the f curves for α values of 0.99 and 1.1. However, for smaller values of α, for example the $\alpha = 0.8$ curve, most of the f values are negative, almost over the complete range of temperatures, indicating that the system in this case absorbed large amount of energy into its oscillatory system, eventually, at smaller α the oscillations transform into fast combustion-

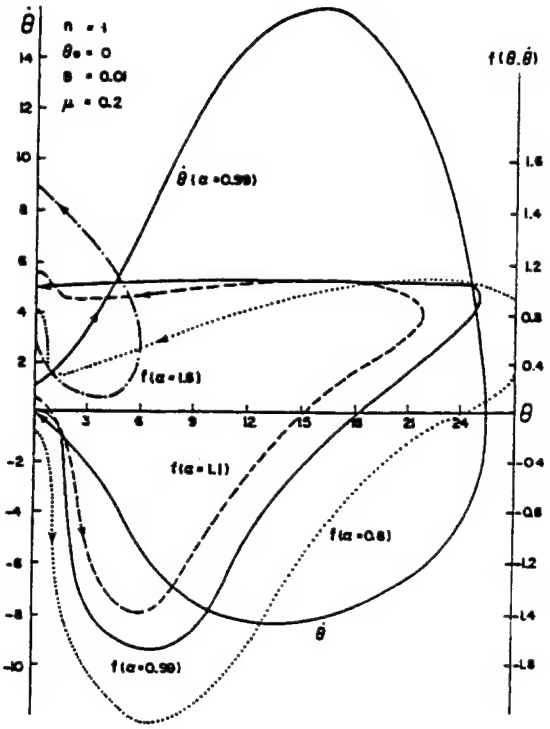

Fig. 12 $f(\theta, \dot{\theta})$ and $\dot{\theta}$ variation with θ for first-order reaction for various initial conditions.

detonation. On the other hand, when α is increased f is shifted to positive values, as seen for $\alpha = 1.6$, where the complete curve has positive values indicating a low temperature combustion without oscillations.

ANNEX 4

CALCULATIONS OF COMBUSTION IN A SCRAMJET ENGINE MODEL USING THE EXTERNAL PROPULSION ACCELERATOR AS A TEST FACILITY

J. Rom[1], M.J. Nusca[2], M.J. Lewis[3], A.K. Gupta[4] and J. Sabean[5]

EXTENDED ABSTRACT

ABSTRACT

The combustion-detonation phenomena in a scramjet engine as well as in an Oblique Detonation Wave Engine can be studied in the External Propulsion Accelerator. This facility provides the means to investigate the combustion-detonation process independently from the fuel mixing process. In this case, a projectile simulates the engine geometry and the combustion of the premixed fuel/oxidizer mixture is initiated in the model flying in the External Propulsion Accelerator. The scramjet combustion also provides net thrust for the model flight in the Accelerator. Thus, this facility enables testing of the combustion characteristics as function of inlet, combustor and nozzle geometry, fuel/oxygen chemical parameters and flight velocity. The effects of various fuel/oxidizer mixtures can be studied by including sections separated by diaphragms in the accelerator tube. These sections can be filled with various mixtures to different initial pressures, so that effects of various pressure levels can also be simulated in this facility.

INTRODUCTION

The External Propulsion Accelerator was proposed by J. Rom (Ref. 1) and certain preliminary aspect of its characteristics were presented in Refs. 2, and 3. Some analytical investigations, based on many simplifying assumptions, for the establishment of combustion front ahead of the forward facing step and on spherical nosed blunt bodies in hypersonic flows of detonable mixtures, including the studies of the oscillations that may occur were investigated by Tivanov and Rom (Ref. 4, 5 and 6). A more detailed study of the combustion-detonation characteristics using the solutions of the full Navier-Stokes equations with chemical processes on projectiles in the External propulsion Accelerator is presented in Ref. 7. The External Propulsion Accelerator has been developed following the development of the Ram Accelerator by A. Hertzberg (Ref. 8) at the University of Washington. The Ram Accelerator method utilizes the idea of using a premixed fuel/oxidizer mixture in the launcher barrel and injecting a projectile at supersonic speeds into this mixture. Thrust is generated by the ramjet combustion obtained between the tube wall and the projectile, where the projectile acts as a ramjet centerbody and the barrel is basically a long cowling, and combustion is initiated and stabilized by the interaction of the shock waves from the projectile nose with the barrel walls. However, as distinct from the Ram Accelerator, the External Propulsion Accelerator use thrust that is generated purely by the interactions between the shock waves from the projectile nose with combustion generated by normal shock waves generated on the projectile body by a ramp or a forward facing step, or by a ring wing, completely independent of the barrel walls. Since the projectile flies in a premixed fuel/oxidizer atmosphere, the difficult problem of mixing the fuel and oxidizer, which plagues all airbreathing propulsion methods proposed for hypersonic flight, is eliminated. However, some important and difficult combustion issues, including the ability to initiate and stabilize the combustion front in the engine in such a way

[1] Professor, Lady Davis Chair, Faculty of Aerospace Engineering, Technion - Israel Institute of Technology, Visiting Professor, Department of Mechanical Engineering, University of Maryland, Fellow AIAA.
[2] Aerospace Engineer, Weapons Technology Directorate, Aberdeen Proving Ground, Army Research Laboratory.
[3] Associate Professor, Department of Aerospace Engineering, University of Maryland.
[4] Professor, Department of Mechanical Engineering, University of Maryland, Fellow AIAA.
[5] Graduate student, Department of Aerospace Engineering, University of Maryland.

that positive thrust can be generated, can be investigated for a uniformly premixed mixture at various flight conditions. Therefore, with proper simulation of the intake geometry and the flow through the engine, the conditions for the initiation and the stabilization of the combustion in the engine and the corresponding thrust generation can be studied.

In this paper we present the calculation of the flow on a scramjet model simulating a scramjet engine geometry flying in the External Propulsion Accelerator using the numerical programs developed for the calculations of the flow in the External Propulsion Accelerator. The recent study, presented in Ref. 7, utilizes the solution of the Navier-Stokes equations for flows with chemical processes which was adapted for the Ram Accelerator calculations at ARL by Nusca (Refs. 9, 10). Calculations of the flow with combustion on the projectile designs proposed for the External Propulsion Accelerator are presented in Ref. 7. This calculation uses the Rockwell Science Center USA-RG (Unified Solution Algorithm Real Gas) code written by Chakravarthy et al (Refs. 11, 12). This CFD code includes the full 3D unsteady Reynolds-Averaged Navier-Stokes (RANS) equations including equations for chemical kinetics (finite-rate and equilibrium). These equations are cast in conservation form and converted to algebraic equations using upwind finite-difference and finite-volume formulations. The equations are solved using a second-order TVD (total variation diminishing) scheme which is used to insure non-oscillatory numerical behavior. Following these calculations, a scramjet model configuration will be proposed for tests in the ARL Ram Accelerator facility (Refs. 13, 14) using subcaliber models.

The scramjet model will be composed of a shallow sharp nosed cone acting as the scramjet inlet, a ring wing simulating the cowling of the scramjet around a cylindrical center body and a conical afterbody simulating the scramjet exhaust. Combustion is generated behind the shock wave established in front of the wedge shape lip of the ring wing. The scramjet combustion in this configuration will produce high temperature high pressure combustion products resulting in significant net positive thrust.

HYPERSONIC SCRAMJET TEST FACILITY BASED ON THE EXTERNAL PROPULSION ACCELERATOR

In this application, the hypersonic scramjet testing facility will be comprised from: 1. The External Propulsion Accelerator section. 2. Transparent test section. 3. Deccelerator section for model retrieval.

1. The External Propulsion Accelerator Section

The tests are conducted in a regular External Propulsion Accelerator using a specially designed model for the scramjet simulation. The model with its sabot are accelerated by a gun powder charge to the required insertion speed of 1,000 up to 1,900 m/sec. (Mach number between 3 to 5). In a simple configuration the projectile body will simulate the engine centerbody and a properly shaped ring wing around this centerbody will represent the engine cowling. The shapes of the engine intake and the shape of the combustion region inside the engine can be also simulated by this model. Combustion-detonation will be initiated by the shock waves generated at the intake to the ring wing and it will cause combustion in the space between the centerbody and the ring-cowling. The flow will be then expanded on the aft-body of the model, simulating the engine exhaust and nozzle flow characteristics. The operation of the scramjet will produce net thrust for the acceleration of the model. Therefore, measurements of the model acceleration-deceleration will enable the evaluation of the thrust obtained by this scramjet engine as a function of model velocity. More sophisticated measurements can be obtained using on-board instrumentation with telemetering. Models with hardened on-board instrumentation can be built to operate up to 50,000 g's acceleration level. The acceleration level in the projectile will depend on the thrust generated by the scramjet. Since the gas mixtures can be varied in the accelerator, this will be a method to study the effects of various chemical fuel compounds on the combustion and the thrust generation. Such studies can be made when the accelerator tube is divided into a number of sections separated by diaphragms. Each section of the accelerator tube can be filled with a certain fuel/oxidizer mixture at various initial pressures. So that in a single experiment the combustion characteristics of flight in various mixtures at specified initial pressures can be studied These test sections can be positioned at the end of the basic accelerator tube in which the projectile is accelerated to the desired velocity.

The length of the facility will be determined by the acceleration of the model and the speed range for the tests. The External Propulsion launcher for 50,000 g's will be about 10 meters for M = 7 testing, 40 meters for M = 10 testing and about 150 meters for M = 15 testing. More sophisticated models requiring lower values of acceleration can be used by proper modifications to the launcher. Lower initial accelerations can be achieved by initial acceleration of either a Ram Accelerator stage initiated by a small light gas gun or a small rocket or the initial acceleration be achieved directly by a rocket motor which will separate at the entrance to the External Propulsion launcher. The length of this launcher varies inversely as the acceleration levels, i.e. lower acceleration will require the correspondingly longer lengths.

The External Propulsion launcher diameter should be about 4 times the model maximum diameter. Therefore, a

launcher of 1m diameter will enable launching of models of 25 cm. diameter and the launcher tube diameter can be reduced to 40 cm for 10 cm models. Of course larger models can be considered with increase in size of the facility.

2. Transparent Test Section.

The possibility of including a transparent section into the Ram Accelerator facility was studied at ARL by Kruczynski et al. (Ref. 15). Such a transparent section at the end of the launcher tube will enable flow visualization photographs on the model, particularly, at the intake and exhaust regions.

3. Deceleration Section.

The energy imparted to the model traveling at Mach 6 to 15 is very large and must be absorbed in order to stop the model. For simple models, the models can be expandable and a conventional "catcher" can be used. For more sophisticated and expansive models there may be some possibilities of some energy absorbing methods for arresting the models, at least in the lower hypersonic speed range.

REFERENCES

1. Rom, J., "Method and Apparatus for Launching a Projectile at Hypersonic Velocity" U.S. Patent 4,932,306, June 12 1990.

2. Rom, J. and Kvity, Y., "Accelerating Projectiles up to 12 km/sec. Utilizing the Continuous Detonation Propulsion Method", AIAA Paper 88-2969, 1988.

3. Rom, J. and Avital, G., "The External Propulsion Accelerator: Scramjet Thrust Without Interaction with the Accelerator Barrel", AIAA Paper 92-3717, 1992.

4. Tivanov, G. and Rom, J., "Investigation of Hypersonic Flow of a Detonable Gas Mixture Ahead of a Forward Facing Step" AIAA Paper 93-0611, 1993.

5. Tivanov, G. and Rom, J., "Stability of Hypersonic Flow of a Detonable Gas Mixture in the Stagnation Region of a Blunt Body and a Forward Facing Step ", Proceedings of the 33rd Israel Annual Conference of Aeronautics and Astronautics, Feb. 1993.

6. Tivanov, G. and Rom, J., "Analysis of the Stability Characteristics of Hypersonic Flow of a Detonable Gas Mixture in the Stagnation Region of a Blunt Body", AIAA Paper 93-1918, 1993.

7. Rom. J., Nusca. M., Kruczynski, D., Lewis, M., Gupta, A. and Sabean, J., "Investigations of the Combustion Induced by a Step on a Projectile Flying at Hypersonic Speed in the External Propulsion Accelerator", AIAA Paper 95-0259, to be presented at the AIAA 33rd Aerospace Sciences Meeting, Reno, ND, January 1995.

8. Hertzberg, A., Bruckner, A.P. and Bogdanoff, D.W., "Ram Accelerator: A New Chemical Method for Accelerating Projectiles to Ultrahigh Velocities" AIAA Journal, Vol. 26, No. 2, 1988, pp 195-203.

9. Nusca, M.J., "Numerical Simulation of Fluid Dynamics with Finite-Rate and Equilibrium Combustion Kinetics for the 120 mm Ram Accelerator" AIAA Paper 93-2182, 1993.

10. Nusca, M.J., "Numerical Simulation of Gas Dynamics and Combustion Kinetics for a 120 mm Ram Accelerator" First International Workshop on Ram Accelerator, ISL, France, 1993.

11. Chakravarthy, S.R., Szema, K.Y., Goldberg, U.C., Gorski, J.J. and Osher, S., "Application of a New Class of High Accuracy TVD Schemes to the Navier-Stokes Equations" AIAA Paper 85-0165, 1985.

12. Palaniswamy, S., Ota, D.K. and Chakravarthy, S.R., "Some Reacting Flow Validation Results for USA-Series Codes" AIAA Paper 91-0583, 1991.

13. Kruczynski, D.L. and Nusca, M.J., "Experimental and computational Investigation of Scaling Phenomena in a Large Caliber Ram Accelerator" AIAA Paper 92-3425, 1992.

14. Kruczynski, D.L., "New Experiments in a 120 mm Ram Accelerator at High Pressures" AIAA Paper 93-2589, 1993.

15. Kruczynski, D., Liberatore, F. and Kiwan, M., "Flow Visualization of Steady and Transient Combustion in a 120 mm Ram Accelerator" AIAA Paper 94-3344, 1994.

AIAA-95-6138
Hypersonic Aerodynamics Test Facility Using the External Propulsion Accelerator

J. Rom
Technion-Israel Institute of Technology
Haifa, Israel
M. Lewis, A. Gupta, and J. Sabean
University of Maryland
College Park, MD

AIAA SIXTH INTERNATIONAL AEROSPACE PLANES AND HYPERSONICS TECHNOLOGIES CONFERENCE
3-7 APRIL 1995 / CHATTANOOGA, TN

HYPERSONIC AERODYNAMICS TEST FACILITY USING THE EXTERNAL PROPULSION ACCELERATOR

Josef Rom*
Technion-Israel Institute of Technology, Haifa, Israel 32000
Mark J. Lewis†, Ashwani K. Gupta‡ and John Sabean§
University of Maryland, College Park, Maryland 20742

Abstract

The use of the External propulsion Accelerator (EPA) for launching models of hypersonic aerodynamic configurations into an instrumented ballistic range is discussed. The aerodynamic model is encased inside an axisymmetric projectile designed to be accelerated to high speed in the EPA. Accelerator lengths required to achieve hypersonic speeds are estimated to vary from 10 meters for Mach 7, 40 meters for Mach 10, 150 meters for Mach 15, and 700 meters for Mach 30, assuming a limit of 50,000 g's acceleration. For a model span of 10 cm to 25 cm, the launch tube diameters are 40 cm and 100 cm, respectively. Using this EPA launcher will enable exact simulation of hypersonic flight in ground facilities where both the gas composition and pressure can be controlled in the ballistic range.

Introduction

One of the practical applications of the External Propulsion Accelerator (EPA) is it's use as the launcher of aerodynamic models to hypersonic speeds in a ground test facility. The models, encased in a properly designed sabot, are accelerated in the EPA to the desired hypersonic speed and fired into an instrumented ballistic range. In the conventional ranges the model velocity is limited to the launch velocities of the chemical explosives, which is less than 2000 m/sec., so that these ballistic ranges cannot simulate flight above Mach number 6 in room temperature air.

The EPA is theoretically capable to launch projectiles to velocities of up to 6 times the detonation velocity of the fuel-oxidizer mixture, in the order of 12,000 m/sec, so that it is well suited to be a launcher for the hypersonic ballistic range. The requirements for a hypersonic ground based flight test range and the feasibility of the use of light-gas gun launcher was discussed by Witcofski et al (Ref. 1). In this study the use of an Electromagnetic launcher (EML) and of the Ram Accelerator (RA) where also considered. It was concluded that with the present state of technology the most suitable candidate is the two-stage light-gas gun which can be made to launch models of about 20 cm. span and length of up to 90 cm. to speeds of up to 6 km/sec. It was contemplated, that at a later stage, using more advanced launcher technology, the models can be increased to 30 cm - 45 cm in span and the velocity range will be increased to 10 km/sec to 15 km/sec.

The free flight range technology seems to enable the best simulation of atmospheric free flight conditions in a ground based facility. The range concept is most suitable since it uses quiescent arbitrary gas in its test sections in which the model flies at the design hypersonic speed. While in other test facilities, such as the various types of shock tunnels and gun tunnels, it is required to compress and heat the test gas to high stagnation temperatures and pressures followed by a rapid expansion in high Mach number nozzles. This process causes disturbances due to dissociation and ionization of the gas in the stagnation region as well as disturbances due to nozzle expansion non-uniformities, boundary layer effects, etc. which are encountered in such facilities.

The External Propulsion Accelerator was proposed by J. Rom (Ref. 2) and certain preliminary aspect of its characteristics were presented in Refs. 3, and 4. Some analytical investigations, based on many simplifying assumptions, for the establishment of combustion front ahead of the forward facing step and on spherical nosed blunt bodies in hypersonic flows of detonable mixtures, including the studies of the oscillations that may occur were investigated by

*Professor, Lady Davis Chair, Faculty of Aerospace Engineering, technion-Israel Institute of Technology. Fellow AIAA.

†Associate Professor, Department of Aerospace Engineering. Senior Member AIAA.

‡Professor, Department of Mechanical Engineering. Fellow AIAA.

§Graduate Research Assistant, Department of Aerospace Engineering

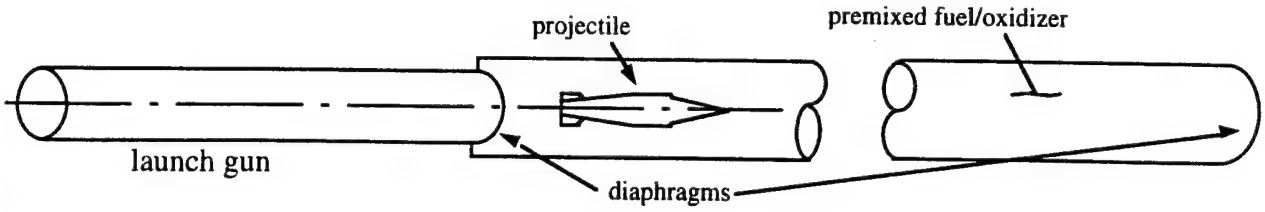

Figure 1. External propulsion accelerator facility.

Tivanov and Rom (Ref. 5, 6 and 7). A more detailed study of the combustion-detonation characteristics using the solutions of the full Navier- Stokes equations with chemical processes on projectiles in the External propulsion Accelerator is presented in Ref. 8.

The External Propulsion Accelerator has been developed following the development of the Ram Accelerator by A. Hertzberg and his co-workers (Ref. 9) at the University of Washington. The Ram Accelerator method utilizes the idea of using a premixed fuel/oxidizer mixture in the launcher barrel and injecting a projectile at supersonic speeds into this mixture. Thrust is generated by the ramjet combustion obtained between the tube wall and the projectile, where the projectile acts as a ramjet centerbody and the barrel is basically a long cowling, and combustion is initiated and stabilized by the interaction of the shock waves from the projectile nose with the barrel walls.

In contrast to the Ram Accelerator, in the External Propulsion Accelerator the thrust is generated purely by the interactions between the shock waves from the projectile nose with combustion generated by normal shock waves generated on the projectile body by a ramp or a forward facing step or by a ring wing, completely independent of the barrel walls. A schematic diagram of this facility is shown in Fig. 1.

Since the projectile flies in a premixed fuel/oxidizer atmosphere, the difficult problem of mixing the fuel and oxidizer, which plagues all airbreathing propulsion methods proposed for the remaining difficult issues of the ability to initiate and stabilize the combustion front on the projectile in such a way that positive thrust can be generated. The previous studies (Refs. 3, 4 and 8) indicated that a relatively small forward facing step on the projectile shoulder will be able to induce a detonation wave and induce large combustion around the projectile aft-body and base resulting in reasonably high thrust levels.

The recent study, presented in Ref. 8, utilizes the solution of the Navier-Stokes equations for flows with chemical processes which was adapted for the Ram Accelerator calculations at ARL by Nusca (Refs. 10, 11). Calculations of the flow with combustion on the projectile designs proposed for the External Propulsion Accelerator are presented. This calculation uses the Rockwell Science Center USA-RG (Unified Solution Algorithm Real Gas) code written by Chakravarthy et al (Refs. 12, 13). This CFD code includes the full 3D unsteady Reynolds-Averaged Navier-Stokes (RANS) equations including equations for chemical kinetics (finite-rate and equilibrium).

These equations are cast in conservation form and converted to algebraic equations using upwind finite-difference and finite-volume formulations. The equations are solved using a second-order TVD (total variation diminishing) scheme which is used to insure non-oscillatory numerical behavior. Following these calculations, the forward facing step configuration is tested in the ARL Ram Accelerator facility (Refs. 14, 15) using subcaliber models.

The projectile external shape is composed of a shallow sharp nosed cone followed by a forward facing step, a short length of a cylindrical body and a conical afterbody with a blunt base. Combustion is generated by the detonation wave established in front of the step, using steps of about 1 mm height. The combustion results in a region of high pressure, high temperature gas engulfing the back parts of the projectile resulting in significant net positive thrust. This region of combustion is confined by the hypersonic flow structure generated by the interactions of the shock wave ahead of the step which is followed by the combustion - detonation front. This is an excellent demonstration of external propulsion in which supersonic combustion is confined by the external flow without any structural boundaries. The step projectile geometry and non-reacting flow structure is illustrated for a 1 mm step projectile in Fig. 2.

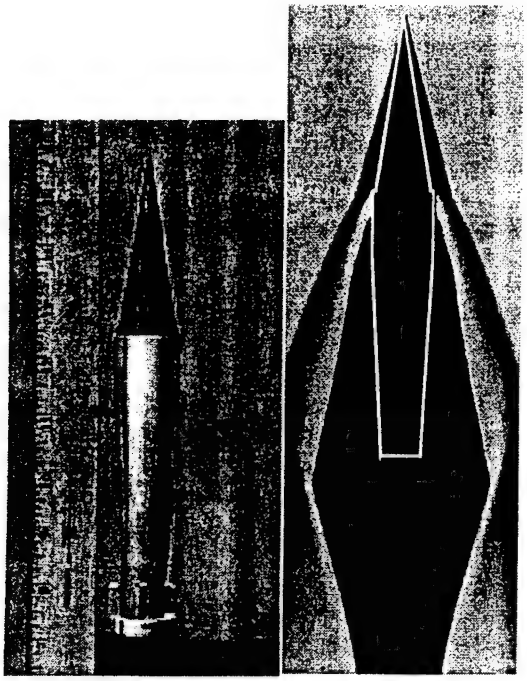

a.) b.)

Figure 2. External propulsion hypersonic projectile with forward-facing step. a.) projectile fired at U.S.. Army research Laboratory 120 mm accelerator b.) computational solution for pressure contours over this projectile (non-reacting case.)

The calculations in Ref. 8 indicated that the thrust levels which can be achieved in the EPA are on the order F/pA = 3. This thrust level can be increased with optimized configurations of the projectile and more energetic mixtures. The axisymmetric projectile configuration needed for the thrust generation in the launcher can be used as the cover for the hypersonic model which can be installed inside the projectile. Upon exit of the hypervelocity projectile from the launcher tube the projectile can be opened an separated from the model which is then free to fly at the launching hypersonic speed in the instrumented range.

Hypersonic Test Facility

In this application, the hypersonic testing facility will be comprised from: 1. The Accelerator section. 2. Sabot separation section. 3. Ballistic Range for aerodynamic models free flight testing. 4. Decelerator section for model retrieval. These parts are described below:

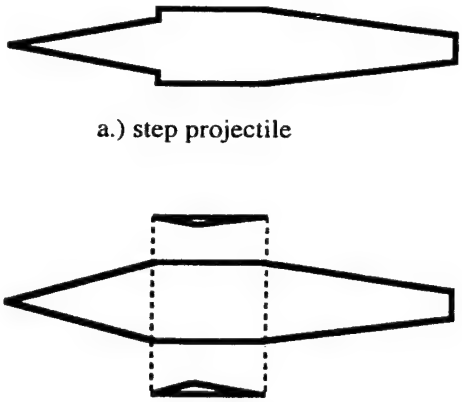

a.) step projectile

b.) ring "scramjet" projectile

Figure 3. External propulsion accelerator projectile types. a.) forward-facing step with shock-induced combustion b.) ring projectile with concentric cowl, which can operate as a scramjet.

1. *The Accelerator Section*

The accelerator is comprised of two parts, an initial accelerator for accelerating the model with its sabot to the required insertion speed of 1,000 to 1,400 m/sec. (M between 3 to 4) and the External Propulsion launcher tube which will accelerate the model with its sabot into the test range. The flight Mach Number in the ballistic range can be then set to the required hypersonic speed with the possibility of reaching M = 30.

The type of initial accelerator and the length of the External Propulsion Launcher depend on the allowable acceleration for the model. Simple aerodynamic shapes used for hypersonic flight, such as blunt reentry bodies, slender shuttle type configurations and wave riders with hardened on board instrumentation can be built to operate up to 50 Kg's acceleration level. In this case, a gun powder launcher can be used for the initial acceleration and the acceleration level of the External Propulsion launcher can be adjusted to the desired level.

The gun launcher will require lengths of up to 5 meters and the External Propulsion launcher for 50 Kg's will be about 10 meters for M = 7 testing, 40 meters for M = 10 testing and about 150 meters for M = 15 testing. For Mach number 30 testing a launcher length of about 700 meters will be required. For more sophisticated models

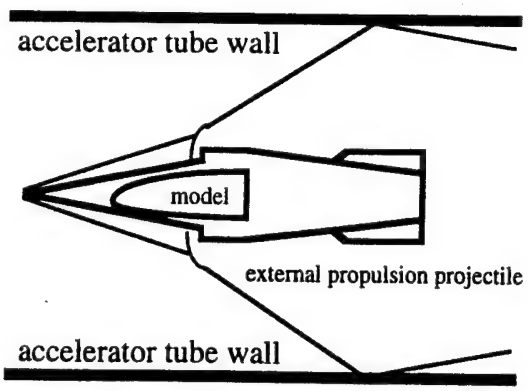

Figure 4. Proposed scheme for using an external propulsion projectile for sabot launching of a hypersonic freeflight model.

requiring lower values of acceleration, the initial accelerator can be either a Ram Accelerator stage initiated by a small light gas gun or a small rocket or the initial acceleration can be achieved directly by a rocket motor which will separate at the entrance to the External Propulsion launcher. The length of this launcher varies inversely with the acceleration levels, i.e. lower acceleration will require the correspondingly longer lengths.

The External Propulsion launcher diameter should be about 4 times the model maximum diameter or span. Therefore, a launcher of 1m diameter will enable launching of models of 25 cm. span or diameter and the launcher tube diameter can be reduced to 40 cm for 10 cm models. Of course larger models can be considered with increase in size of the facility.

2. *Sabot Separation Section.*

Since the projectile shapes required for the initial accelerator and for the External propulsion Accelerator should be of a specified axisymmetric shape, the aerodynamic model must be encased in a sabot, as illustrated in Fig. 4. The outside shape of this sabot should be in accordance with the external propulsion projectile design while supporting the model to withstand the acceleration levels. Upon exit from the accelerator launcher the sabot should be separated either mechanically or by special mechanism which will be initiated at the exit and the sabot parts should be retained in this separation section while the free model flies into the test range.

3. *Ballistic Range Section.*

The free model can now fly in the instrumented ballistic range where its instantaneous trajectory positions and attitudes can be photographed and measured as well as any on board instrumentation can be monitored by telemetering system. If we consider models of 10 cm to 25 cm in diameter or span, such models are sufficiently large to include most details of the aerodynamic design, including deflected control surfaces and/or small control jets actuated by small rockets or gas supply.

The ballistic range can either be an atmospheric range or be enclosed in a large tube enabling controlled atmosphere for simulation of pressure-altitude effects and also atmospheric composition effects studies.

4. *Deceleration Section.*

The energy imparted to the model traveling at Mach 6 to 30 is very large and must be absorbed in order to stop the model. For simple models, the models can be expandable and a conventional "catcher" can be used. For more sophisticated and expansive models there may be some possibilities of some energy absorbing methods for arresting the models, at least in the lower hypersonic speed range.

Conclusions

The concept of using the EPA for launching large aerodynamic models to hypersonic speeds has been introduced. It has been shown that with acceleration levels which can be achieved in the EPA, about 50,000 g's, the length of launcher needed for hypersonic speeds would be reasonable, about 150 meters for Mach 15 flight.

A ballistic range for testing aerodynamic models of span 25 cm could be constructed using an accelerator tube of diameter 100 cm. The model would be encased in an EPA projectile-sabot and separated before entering the free flight ballistic range. This would enable exact simulation of hypersonic flight

Acknowledgments

This work has been conducted as part of the Maryland Center for Hypersonic Education and Research is supported under NASA grant NAGW-3715, with Mr. Stephen Wander as technical monitor, to whom appreciation is expressed.

Thanks are also expressed to Michael Nusca and David Kruczynski of the U.S. Army Research Laboratory at Aberdeen Proving Grounds. The participation of the first author in this research program has been supported in part by the U.S. government through the European Office of the U.S. Army Research Office, contract number N6817194C 9065.

References

1. Witcofski, R., Scallion, W., Carter, D. Jr. and Courter, R., "An Advanced Hypervelocity Aerophysics Facility: A Ground-Based Flight-Test Range," AIAA Paper 91-0296, 1991.

2. Rom, J., "Method and Apparatus for Launching a Projectile at Hypersonic Velocity" U.S. Patent 4,932,306, June 12 1990.

3. Rom, J. and Kvity, Y., "Accelerating Projectiles up to 12 km/sec. Utilizing the Continuous Detonation Propulsion Method," AIAA Paper 88-2969, 1988.

4. Rom, J. and Avital, G., "The External Propulsion Accelerator: Scramjet Thrust Without Interaction with the Accelerator Barrel," AIAA Paper 92-3717, 1992.

5. Tivanov, G. and Rom, J., "Investigation of Hypersonic Flow of a Detonable Gas Mixture Ahead of a Forward Facing Step" AIAA Paper 93-0611, 1993.

6. Tivanov, G. and Rom, J., "Stability of Hypersonic Flow of a Detonable Gas Mixture in the Stagnation Region of a Blunt Body and a Forward Facing Step ," Proceedings of the 33rd Israel Annual Conference of Aeronautics and Astronautics, Feb. 1993.

7. Tivanov, G. and Rom, J., "Analysis of the Stability Characteristics of Hypersonic Flow of a Detonable Gas Mixture in the Stagnation Region of a Blunt Body," AIAA Paper 93-1918, 1993.

8. Rom. J., Nusca. M., Kruczynski, D., Lewis, M., Gupta, A. and Sabean, J., "Investigations of the Combustion Induced by a Step on a Projectile Flying at Hypersonic Speed in the External Propulsion Accelerator," AIAA paper 95-0259, January 1995.

9. Hertzberg, A., Bruckner, A.P. and Bogdanoff, D.W., "Ram Accelerator: A New Chemical Method for Accelerating Projectiles to Ultrahigh Velocities" AIAA Journal, Vol. 26, No. 2, 1988, pp 195-203.

10. Nusca, M.J., "Numerical Simulation of Fluid Dynamics with Finite-Rate and Equilibrium Combustion Kinetics for the 120 mm Ram Accelerator" AIAA Paper 93-2182, 1993.

11. Nusca, M.J., "Numerical Simulation of Gas Dynamics and Combustion Kinetics for a 120 mm Ram Accelerator" First International Workshop on Ram Accelerator, ISL, France, 1993.

12. Chakravarthy, S.R., Szema, K.Y., Goldberg, U.C., Gorski, J.J. and Osher, S., "Application of a New Class of High Accuracy TVD Schemes to the Navier-Stokes Equations" AIAA Paper 85-0165, 1985.

13. Palaniswamy, S., Ota, D.K. and Chakravarthy, S.R., "Some Reacting Flow Validation Results for USA-Series Codes" AIAA Paper 91-0583, 1991.

14. Kruczynski, D.L. and Nusca, M.J., "Experimental and computational Investigation of Scaling Phenomena in a Large Caliber Ram Accelerator" AIAA Paper 92-3425, 1992.

15. Kruczynski, D.L., "New Experiments in a 120 mm Ram Accelerator at High Pressures" AIAA Paper 93-2589, 1993.

ANNEX 6

DECEMBER 1994

ANALYSIS OF THE INITIATION OF DETONATION ON A HYPERVELOCITY PROJECTILE AND IT'S MAXIMUM VELOCITY IN THE EXTERNAL PROPULSION ACCELERATOR

by

J. Rom
Faculty of Aerospace Engineering
Technion - Israel Institute of Technology
Haifa, Israel

TAE No. 729

The research was supported in part by the European Research Office
U.S. Army under contract N68171-94-C-9065

ANALYSIS OF THE INITIATION OF DETONATION ON A HYPERVELOCITY PROJECTILE AND IT'S MAXIMUM VELOCITY IN THE EXTERNAL PROPULSION ACCELERATOR

Josef Rom [1]

Technion - Israel Institute of Technology, Haifa 32000, Israel

ABSTRACT

The initiation of detonation and the subsequent acceleration of the projectile in the in-tube chemical launchers for accelerating projectiles to hypervelocity are investigated using an energy balance analysis. The question of initiation of detonation by the hypervelocity projectile is evaluated by the use of the blast wave analogy. In this analysis the blast energy required for the initiation of detonation is equated with the work done by the drag force of the traveling projectile. This analysis can be applied to the two types of in-tube chemical launchers, the Ram Accelerator and the External Propulsion Accelerator. It is shown that in the External Propulsion Accelerator, where the detonation is initiated by the hypersonic flow of a detonable gas mixture flowing into a forward facing step, the drag of this blunt step is more then sufficient to initiate detonation at projectile velocity well below the Chapman-Jouguet detonation velocity. Furthermore, the energy balance analysis is also applied to evaluate the maximum velocity which can be achieved in the in-tube accelerators when the available chemical reaction energy is utilized. It is shown that in the Ram Accelerator, due to the high drag caused by the choking of the flow between the projectile and the tube wall as the projectile Mach number is increasing, the maximum projectile velocity is limited to about 1.2 - 1.3 the Chapman-Jouguet detonation velocity. It is observed that the experimental measurements of the velocity to "unstart" in the Ram Accelerator are at most at 1.15 - 1.2 times the Chapman Jouguet detonation velocity, which is in agreement with the results of this analysis. In the External Propulsion Accelerator, the total drag coefficient of the projectile is much lower and remains almost constant at the hypersonic Mach numbers, while the useful chemical reaction energy increases with increasing flight Mach number. Therefore, the maximum projectile velocity in the

---

[1] Professor, Lady Davis Chair, Faculty of Aerospace Engineering, Fellow AIAA

External Propulsion Accelerator can reach the level of 6 times the Chapman-Jouguet detonation velocity, which can be well above escape velocity into space.

NOMENCLATURE

B	$(Q / c_v) (E / R T^2_s)$
c_p	specific heat coefficient at constant pressure
c_v	specific heat coefficient at constant volume
C_D	drag coefficient
d	diameter
D	detonation speed
Dam	Damkohler number
e	natural log base
E	activation energy
H	step height
M	Mach number
p	pressure
Pr	Prandtl number
Q	heat of chemical reactions
R	gas constant
R_b	radius of nose of the body

R_s	distance between normal shock and step face
Re	Reynolds number
t	time
T	Temperature
u, v	velocity components in the x, y direction
$\bar{v}$	effective velocity
V	velocity vector
x, y, z	Cartesian coordinates
Z	coefficient of chemical reaction in the Arrhenius rate equation
β	mass fraction of species; ratio of combustion tube to projectile diameters
γ	specific heat ratio
η_c	Carnot efficiency
λ	detonation cell size
Λ	$H e B/\gamma \ \bar{v} \tau_r$
θ	$E (T - T^*) / R T^{*2}$
ρ	density
τ	induction time
τ_q	measure of time of flow between shock wave and step face
τ_r	measure of time of chemical reaction

INTRODUCTION

The in-tube chemical launchers for accelerating projectiles to hypervelocity utilize, in the superdetonative mode of operation, the possibilities of generating continuous thrust by initiating detonation in the premixed fuel/oxidizer mixture by a shock wave. The first method proposed for an in-tube chemical launcher was the Ram Accelerator, originated and developed by A. Hertzberg and his colleagues at the University of Washington (Ref. 1). The concept of the Ram Accelerator, operating in the superdetonative mode, is based on utilization of the scramjet cycle, where the projectile acts as a free centerbody and the tube as an extended cowling. The projectile is fired at high initial speed into the tube which is filled with the premixed fuel/oxidizer mixture, where the detonation velocity in this mixture is lower than the projectile velocity. The sharp nosed projectile diameter is slightly less than the tube diameter (typically 70% to 80%) therefore the nose shock wave is reflected from the tube wall into the projectile centerbody. Under proper conditions this reflected shock wave initiates a detonation process so that when the products of the chemical reactions are expanded on the rear part of the projectile, thrust is generated. Another method for operating the chemical in-tube accelerator is based on the utilization of the external propulsion cycle, proposed by Rom (Ref. 2,3). In deference from the Ram Accelerator, in the External Propulsion Accelerator the projectile diameter is much smaller than the tube diameter so that there is no interaction between the flow over the projectile and the tube wall over the complete length of the projectile. In this case the detonation is established by aerodynamic means on the projectile, such as a forward facing step on the projectile shoulder (or a blunt leading edge of a ring wing positioned on the rear part of the projectile). In the case of the projectile with the forward facing step, a normal shock wave is established ahead of the forward facing step in supersonic and hypersonic flows. When a detonable gas mixture is flowing at these high speeds into the forward facing step, this normal shock wave compresses and heats up the mixture to very high pressures and temperatures. For high enough projectile velocity, the heating and compression of the combustible mixture by this shock wave can result in initiation of a detonation front in the region between the shock wave and the face of the step. Due to the interaction between the shock wave from the projectile nose with the detached shock-detonation wave established in front of the step, the high pressure high temperature chemical reaction products are

confined by the contact surface generated at the wave intersection point. Therefore, the aerodynamically confined region filled with the chemical reaction products is in effect an "external combustion chamber" which extends further on the rear part and in the base region of the projectile and is used to produce thrust on the projectile.

It is obvious that the projectile configurations and therefore the initiation of detonation and the combustion process are very different in the cases of the Ram Accelerator (RA) and in the External Propulsion Accelerator (EPA). In the EPA, using the projectile configuration with a forward facing step, the detonation is initiated by the detached (nearly normal) shock wave which is established at hypersonic speed in front of the step. An investigation of the required step height and of the position of the reaction front ahead of the step was presented by Tivanov and Rom (Ref. 4). Furthermore, there are numerical solutions for the flow over a projectile with a step, presented by Rom et al (Ref. 5) and an example of such a calculation is also included in a paper by Nusca (Ref. 6). It was shown by Tivanov and Rom (Ref. 4) that step heights of less than 1 mm may enable initiation of detonation for hydrocarbon fuels, such as methane and acetylene, as well as hydrogen, where all of these fuels are premixed with oxygen. Since these studies are based on rough approximations, it is important to investigate further, based on the present knowledge of detonation processes, the initiation of detonation and the type of combustion process that we may expect around the forward facing step and the over the projectile in the EPA.

In the present paper the initiation of detonation and the subsequent acceleration of the projectile in the in-tube chemical launchers for accelerating projectiles to hypervelocity are investigated using an energy balance analysis. The question of initiation of detonation by the hypervelocity projectile is evaluated by the use of the blast wave analogy. In this analysis the blast energy required for the initiation of detonation is equated with the work done by the drag force of the traveling projectile. In the case of the Ram Accelerator, due to the large drag caused by the choking of the flow between the projectile and the tube wall as the projectile Mach number increases, the drag work is sufficient to induce detonation after the projectile is accelerated to above a certain velocity. It is shown that in the External Propulsion Accelerator, where the detonation is initiated by the hypersonic flow of a detonable gas mixture flowing

into a forward facing step, the drag of this blunt step is more then sufficient to initiate detonation at projectile velocity well below the Chapman-Jouguet detonation velocity.

The energy balance analysis is also applied to evaluate the maximum velocity which can be achieved in the in-tube accelerators. It is shown that in the Ram Accelerator, due to the high drag caused by the choking of the flow between the projectile and the tube wall, the maximum projectile velocity is limited to about 1.2 - 1.3 the Chapman-Jouguet detonation velocity. It is observed that the experimental measurements of the velocity to "unstart" in the Ram Accelerator are at most 1.15 - 1.2 times the Chapman Jouguet detonation Mach number, which are in agreement with the results of this analysis.

When this analysis is applied to the External Propulsion Accelerator, it is noted that the total drag coefficient of the projectile is much lower and remains almost constant at the hypersonic Mach numbers. In this case the available chemical reaction energy increases with increasing flight Mach number. It is shown that the maximum projectile velocity in the External Propulsion Accelerator can be in the order of 6 times the Chapman-Jouguet detonation velocity, which is well above escape velocity into space.

INITIATION OF DETONATION BY A BLUNT BODY

A discussion on the initiation of detonation on a blunt nosed projectile is presented by Lee (Ref. 7,8). It is proposed there to estimate the requirement for initiation of detonation by a hypervelocity projectile by the use of the blast wave analogy, thus equating the blast energy required for the initiation of detonation with the work done by the drag force of the traveling projectile. Various results of the measurement of the energy for direct initiation of detonation are discussed by Lee (Refs. 7,8). The analysis is then based on the relation, first stated by Zeldovich, that this critical energy is dependent on the third power of the induction time (or induction length) for spherical blast waves. Using strong-blast theory, Lee derived the following expression for the critical energy, E_o , for spherical detonation

$$E_o = 1.692\pi\rho_o D^2 (2.5D\tau_r)^3 \qquad (1)$$

and for cylindrical detonation

$$E_o = 1.252\pi\rho_o D^2 (2D\tau_r)^2 \qquad (2)$$

where D is the detonation velocity for the Chapman-Jouguet conditions and τ_r is the induction time. In Ref. 8 Lee states that "if the induction time evaluated at the shock temperature corresponding to a Chapman-Jouguet detonation is used for τ_r than the value of E_o evaluated from Eq. 1 is about three orders of magnitude smaller than the experimental values". The experimental values, to which Lee refers, are determined from the measurements of the average cell size, λ, and from the evaluation of the critical tube diameter determined for detonation waves traveling into a stationary detonable mixture. Lee then assumed that the characteristic chemical length is the cell size, so that the characteristic time is proportional to λ/D.

Using semi-empirical considerations, Lee suggests the following relations for the energy for direct initiation, for the spherical and cylindrical detonation cases for fuel-air mixtures,

For spherical detonation (Ref. 7),

$$E_o = 252 p_o M_{CJ}^2 \lambda^3 \qquad (3)$$

For cylindrical detonation, the critical energy per unit length is (Ref. 7),

$$E_o = 14.5 p_o M_{CJ}^2 \lambda^2 \qquad (4)$$

where λ, the cell size, is related to the induction time. The cell size was measured for detonations traveling into a stationary gas mixture at relatively low pressures, p_o in the range of 10 torr. to 200 torr. and up to atmospheric pressure.

The large discrepancy between the critical energy which is evaluated by applying the strong-blast theory as presented in Eqs. 1 and 2, using the induction time, τ_r , evaluated at the temperature corresponding to the Chapman-Jouguet detonation and the critical energy evaluated using the experimentally measured cell size, Eqs. 3 and 4, indicates a strong deficiency in our ability to evaluate correctly this energy for

initiation of detonation on a traveling projectile. It seems reasonable to expect that in the case of the flow of a detonable mixture at hypersonic speeds in and about the stagnation region of a blunt body the characteristic time for detonation should be the induction time evaluated from the chemical reaction rates at the temperature and pressure corresponding to the Chapman-Jouguet detonation. This discrepancy, which was pointed out by Lee in Ref. 7, should be investigated. Particularly since there are number of numerical calculations by Yungster et al (Ref. 9), Nusca (Ref. 6) and Li et al (Ref. 10) and supported by some RA experiments which indicate that the initiation of detonation is obtained and is computed using the induction time evaluated from the chemical reaction rates. In this respect, it will be extremely important to measure directly the initiation of detonation on a flying projectile in the EPA where the detonation will be initiated by a forward facing step.

When we consider the initiation of detonation ahead of a blunt body in hypersonic flow, it was also pointed out by Zeldovich that detonation will occur when the induction time is shorter than the flow time from the detached shock wave to the face of the body. The induction time is determined by the chemical reaction kinetics of the mixture at the conditions behind the detached shock wave while the flow time is a function of the detachment distance which varies with the radius of curvature of the blunt nose of the body. Analysis of certain aspects of the hypersonic flow over blunt bodies with chemical reactions were presented by Sichel and Galloway (Ref. 11) , Galloway and Sichel (Ref. 12) and Chernyi (Ref. 13). It was shown in these studies that the establishment of combustion in the stagnation region depends on the ratio of the ignition delay distance to the shock standoff distance. Sichel and Galloway (Ref. 11) define a parameter relating the ignition delay time, the body radius of curvature and the flow velocity. When this ignition delay parameter, $\kappa = u_\infty \tau / R_b$ (where u_∞ is the free stream velocity, τ is the ignition delay time and R_b is the spherical nose radius), is less than 1, then combustion will occur between the detached shock wave and the body surface.

Studies of hypersonic flows with oblique detonation are presented in Refs. 14 and 15. A study of the hypersonic flow of a premixed fuel/oxidizer mixture over a wedge and the characteristics of the oblique

detonation wave is presented by Powers and Stewart (Ref. 14) and studies of the oblique detonation wave by Li et al in Ref. 15.

INITIATION OF DETONATION BY A FORWARD FACING STEP

Since the forward facing step has an infinite radius of curvature at the stagnation region, the initiation of detonation will occur when the temperature behind the detached shock wave will be above the minimum auto-ignition temperature of the mixture. Therefore, above a minimum projectile velocity the temperature behind the detached shock wave will be higher then the auto-ignition temperature, and a detonation process will be initiated. Above the step, the shock wave will curve, reducing the radius of curvature as the distance above the step increases. As discussed by Lee in Ref. 7, when the shock wave curvature is reduced below a critical value and hence the flow divergence is too severe, then the reactions may be quenched even when the initial shock temperature, in the stagnation point, exceeds the auto-ignition limit. Therefore, in order to insure stabilization of the reaction front behind the detached shock wave a minimum step height is needed. This qualitative argument is in agreement with the results of the analysis of Tivanov and Rom (Ref. 4) where the minimum step height concept was introduced and evaluated by an approximate analysis. In the analysis in Ref. 4, it was shown that when $B\,\tau_q/\tau_r > 1/e$ then detonation can occur. Here, the time of reaction, τ_r / B, and the time of the flow between the detached shock wave and the body, τ_q, are estimated by the following relations:

$$\tau_r^{-1} = (Z/\bar{\rho})\ \exp(-E/R\,T_s) \qquad \tau_q = H/\bar{v}$$

where H is the step height and $\bar{v}$ is an average velocity in the stagnation region which can be evaluated from the solution of the hypersonic blunt body stagnation flow field (Ref. 16). A minimum step height needed for establishing a detonation front is then,

$$H \geq \tau_r\ \bar{v}/e\,B$$

This required step height can be defined in terms of a Damkohler number, Dam = $H / \tau_r \bar{v}$, which must be equal or greater then 1/ eB for detonation to be initiated and stabilized, and is determined by the mixture properties. This minimum step height was evaluated in Ref. 4 and is presented for mixtures of hydrogen-oxygen, acetylene-oxygen and methane oxygen as a function of the flow Mach number in Fig. 1a and 1b. It is possible to define a parameter $\Lambda = H\, e\, B / \tau_r \bar{v}$, which indicates the possibility of detonation. If $\Lambda > 1$ then detonation can develop while for $\Lambda < 1$ only deflagration can occur. This analysis is in agreement with the phenomenological analysis of Sichel and Galloway (Ref. 5). Their criterion for initiation of the combustion front on a blunt body represented by the ignition delay parameter $\kappa = u_\infty \tau / R_b$ (where τ is the ignition delay time and R_b is the spherical nose radius) is inversely proportional to the parameter Λ.

THE ENERGY REQUIRED TO INITIATE DETONATION

In order to define the conditions for the establishment of detonation on a projectile, consider the flow of the fuel/oxidizer mixture at hypersonic velocity over the conical nose of the projectile, as illustrated in Fig. 2. An oblique shock wave is formed on the cone, attached to the cone tip, compressing and heating the gas mixture. The nose cone angle is selected so a to keep the temperature behind the conical shock wave low enough so as to prevent significant chemical reaction from occurring on the projectile nose due to this shock wave over the range of the design flight Mach numbers. A forward facing step is positioned at the shoulder of the cone causing a normal shock wave ahead of the step which compresses and heats up the mixture so that exothermic reactions are sustained between the shock wave and the face of the step. As the temperature and pressure behind the detached normal shock wave increase the reaction front moves closer to the shock wave until a detonation front is established in front of the step. As the flows nears the outer corner of the step, the expansion fan from the corner will weaken and curve the initially normal detached shock wave. The reduced radius of curvature above the step corner will reach a value where the reaction front will separate from the curved shock wave. However for flows of high enough Mach numbers the reaction will be attached to the detached shock wave at least till it's intersection point

with the conical shock wave from the nose. So that all the incoming flow into the projectile nose up to the intersection point between the detached shock wave and the conical shock wave will pass through the reaction front initiated by the detached shock wave. Furthermore, at increasing flow Mach numbers the transmitted shock wave beyond the intersection may be still strong enough to sustain the reaction front further into the flow above the projectile until the local radius of curvature of the shock wave will be reduced so as to quench the reaction. In this case the layer of the high temperature high pressure reaction products confined by the contact sheet acts as an "external combustion chamber" for the projectile and its energy can be used to generate thrust on the rear part of the projectile.

A. Evaluation of the Minimum Mach Number for Initiation of Detonation on the Hypervelocity Projectile

The minimum Mach number for the initiation of detonation on a projectile with a forward facing step in the EPA can be evaluated by equating the critical energy required for direct initiation of cylindrical detonation, given by Eq. 2 with the work done by the drag force of the hypervelocity projectile of diameter d with a step H (where H/d << 1), thus

$$E_o = 1.252\pi\rho_o D^2 (2D\tau_r)^2 = 0.5\rho_o V_\infty^2 (2\pi dH) C_{D_{step}} \qquad (5)$$

Thus the minimum projectile speed in this case is expressed, as follows:

$$\frac{V_\infty^2}{D^2} = 2.504 \frac{H}{d}\left(\frac{D\tau_r}{H}\right)^2 \frac{1}{C_{D_{step}}} \qquad (6)$$

Since typical H/d values can be 1/30 and smaller , $D\tau_r$ /H should be less than 1(probably in the range of 1/3 to 1/5) for detonation to occur and $C_{D_{step}}$ for a forward facing step is about 1. Therefore, introducing these values into Eq. 6, the minimum projectile velocity that produces energy to balance the critical initiation energy for detonation is evaluated to be much below the detonation velocity. Since the projectile in the EPA is expected to fly well above the detonation speed then there is no problem of securing the energy required to initiate the detonation.

The energy balance, presented in Eq. 5, can be applied also to the projectile in the RA. In this case, the drag coefficient is equated with that of the drag of the projectile including the effects of the interaction between the projectile and the tube wall and the reference area is the cross section of the projectile body. As the projectile speed increases the drag force on the projectile increases so as to provide the energy for initiation of the detonation. At the lower initial speeds the required drag is provided by the perforated piston orbutrator which is used in the RA for initiation of the process.

B. Evaluation of the Maximum Velocity by the Energy Balance on the Hypervelocity Projectile in the EPA

As discussed before, the work done by the drag force acting on the hypervelocity projectile is balanced by the energy released by the detonating gas mixture. Following the discussion by Lee in Ref. 7, it is possible to evaluate the maximum velocity that can be reached by the projectile when all the combustion energy of the reacting mixture is utilized. This energy balance can be expressed by the following relation,

$$\rho_o\left(\frac{\pi(\beta d)^2}{4}\right)Q\eta_c = 0.5\rho_o V_{\infty_{max}}^2\left(\frac{\pi d^2}{4}\right)C_D \qquad (7)$$

where Q is the chemical energy per unit mass and η_c is the Carnot cycle efficiency. Now,

$$Q = \frac{D^2}{2(\gamma^2 - 1)} \qquad (8)$$

and then using Eq. 7 it can be shown that

$$\frac{V_{\infty_{max}}^2}{D^2} = \frac{\beta^2\eta_c}{C_D(\gamma^2 - 1)} \qquad (9)$$

and following Lee (Ref. 7), we can assume a value of 2/3 for η_c (assuming high combustion temperature of 3000° K and low temperature of 1000° K). In Eqs. 7 and 9, β is defined as the ratio of the outside diameter of the external combustion zone to the projectile diameter. In the EPA the thickness of the external combustion layer varies as a function of the flow Mach number. It was found from the numerical

calculations, which are reported in part in Refs. 5,6 that for the 32 mm diameter projectile with a 1 mm step the combustion layer thickness varies from 3 step heights at Mach number 5 to 5.5 step heights at Mach number 6 and to 17 step heights at Mach number 10. The value of C_D for the cone with the 1 mm step is about 0.26-0.28 for Mach numbers above 5 (for cone-cylinder without the step the drag coefficient is about 0.07-0.08). Then, using Eq. 9, the maximum projectile velocity can be about 1.9 times the detonation velocity at Mach number 5, about 2.1 times the detonation velocity at Mach number 6 and about 3.3 times the detonation velocity at Mach number 10. At higher flight Mach numbers the combustion may extend to the tube wall, then for the 120 mm tube with the 32 mm projectile the maximum velocity is about 6 times the detonation velocity, which is well above the escape velocity to orbit into space. Therefore, when the projectile is injected at initial velocity between Mach 5 to 6, only about 21% to 28% of the energy of combustion is used to overcome the drag, so that about 72% to 79% of the combustion energy is available for accelerating the projectile. Actually the available combustion energy increases as the Mach number increases, reaching to about 90% at Mach number 10 and will be even higher as the Mach number is increased further. In this case of accelerating the projectile in the EPA we can conclude that only a small fraction of the available combustion energy which can be released in the detonation process is needed to overcome the drag of the hypervelocity projectile and this available energy can be used for accelerating the projectile to higher hypervelocity. Of course as the projectile velocity increases the problems of heating and ablation of the projectile surfaces and the aerodynamic and acceleration loads on the projectile structure become more critical.

C. Evaluation of the Maximum Velocity by the Energy Balance on the Hypervelocity Projectile in the RA

It is of interest to evaluate the maximum velocity of the projectile in the RA by this energy balance analysis. Particularly, since there are some experimental results on the operational limits in the RA. Thus using a similar analysis, we can apply the energy balance and evaluate the maximum velocity applying Eq. 9 to the case of the projectile in the RA. Such evaluation was first done by Lee in Ref. 7. There Lee assumes a value of the drag coefficient for the projectile flying in the RA tube to be of order 1, $C_D = O(1)$, which is equal to the drag coefficient of a blunt body at hypersonic speeds. So, using Eq. 9 with $\gamma = 1.4$

and $\beta = 1.5$, he estimates the value of the maximum projectile velocity to be about 1.3 times the detonation velocity. He then concludes that when the projectile velocity is equal to the detonation velocity about 75% of the available energy is used to overcome the drag so that only a small fraction of the energy is available for additional acceleration of the projectile.

The projectiles used in the RA of the University of Washington and ARL, as presented in Refs. 1 and 6, has a drag coefficient of about 0.2 -0.25 at Mach numbers above 5 in free flight without the tube wall interference. However, the multiple shock wave reflections from the tube wall to the projectile center-section and the blunt leading edges of the fins which may initiate detonation increase the drag coefficient of the projectile considerably in its flight in the accelerator tube. As the projectile velocity increases the strength of the reflected oblique shock waves increase and the total pressure loss in the shock interference region on one hand provides energy for the initiation of the detonation but on the other hand due to the extremely high drag consumes an increasing portion of the available reaction energy until the energy required to overcome the drag force will be larger than the available energy from the chemical reaction and we will face the conditions of "unstart". At these conditions the assumption of a drag coefficient of about 1, which is the value for a blunt body, seems reasonable.

An experimental investigation as to the limit of operation in the RA was conducted at the University of Washington (Ref. 17). The RA tube diameter is 38 mm while the diameter of the projectile body is 29 mm. Therefore, using $C_D = 0.8\text{-}0.9$ in Eq. 9, and the appropriate values of the other parameters, i.e. $\gamma = 1.4$ and $\beta = 1.31$, we obtain that the maximum value of the projectile speed in the University of Washington RA facility is about 1.2-1.3 times the detonation velocity. The experiments were conducted with groups of mixtures. The first group was based on a methane-oxygen diluted with varying amounts of nitrogen, that is $2.8\ CH_4 + 2\ O_2 + X\ N_2$. The second group was based on a hydrogen-oxygen diluted with methane, that is $2\ H_2 + 2\ O_2 + X\ CH_4$. The five finned projectile was fired into these mixtures and its flight characteristics measured. It was found that for the very energetic mixtures, where the dilutant was very small, the projectile unstarted at relatively low velocity, even below the Chapman-Jouguet velocity. This can be explained by the fact that for these very energetic mixtures the energy release by the

detonation generated by the reflected shock wave is so large that it chokes the flow, increasing the effective drag of the projectile so that the projectile is "stopped" - then the "unstart" in the terminology of Ref. 17 occurs since the stopped projectile cants hits the wall and is destroyed. However, for moderate dilutants the projectile accelerated from an initial Mach number of 3.8 to above the Chapman-Jouguet detonation velocity reaching Mach numbers up to about 5.8. In these experiments, as the projectile velocity increased, at a certain speed the projectile experienced the phenomenon of "unstart", which was generally followed by disintegration of the projectile. These measurements of the projectile velocity to "unstart", which are reported in Ref. 17, are presented in Figs. 3a and 3b, for the nitrogen diluted mixtures and for the methane diluted mixtures, respectively. Observing the results of the measurements of the Mach number at "unstart" conditions, it turns out that the ratio of M_{unstat}/ M_{CJ} is constant for all the runs with the methane-oxygen with the nitrogen dilutants, $M_{unstat}/ M_{CJ} = 1.2$, and for the hydrogen-oxygen with methane dilutants the value was also constant, $M_{unstat}/ M_{CJ} = 1.15$ (as shown in the tables attached to Figs. 3a and 3b). This is in remarkable close agreement with the energy balance analysis results (when we identify that the maximum velocity is just above the velocity to unstart), which was calculated to be, $M_{unstat}/ M_{CJ} = 1.2$-1.3. We find that there is an excellent qualitative agreement, the fact that $M_{unstat}/ M_{CJ} =$ constant, and also reasonable quantitative agreement, less than 10% deviation in the value of the maximum Mach number, considering the rough evaluation of the drag coefficient for the projectile with the tube walls interference.

In the discussion in Ref. 17, it is suggested that the "unstart" phenomenon is caused by projectile disintegration due to configuration distortion by aerodynamic heating and mechanical stresses. It is assumed that this distortion is a result of the aerodynamic heating and pressure and acceleration loads which cause the projectile to cant and be destroyed, as shown in Ref. 18. A test of this assumption was performed by firing a titanium nosed projectile instead of the aluminum projectiles used in all previous tests. The titanium projectile was able to withstand the choking effects at the maximum velocity without significant distortions and actually exited from the accelerator tube. A flight trajectory comparison between the aluminum and titanium projectiles was presented in Ref. 17 and is shown in Fig. 4. It is interesting to note, that this titanium projectile reached a maximum velocity after traveling about 13 m in

the tube and for the last 2-3 meters it continued at constant velocity of 2300 m/sec. The aluminum projectile had an unstart at a velocity of 2200 m/sec after traveling about 10 m in the tube. For this aluminum projectile the Mach number at unstart was 1.15 times the Chapman-Jouguet Mach number while the maximum Mach number of the titanium projectile is 1.2 times M_{CJ}, which is in close agreement with the estimated value from the energy balance analysis.

SUMMARY AND CONCLUSIONS

It is shown that the energy balance analysis of the projectile flight in the in-tube chemical accelerators can be used to evaluate the velocity required to initiate the detonation process on the rear part of the projectile. Applying this analysis to the projectile designed for the External Propulsion Accelerator, where the detonation is initiated on the blunt forward facing step, it is shown that even at velocities below the Chapman-Jouguet detonation velocity the drag work of the step on the projectile is sufficient to initiate the detonation.

It is shown that using the energy balance analysis it is possible to evaluate the maximum velocity that can be achieved in the in-tube chemical accelerators by balancing the drag work of the projectile with the utilization of the total available chemical reaction energy.

In the Ram Accelerator case, the high drag experienced by the projectile due to the choking of the flow at increasing Mach numbers results in limiting the projectile velocity to about 1.2 - 1.3 times the Chapman-Jouguet detonation velocity. This result is supported by the measurements of the "unstart" phenomenon in the RA at the University of Washington (Ref. 17).

Using this analysis, it is shown that the maximum projectile velocity in the External Propulsion Accelerator can be few times the Chapman-Jouguet detonation velocity and may reach 6 times this velocity, which is well above the escape velocity into space.

ACKNOWLEDGMENTS

The research was supported in part by the European Research Office U.S. Army under contract N68171-94-C-9065.

REFERENCES

1. Hertzberg, A., Bruckner, A.P. and Bogdanoff, D.W., " Ram Accelerator: A New Chemical Method for Accelerating Projectiles to Ultrahigh Velocities", AIAA Journal, Vol. 26, No. 2, 1988, pp. 195-203.

2. Rom, J., "Method and Apparatus for Launching a Projectile at Hypersonic Velocity", U.S. Patent 4,932,306, June 12, 1990.

3. Rom, J. and Avital, G., "The External Propulsion Accelerator: Scramjet Thrust Without Interaction With Accelerator Barrel" , AIAA Paper 92-3717, 1992.

4. Tivanov, G. and Rom, J., "Investigation of Hypersonic Flow of a Detonable Gas Mixture Ahead of a Forward Facing Step", AIAA Paper 93-0611, 1993.

5. Rom, J., Nusca, M.J., Kruzcynski, D., Lewis, M., Gupta, A.K. and Sabean, J., "Investigations of the Combustion Induced by a Step on a Projectile Flying at Hypersonic Speeds in the External Propulsion Accelerator", AIAA Paper 95-0259, 1995.

6. Nusca, M.J., "Reacting Flow Simulations for Large Scale Ram Accelerator", AIAA Paper 94-2963, 1994.

7. Lee, J.H.S., "On the Initiation of Detonation by a Hypervelocity Projectile", Paper presented at the Zeldovich Memorial Conference on Combustion, Sept. 12-17, 1994, Voronovo, Russia.

8. Lee, J.H.S., "Dynamic Parameters of Gaseous Detonations", Annual Review of Fluid Mechanics, Vol. 16, 1984, pp 311-316.

9. Yungster, S., Eberhardt, S. and Bruckner, A.P., "Numerical Simulation of Shock Induced Combustion Generated by High Speed Projectiles in Detonable Gas Mixtures", AIAA Journal, Vol. 29, No. 2, 1991, pp. 187-199.

10. Li, C., Kailasanath, K. and Oran, E.S., "Detonation Structures on Ram-Accelerator Projectiles", AIAA Paper 94-0551, 1994.

11. Sichel, M. and Galloway, A.J., "Regimes of Exothermic Blunt Body Flow", Astro. Acta, Vol. 13, 1967, pp. 137-145.

12. Galloway, A.J. and Sichel, M., "Hypersonic Blunt Body Flow of $H_2 + O_2$ Mixtures", Astro. Acta, Vol. 15, 1969, pp. 89-105.

13. Chernyi, G., "Supersonic Flow Past a Sphere of a Hot Gas Mixture With Consideration of Ignition delay Time", Akad. Nauk. SSSR, Mekh. Zhidkosti Gaza, No.1, 1968, pp. 20-32.

14. Powers, J.M. and Scot Stewart, D., "Approximate Solution for Oblique Detonation in Hypersonic Limit" AIAA Journal, Vol. 30, No. 3, 1992, pp 726-736.

15. Li, C., Kailasanath, K. and Oran, E.S., "Structure of Reaction Waves Behind Oblique Shocks", The 13th International Colloquium on Dynamics of Explosions and Reactive Systems, Nagoya, Japan, 1991.

16. Hayes, W.D. and Probstein, R.F., "Hypersonic Flow Theory", Academic Press, 1959.

17. Knowlen, C., Higgins, A. and Bruckner, A., "investigation of Operational Limits to the Ram Accelerator", AIAA Paper 94-2967, 1994.

18. Hinkey, J.B., Burnham, E.A. and Bruckner, A.P., "Investigation of Ram Accelerator Flow Fields Induced by Canted Projectiles", AIAA Paper 93-2186, 1993.

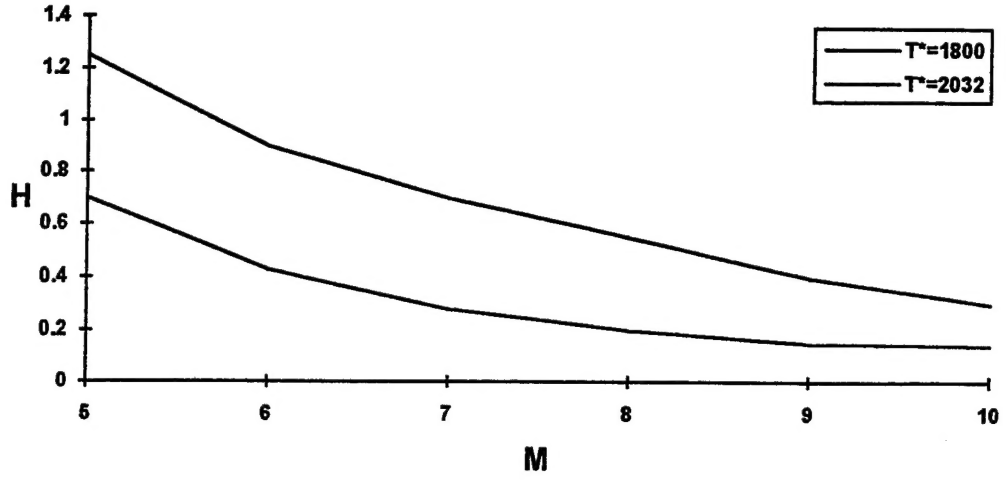

Fig. 1a. The calculated minimum step height for hydrogen - oxygen mixture (from Ref. 4).

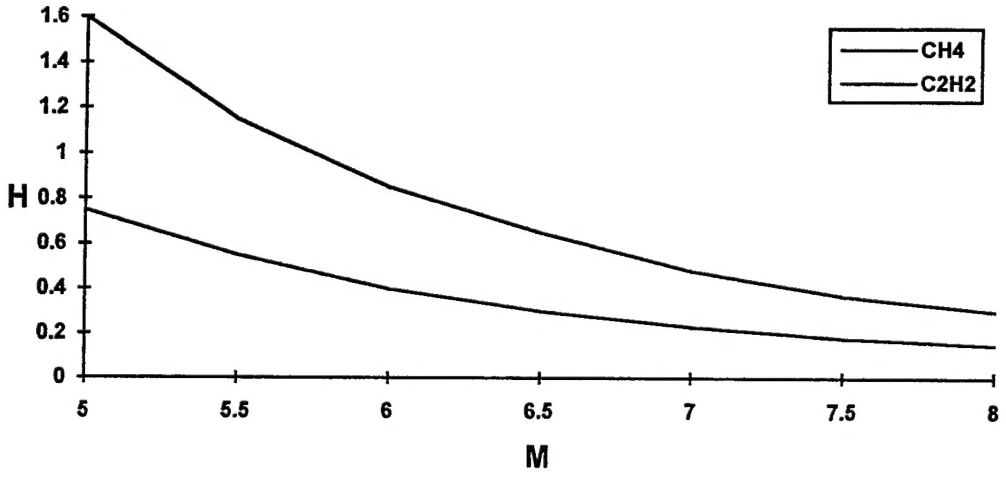

Fig. 1b. The calculate minimum step height for the acetylene - oxygen and for the methane - oxygen mixtures (from Ref. 4).

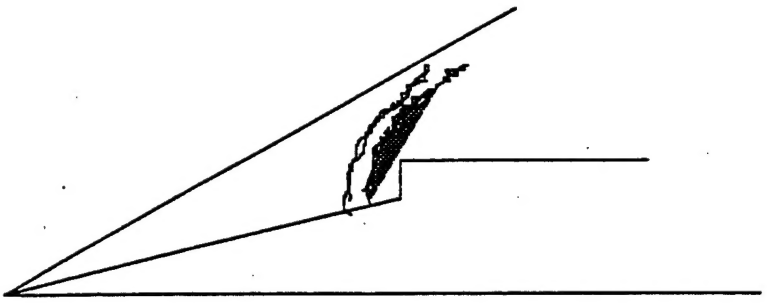

2. The flow structure on the conical nose with the forward facing step.

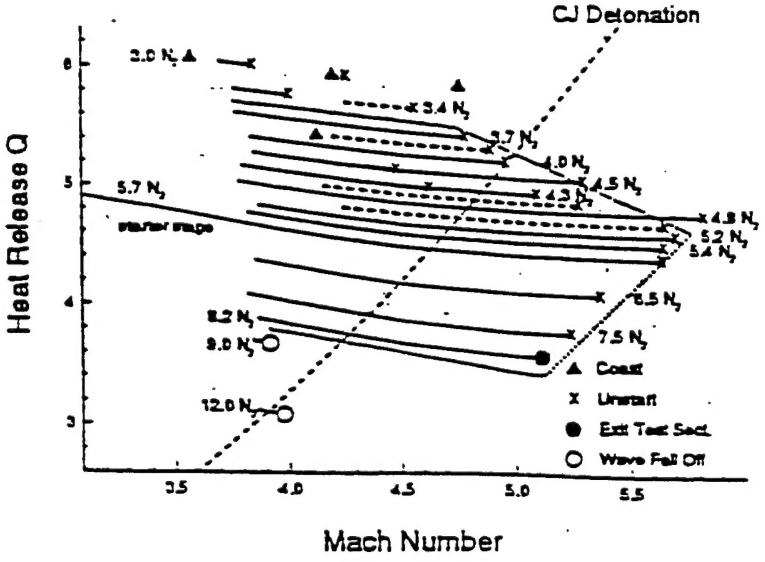

MIXTURE: 2.8 CH_4 + 2 O_2 + X N_2

X	M_{CJ}	M_{us}	Q_{us}	M_{CJ} / M_{us}
4.8	4.8	5.82	4.65	1.21
5.2	4.70	5.7	4.6	1.21
5.4	4.65	5.65	4.5	1.21
5.7	4.62	5.65	4.4	1.22
6.5	4.5	5.4	4.05	1.2
7.5	4.35	5.25	3.8	1.21

3a. Results of variable nitrogen experiments plotted as thermally choked heat release vs. flight Mach number (from Ref. 17).

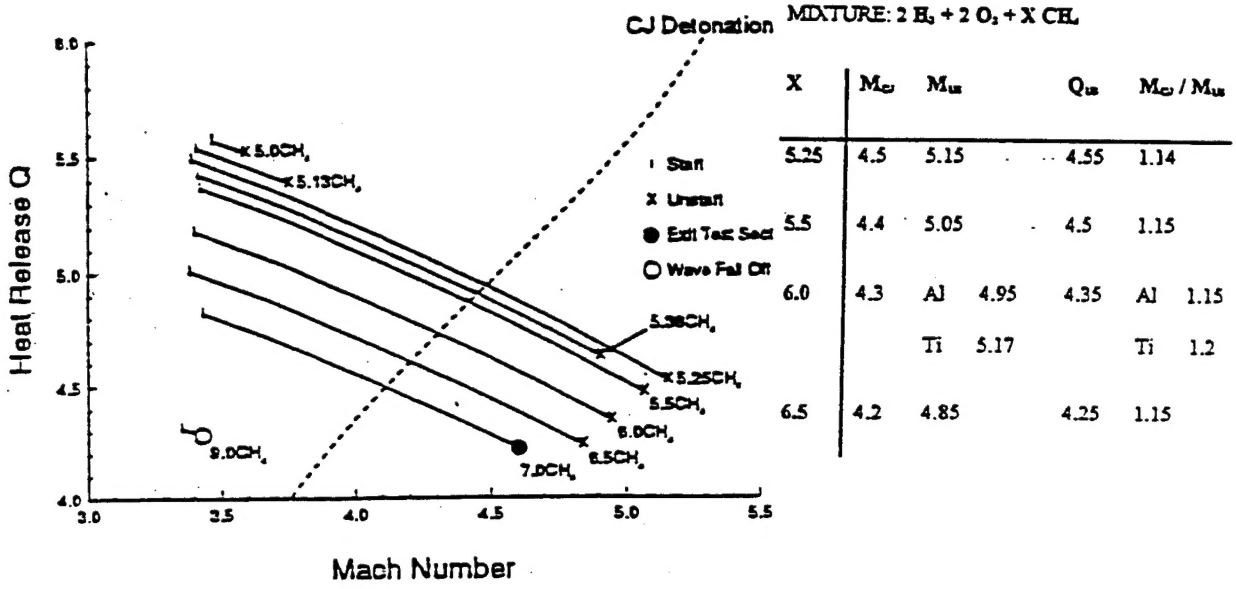

X	M_{ci}	M_{us}		Q_{us}	M_{ci}/M_{us}
5.25	4.5	5.15		4.55	1.14
5.5	4.4	5.05		4.5	1.15
6.0	4.3	Al	4.95	4.35	Al 1.15
		Ti	5.17		Ti 1.2
6.5	4.2	4.85		4.25	1.15

3b. Results of variable methane experiments plotted as thermally choked heat release vs. flight Mach number (from Ref. 17).

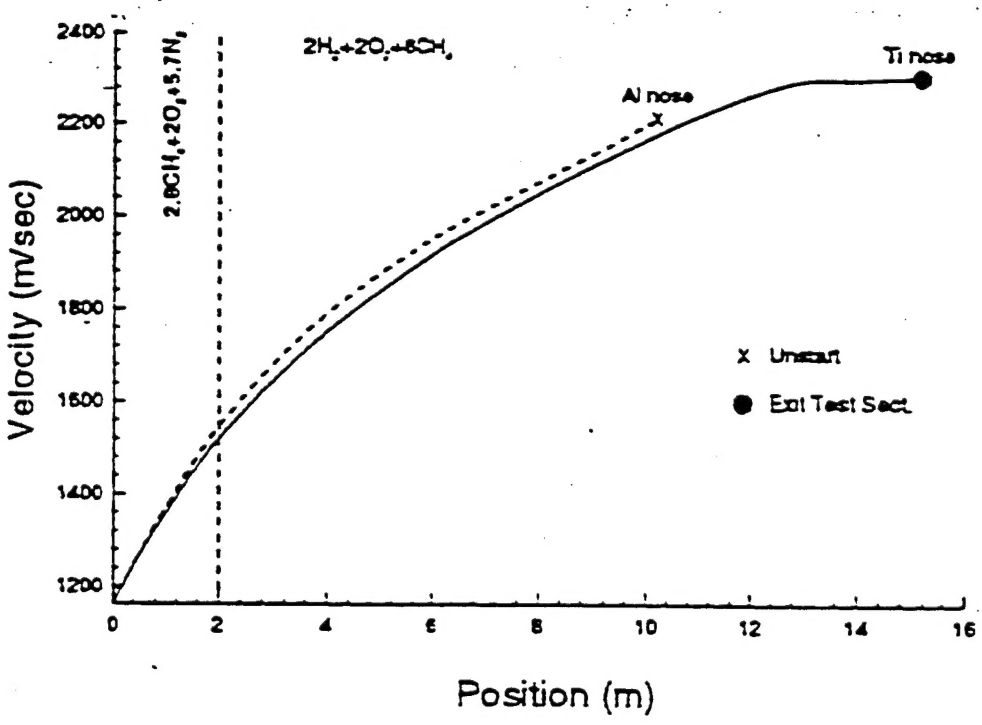

4. Velocity-distance data comparing aluminum and titanium nose projectiles (from Ref. 17).